The role of TRPV6 in the progression and aggressiveness of pancreatic cancer

Gonçalo Mesquita

Thesis submitted for the degree of:

DOCTOR

THE UNIVERSITY OF LILLE

THE UNIVERISTY OF MÜNSTER

Discipline: Molecular and cellular aspects of biology

The role of TRPV6 in the progression and aggressiveness of pancreatic cancer

Gonçalo Mesquita

15th of December 2023

Composition of the jury:

Prof. Dr. Natacha Prevarskaya – University of Lille - Head of the jury

Dr. (HDR) V'yacheslav Lehen'kyi – University of Lille - Thesis director

Prof. Dr. Albrecht Schwab – University of Münster - Thesis director

Prof. Dr. Alessandra Fiorio Pla – University of Turin - Rapporteur

Prof. Dr. Bruno Constantin – University of Poitiers - Rapporteur

Dr. (HDR) Rosangela Cardone – University of Bari - Examiner

Dr. (HDR) Nicolas Jonckheere – University of Lille - Examiner

Dr. (HDR) Zoltan Pethö – University of Münster - Examiner

Thèse présentée en vue de l'obtention du grade de:

DOCTEUR

L'UNIVERSITÉ DE LILLE

L'UNIVERSITÉ DE MÜNSTER

Discipline: Aspects moléculaires et cellulaires de la biologie

Le rôle de TRPV6 dans la progression et l'agressivité du cancer du pancréas

Gonçalo Mesquita

Le 15 décembre 2023

Composition du jury:

Natacha Prevarskaya - Université de Lille - President du jury

Dr. (HDR) V'yacheslav Lehen'kyi – University of Lille - Directeur de thèse

Prof. Dr. Albrecht Schwab – University of Münster - Directeur de thèse

Alessandra Fiorio Pla - Université de Turin - Rapporteur

Bruno Constantin - Université de Poitiers - Rapporteur

Dr. (HDR) Rosangela Cardone - Université de Bari - Examinateur

Dr. (HDR) Nicolas Jonckheere - Université de Lille - Examinateur

Dr. (HDR) Zoltan Pethö - Université de Münster - Examinateur

Acknowledgements

I have to start this chapter by thanking both of my supervisors, Dr. V'ycheslav Lehen'kyi and Prof. Dr. Albrecht Schwab. Without them, the conclusion of this thesis would have never been possible. Thank you for the opportunity given 3 years ago. Throughout all the hardships, all the disappointments, all the doubts, you gave me the hope and the assurance needed to keep pushing. For all that we have been through, I hope to have made you proud of all the work done and the resulting thesis.

A word of appreciation for the two" senior" researchers of each lab, Dr. Aurélien Haustrate and Dr. Zoltan Pethö. They were relentless in their support. Even during more busy times, they would spare me their time to teach or correct me, making me improve as a researcher on every occasion.

I would also like to extend my appreciation to all my colleagues, and above all, friends. In Lille, I was lucky to be received by Lina, Madeleine and Dheeraj. Even on those dark times of the pandemic, you were a big support and all our time together was lovely. In Münster I found my family for the last 2 years: Micol, Ben, Matteo, Dominika, Jakub, Rieke and Thorsten. Thank you for all the beautiful moments I got to spent in this time. I'll carry you with me wherever I go.

To my girlfriend, Sara, thank you for putting up with these 3 hard years. You were the boat that hold me on the hardest days, and without you this would have been impossible to achieve.

To my family, you are the reason I am here. For all the continuous support and dedication to improve my academic path, I will be forever grateful. You gave me the tools to build my future and I just hope one day I can repay you.

Lastly, thank you to my friends in my home country. You maintained your connection with me all the time, never letting me feel alone. You are part of my strength and I am deeply thankful for having you.

Summary

Pancreatic ductal adenocarcinoma stands as a highly aggressive and lethal cancer, characterized by a grim prognosis and scarce treatment alternatives. Within this context, TRPV6, a calcium-permeable channel, emerges as a noteworthy candidate due to its overexpression in various cancers of epithelial origin, capable of influencing the cell behaviour in different cancer entities. Nonetheless, the exact expression pattern and functional significance of TRPV6 in the context of PDAC remains enigmatic.

This study scrutinizes the expression of TRPV6 in tissue specimens obtained from 46 PDAC patients across distinct stages and grades. This allowed for a correlation to be made between TRPV6 expression and tissue staging, differentiation and proliferation. TRPV6 expression was also manipulated (knockdown, overexpression) in the human PDAC cell lines Panc-1 and Capan-1. Subsequently we analysed its impact on multiple facets, encompassing Ca^{2+} influx, proliferation, apoptosis, migration, chemoresistance, and tumour growth, both *in vitro* and *in vivo*.

Notably, the data indicates a direct correlation between TRPV6 expression levels, tumour stage, and grade, establishing a link between TRPV6 and PDAC proliferation in tissue samples. Decreasing TRPV6 expression via knockdown hampered Ca^{2+} influx, resulting in diminished proliferation and viability in both cell lines, and cell cycle progression in Panc-1. The knockdown simultaneously led to an increase in apoptotic rates and increased the susceptibility of cells to 5-FU and gemcitabine treatments. Moreover, it accelerated migration and promoted collective movement among Panc-1 cells. Conversely, TRPV6 overexpression yielded opposing outcomes in terms of proliferation in Panc-1 and Capan-1, and migration of Panc-1 cells. Intriguingly, both TRPV6 knockdown and overexpression diminished the process of tumour formation in vivo.

Overall, this thesis suggests that PDAC aggressiveness relies on a fine-tuned TRPV6 expression, raising its profile as a putative therapeutic target. An intricate interplay of TRPV6 expression is commonly found in all experiments performed.

Table of Contents

List of figures

List of tables

Abbreviations

5-FU = 5-fluorouracil

AKT = PI3K-protein kinase B

ANOVA = Analysis of variance

ASPC-1 = Pancreatic cancer cell line

ATP = Adenosine triphosphate

BCA = Bicinchoninic acid assay

BxPC-3 = Pancreatic cancer cell line

CA19-9 = Carbohydrate antigen 19-9

CAF = Cancer-associated fibroblasts

CAPAN-1 = Pancreatic cancer cell line

CAPAN-2 = Pancreatic cancer cell line

CAT1 = Calcium transport protein 1

CDK1 = Cyclin-dependant kinase 1

CDKN2A = Cyclin-dependent kinase inhibitor 2A

cDNA = Complementary DNA

COLO357 = Pancreatic cancer cell line

DESeq2 = Differential gene expression analysis based on the negative binomial distribution

DMSO = Dimethyl sulfoxide

DNA = Deoxyribonucleic acid

dNTP = Deoxynucleotide

ECM = Extracellular matrix

EDN1 = Endothelin 1

EDTA = Ethylenediaminetetraacetic acid

EGFR = Epidermal growth factor receptor

EMT = Epithelial-mesenchymal transition

ER = Endoplasmic reticulum

ERK = Extracellular signal-regulated kinase

FBS = Fetal bovine serum

FGFR3 = Fibroblast growth factor receptor 3

FOLFIRINOX = Combination treatment of FOL (folinic acid), F (5-fluorouracil), IRIN (irinotecan) and OX (oxaliplatin)

G418 = Geneticin

GAPDH = Glyceraldehyde-3-phosphate dehydrogenase

GO = Gene ontology

HEPES = 4-(2-hydroxyethyl)-1-piperazineethanesulfonic acid

HES = Haematoxylin-eosin saffron

HPDE = Immortalized epithelial cell line from pancreatic ducts

HR = Hazard ration

IHC = Immunohistochemistry

INS-1E = Pancreatic beta cell line

IP3R = Inositol trisphosphate receptor

K-562 = Human leakaemia cell line

KPC = Mouse model of PDAC

KRAS = Kristen rat sarcoma viral oncogene homolog gene

LNCaP = Prostate cancer cell line

MCF10A = Epithelial cell line from mammary gland in fibrocystic breasts

MEK =Mitogen-activated protein kinase

MIAPACA-2 = Pancreatic cancer cell line

mRNA = Messenger RNA

MTS = 3-(4,5-dimethylthiazol-2-yl)-5-(3-carboxymethoxyphenyl)-2-(4-sulfophenyl)-2H-tetrazolium

NFAT = Nuclear factor of activated T cells

PAGE - Polyacrylamide gel electrophoresis

PBS = Phosphate-buffered saline

PC3 = Prostate cancer cell line

PCR = Polymerase chain reaction

PDAC = Pancreatic ductal adenocarcinoma

PI3K = Phosphatidylinositol 3-kinase

PMCA = Plasma membrane Ca2+ ATPase

PMS = Phenazine methosulfate

PS = Phosphatidylserine

PVDF = Polyvinylidene difluoride

RAF = Rapidly accelerated fibrosarcoma kinase

RAL = Ras-related protein

RNA = Ribonucleic acid

RPMI = Roswell Park memorial institute 1640 medium

SDS = Sodium dodecyl sulphate

SEM = Standard error of the mean

SERCA = Sarcoendoplasmic reticulum calcium ATPase

SMAD4 = Mothers against decapentaplegic homolog 4

SW480 = Colorectal cancer cell line

T-47D = Breast cancer cell line

TCGA = The cancer genome atlas

TFCP2L1 = Transcription factor CP2-like protein 1

TGF-β1 = Transforming growth factor beta 1

THCV = Tetrahydrocannabivarin

TME = Tumour microenvironment

TNM = Tumour, nodule and metastasis classification

TP53 = Transformation-related protein 53

TRP = Transient receptor potential

UV = Ultraviolet light

1. Introduction

1.1. Ions channels and their role in tumour aggressiveness

Ion channels play an important role in many biological processes, such as cell signalling, membrane potential, enzyme activity, and pH regulation. However, ion channels can also be involved in the development and progression of cancer, as they can affect various aspects of tumour biology, such as metabolism, proliferation, invasion, angiogenesis, and resistance to therapy (Bortner and Cidlowski 2014, Litan and Langhans 2015, Prevarskaya, Skryma et al. 2018).

One of the main factors that affects the ion homeostasis in tumours is the tumour microenvironment (TME), which is the complex network of cells and molecules that surrounds and interacts with tumour cells (Andersen, Moreira et al. 2014). The TME can modulate the activity and function of ion channels and transporters in tumour cells and stromal cells, such as fibroblasts (Loeck and Schwab 2023), endothelial cells (Fiorio Pla and Munaron 2014), and immune cells (Bose, Cieslar-Pobuda et al. 2015). For instance, the TME can stimulate the release of growth factors (Koda, Hu et al. 2023), cytokines and chemokines (Zhao, Wu et al. 2021), which can bind to receptors on tumour cells and activate signalling pathways that regulate ion channel expression and activity (You, Xie et al. 2023). Moreover, the TME can alter the composition and structure of the extracellular matrix (ECM), which can affect the mechanical properties and electrical conductivity of the tissue (Brassart-Pasco, Brezillon et al. 2020). These changes influence the ion fluxes and gradients across cell membranes and affect cell behaviour.

The role of ion channels in tumour aggressiveness has been studied for various types of cancer, such as breast cancer (Rhana, Trivelato et al. 2017, Lu, Ma et al. 2020, Xu, Li et al. 2021), lung cancer (Bulk, Todesca et al. 2021), prostate cancer (Valero, Mello de Queiroz et al. 2012, Raphael, Lehen'kyi et al. 2014, Han, Liu et al. 2019), glioblastoma (Molenaar 2011, Zhang, Cruickshanks et al. 2017, Liu, Qu et al. 2019), and colorectal cancer.

1.2. The Transient Receptor Potential channels

Transient receptor potential (TRP) channels are a large and diverse family of ion channels that are involved in various physiological processes, such as sensation, thermoregulation, pain, inflammation, and vascular function (Song and Yuan 2010, Julius 2013, Vriens, Nilius et al. 2014, Khalil, Alliger et al. 2018). However, TRP channels can also play a role in the development and progression of cancer by modulating several cellular functions that are associated with the hallmarks of cancer, such as proliferation (Chigurupati, Venkataraman et al. 2010, Lodola, Laforenza et al. 2012), survival (Zhang, Liu et al. 2017), migration (Fiorio Pla and Gkika 2013) and metastasis (Fels, Bulk et al. 2018, Bai, Wei et al. 2023).

The history of TRP channels began with the discovery of a mutant strain of the fruit fly Drosophila that had defective vision (Cosens and Manning 1969). The mutant flies had a transient response to light, instead of a sustained one, and were named "transient receptor potential" or trp mutants. The gene *trp* responsible for this phenotype was cloned and sequenced in 1989 and from then on, the TRP family started growing with several members being discovered in numerous independent studies (Minke 2010). It was found that *trp* was not the only gene involved in the phototransduction pathway in Drosophila. Another gene, named *trpl* (for *trp*-like), was also identified as a cation channel that had similar structure and function to *trp* (Phillips, Bull et al. 1992). Together, *trp* and *trpl* formed a heteromultimeric channel complex that was essential for the maintenance of the light-induced current in the photoreceptors. The discovery of trp and trpl sparked the interest in finding other homologous genes in different organisms. Soon, several mammalian genes were identified that shared sequence similarity with *trp* and *trpl*. In 2002 there was a standardization of the nomenclature that led to the formation of the superfamily TRP (Montell, Birnbaumer et al. 2002). These genes were classified into seven subfamilies based on their sequence homology and functional properties: TRPC (canonical), TRPV (vanilloid), TRPM (melastatin), TRPA (ankyrin), TRPML (mucolipin) and polycystin (Fig. 1). Each subfamily contains several members that have distinct biophysical and pharmacological characteristics, as well as different expression patterns and regulatory mechanisms. Some TRP channels are activated by physical stimuli, such as temperature, pressure or stretch (Strotmann, Harteneck et al. 2000, Oancea, Wolfe et al. 2006, Inoue, Jensen et al. 2009), while others are activated by chemical stimuli, such as pH, oxidative stress, or ligands (Dhaka,

Uzzell et al. 2009, Huang, Liu et al. 2010, Muller, Morales et al. 2018, Hellenthal, Brabenec et al. 2021).

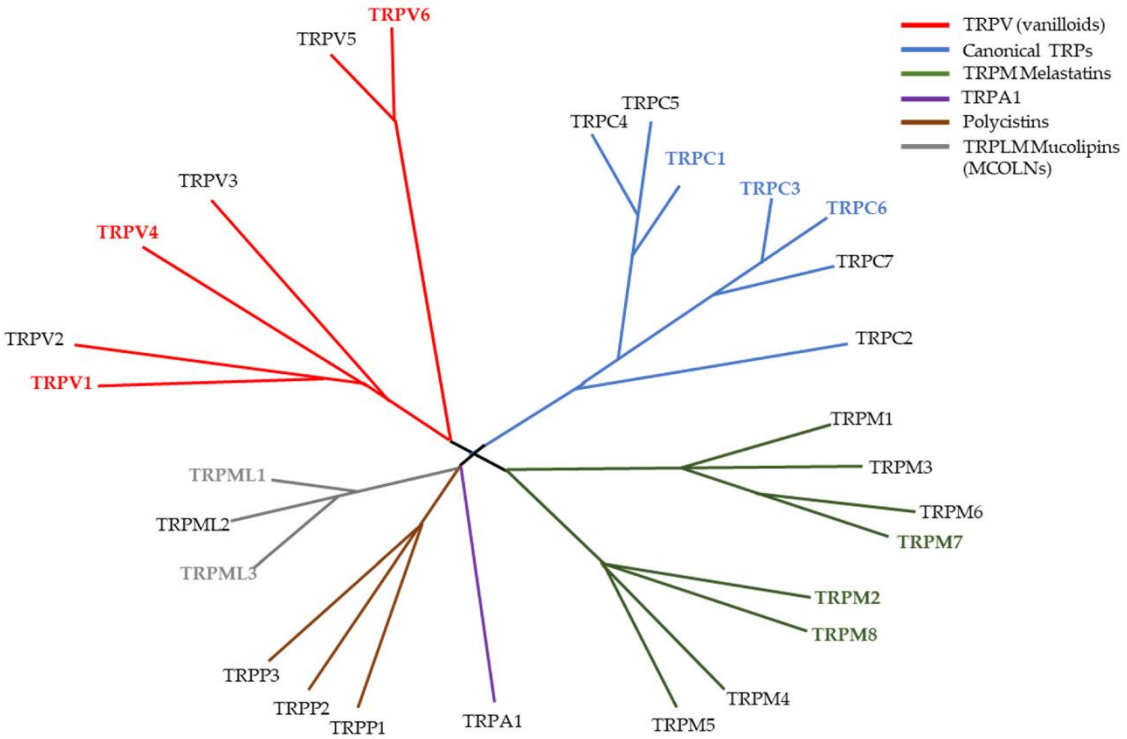

Figure 1 - **Phylogenetic tree of the TRP superfamily in vertebrates**. Highlighted TRP channels (TRPV1, TRPV4, TRPV6, TRPC1, TRPC3. TRPC6, TRPM2, TRPM7, TRPM8, TRPML1 and TRPML3) identify channels that already been study in the context of PDAC and/or pancreatitis. Figure taken from Mesquita *et al* (Mesquita, Prevarskaya et al. 2021). Figure inspired by Clapham D. (2003) (Clapham 2003).

The structure of TRP channels has been elucidated by various methods, such as X-ray crystallography, electron microscopy, and molecular modelling. The basic structure of TRP channels consists of six membrane-spanning helices (S1-S6) with intracellular N- and C-termini (Clapham 2003, Hellmich and Gaudet 2014). The S1-S4 segments form the voltage-sensing domain, while the S5-S6 segments form the pore domain. The pore domain contains a selectivity filter that determines the ion permeability of the channel. The N- and C-termini contain various domains that mediate the interactions with other proteins or molecules that modulate the channel activity (Nilius and Owsianik 2011, Hellmich and Gaudet 2014).

Some TRP channels have additional domains that confer specific functions or properties to them. For example, some TRP channels have ankyrin repeats in their N-terminus that are involved in protein-protein interactions or channel gating (Schindl, Frischauf et al. 2008, Bodkin and Brain 2011). Some TRP channels have a TRP domain in their C-terminus that is important for channel assembly or trafficking (Garcia-Sanz, Fernandez-Carvajal et al. 2004, Rohacs, Lopes et al. 2005). Some TRP channels have other domains that bind to ligands or second messengers that regulate the channel activity (Clapham 2003).

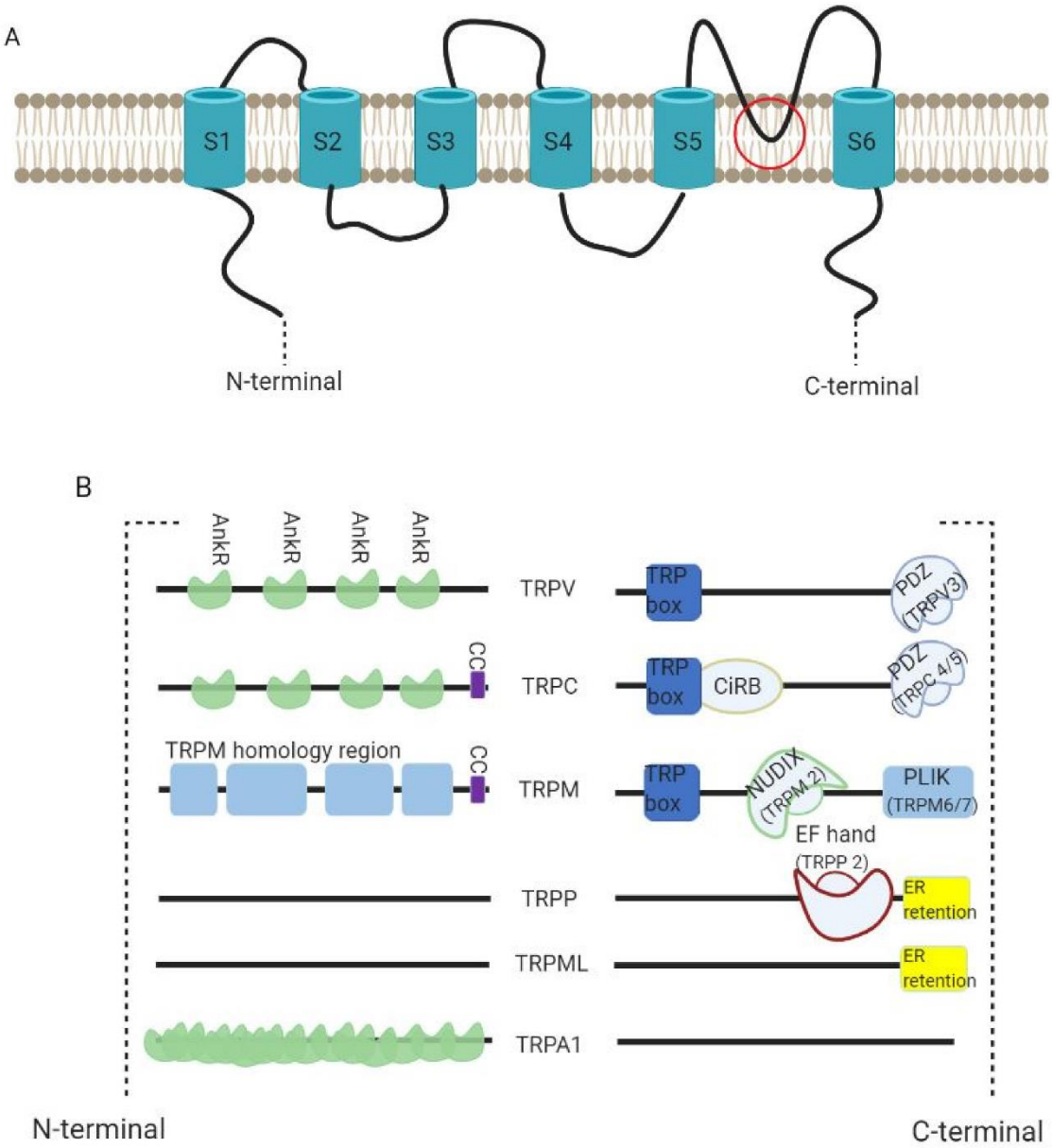

Figure 2 - **TRP channel structure**. (A) All the channels possess a six-transmembrane (S1 to S6) polypeptide subunits (with a pore-forming re-entrant loop between S5 and S6 as marked in the figure) that assemble as tetramers to form cation-permeable pores. (B) The diversity of the channels is dependent on their C- and N- termini. All TRPV channels have a TRP box at their C-termini and TRPV3 has an additional PDZ binding motif. They have 3–4 Ankyrin repeats (AnkR) in their N-termini. TRPC channels have a TRP box containing the motif EWKFAR plus CIRB (a calmodulin- and inositol triphosphate receptor-binding site). Much like TRPV3, TRPC4/5 have a PDZ binding motif. This subfamily has 3–4 AnkR with an additional coiled-coil domain (CC) in the N-terminus. TRPM channels also have a TRP box in their C-termini. While TRPM2 has NUDIX (a NUDT9 hydrolase protein homologue binding ADP ribose), TRPLM6/7 have PLIK (a phospholipase-C-interacting kinase). In their N-termini, TRPM channels have a CC and a homology region whose functions are unknown. Both TRPP and TRPML have an endoplasmic reticulum retention signal (ER retention) in the C-terminal. TRPP2 also possess a EF-hand (a canonical Ca2+-binding domain) in the N-terminus. TRPA1 channels have a much bigger number of AnkR than TRPV or TRPC. Figure taken from Mesquita *et al* (Mesquita, Prevarskaya et al. 2021). Figure inspired by Clapham D. (2003) (Clapham 2003).

1.3. Role of TRP channels in tumours

The expression and activity of TRP channels can be altered in cancer cells due to genetic mutations or changes in the tumour microenvironment (Prevarskaya, Zhang et al. 2007, Yang and Kim 2020). These alterations can result in aberrant Ca^{2+} signalling and downstream effects on various signalling pathways that are involved in cancer initiation and progression. For example, in oesophageal squamous cell carcinoma cells, the inhibition of TRPC6 leads to decreased Ca^{2+} signalling and cell cycle arrest via Cdk1 (Shi, Ding et al. 2009). Some TRP channels inhibit apoptosis by affecting the expression or function of some proteins. For example, inhibition of TRPV4 in human hepatocellular carcinoma cells leads to increased apoptosis, due to the levels of p-ERK expression being repressed after treatment with the TRPV4 antagonist (Fang, Liu et al. 2018). Some TRP channels can enhance cell migration and invasion by regulating the cytoskeleton dynamics, focal adhesions, or matrix metalloproteinases. For example, TRPM2 activation can induce filopodia formation, loss of actin stress fibres and disassembly of focal adhesions that leads to higher cell motility in HeLa and prostate cells (Li, Abuarab et al. 2016). Some TRP channels can stimulate angiogenesis as shown in prostate tumour where several TRP channels can impact vascularization both *in vivo* and *in vitro* (Bernardini, Brossa et al. 2019). These are some of

the potential functions of TRP channels, whose roles are still being investigated in several types of cancer.

TRP channels have been implicated in various types of cancer, including digestive tract cancers, breast cancer, prostate cancer, lung cancer, skin cancer and brain cancer (Gkika and Prevarskaya 2011, Fusi, Materazzi et al. 2014, Buch, Buch et al. 2018, Stoklosa, Borgstrom et al. 2020, Chinigo, Castel et al. 2021, Saldias, Maureira et al. 2021). The expression and function of TRP channels in cancer cells can vary depending on the tumour type, stage, grade, subtype, or microenvironment (Gkika and Prevarskaya 2011, Saldias, Maureira et al. 2021). Therefore, TRP channels could serve as potential diagnostic biomarkers or therapeutic targets for different cancers (Santoni, Maggi et al. 2019). However, the role of TRP channels in cancer is complex and context-dependent, and more studies are needed to elucidate the molecular mechanisms and clinical implications of TRP channel dysregulation in cancer.

1.4. TRPV6 structure and story

Transient Receptor Potential Cation Channel Subfamily V Member 6 or TRPV6 is a calcium-selective channel that belongs to the TRP channels family of proteins. It was first identified in 1999 (Peng, Chen et al. 1999). Peng and colleagues wanted to clone TRPV6, so they gave rats a diet low in Ca^{2+} for 2 weeks. This increased the expression of channels and proteins that absorb Ca^{2+} in the cells. They only isolated mRNA from the duodenum and cecum, which are parts of the intestine that absorb a lot of Ca^{2+}. They injected this mRNA into Xenopus oocytes and measured how much $^{45}Ca^{2+}$, a radioactive form of Ca^{2+}, they took up. This way, they found a channel by using a method called expression cloning. The protein that formed the channel looked like a typical ion channel, but it had a different way of taking up $^{45}Ca^{2+}$ than prototypical channels but exhibited saturation kinetics of $^{45}Ca^{2+}$ uptake typically associated to transporters. This protein is now known as TRPV6, but when Peng and colleagues discovered it, they called it Ca^{2+} transport protein (CaT1). They thought it was very important for absorbing Ca^{2+} in the intestine. Within two years of finding TRPV6 in the rat intestine (Peng, Chen et al. 1999), researchers also found its counterparts in mice (Suzuki, Ishibashi et al. 2000, Weber, Erben et al. 2001) and humans (Peng, Chen et al. 2000, Hoenderop, Vennekens et al. 2001, Wissenbach, Niemeyer et al. 2001). These early studies

showed that TRPV6 was a key channel for letting Ca^{2+} into the intestinal cells. More than 30 years have passed since TRPV6 was first discovered, and later studies have revealed more details about how this channel is regulated and what it does as a Ca^{2+}-selective channel.

TRPV6 is mainly expressed in epithelial tissues, where it mediates calcium uptake from the extracellular environment (Hirnet, Olausson et al. 2003). The regulation of calcium homeostasis by TRPV6 is crucial for normal physiology and health. Dysregulation of TRPV6 can lead to various pathological conditions, such as hypercalciuria, kidney stones, bone disorders, skin diseases, male infertility, and cancer (Bianco, Peng et al. 2007, Suzuki, Pasch et al. 2008, Weissgerber, Kriebs et al. 2011, Lieben and Carmeliet 2012, Stewart 2020).

The structure and function of TRPV6 have been extensively studied by various experimental and computational methods (Saotome, Singh et al. 2016, McGoldrick, Singh et al. 2018, Sakipov, Sobolevsky et al. 2018). TRPV6 is composed of four identical subunits that form a tetrameric channel with a central pore. Each subunit consists of six transmembrane helices (S1-S6), a pore loop between S5 and S6, an N-terminal domain with six ankyrin repeats, and a C-terminal domain with coiled-coil motifs. The pore loop contains a highly conserved aspartate residue (D541 in human TRPV6) that is responsible for the high calcium selectivity of the channel. The N-terminal domain interacts with the S4-S5 linker and modulates the channel gating. The C-terminal domain mediates the assembly and trafficking of the channel (Sakipov, Sobolevsky et al. 2018).

The activity of TRPV6 is regulated by various factors, such as pH (Peng, Chen et al. 2000), voltage (Bodding 2005), calmodulin (Singh, McGoldrick et al. 2018), and other ligands (Niemeyer, Bergs et al. 2001, McGoldrick, Singh et al. 2018). Several natural and synthetic compounds have been identified as modulators of TRPV6, either as agonists or antagonists (Lee, Lee et al. 2009, Bhardwaj, Lindinger et al. 2020). Some of these compounds have therapeutic potential for treating diseases associated with TRPV6 dysfunction (Fu, Hirte et al. 2017, Neuberger, Nadezhdin et al. 2021). For example, tetrahydrocannabivarin (THCV), a natural cannabinoid extracted from Cannabis sativa, has been shown to inhibit TRPV6 by binding to the portals that connect the membrane environment to the central cavity of the channel pore (Neuberger, Trofimov et al. 2023). THCV has anti-cancer properties and can suppress the proliferation of cancer cells that overexpress TRPV6.

1.5. TRPV6 in cancer

Many human cancers have high levels of TRPV6 mRNA and protein (Schwarz, Wissenbach et al. 2006, Lehen'kyi, Raphael et al. 2012). TRPV6 is already considered an oncochannel and its gene an oncogene (Lehen'kyi, Raphael et al. 2012, Huber 2013). TRPV6 mRNA was initially found to be high in a colorectal cancer cell line (SW480) and human leukaemia cell line (K-562) (Peng, Chen et al. 2000) and rat leukaemia cells (Bodding, Wissenbach et al. 2002). Another study found that TRPV6 mRNA was increased in prostate cancer and in two prostate cancer cell lines, LNCaP and PC3, later confirmed that it contributes to cancer aggressiveness (Peng, Zhuang et al. 2001, Raphael, Lehen'kyi et al. 2014). TRPV6 protein was low or absent in healthy exocrine tissues (e.g. breast, pancreas, prostate) but has elevated amounts in breast, colon and prostate carcinomas (Peng, Zhuang et al. 2001, Zhuang, Peng et al. 2002, Dhennin-Duthille, Gautier et al. 2011)

TRPV6 mRNA and protein are higher in breast cancer than in normal tissue, and they can be 2 to 15 times higher depending on the case (Dhennin-Duthille, Gautier et al. 2011). In most biopsies (93.3%), TRPV6 protein was more abundant in invasive tumour areas, compared to those that were non-invasive. TRPV6 was observed to be up-regulated in oestrogen receptor-negative breast cancers and this was linked to worse outcomes (Peters, Simpson et al. 2012). TRPV6 is also involved in diverse gastrointestinal malignancies, especially in the early stages. TRPV6 mRNA is very low or absent in advanced tumours (Stage III and IV), but 66% of Stage I tumours and 17% of Stage II tumours have high expression of the channel (Peleg, Sellin et al. 2010).

When TRPV6 was reduced with siRNA in breast (T-47D) (Bolanz, Hediger et al. 2008) and prostate (LNCaP) cancer cell lines (Lehen'kyi, Flourakis et al. 2007), and it resulted in decreased cell proliferation and increased apoptosis. A study showed that capsaicin caused TRPV6-dependent apoptosis due to higher calcium levels inside the cells, in a gastric adenocarcinoma cell line (Chow, Norng et al. 2007).

1.6. Pancreatic Ductal Adenocarcinoma

Pancreatic cancer is a type of cancer that originates in the pancreas and is one of the most lethal cancers, with a 5-year survival rate of only 9% (Rawla, Sunkara et al. 2019). This value has even got lower after the Covid-19 pandemic (Madge, Brodey et al. 2022). Pancreatic cancer is often diagnosed at a late stage when it has already spread to other organs and is difficult to treat.

There are different types of pancreatic cancer, depending on the cells that are affected. The most common type is pancreatic ductal adenocarcinoma (PDAC), which accounts for about 90% of all cases (Kleeff, Korc et al. 2016). PDAC develops from the cells that line the ducts that carry the digestive juices from the pancreas to the small intestine. PDAC is usually very aggressive and resistant to chemotherapy and radiation therapy (Carrato, Falcone et al. 2015).

The causes of PDAC are not fully understood, but some risk factors have been identified, such as smoking, obesity, diabetes, chronic pancreatitis, family history, and genetic mutations (Hu, Zhao et al. 2021). Chronic pancreatitis can also progress into Some of the genes that are frequently mutated or altered in PDAC are KRAS (Zhang, Zhang et al. 2023), TP53 (Maddalena, Mallel et al. 2021), CDKN2A (Klatte, Boekestijn et al. 2022), and SMAD4 (Dardare, Witz et al. 2020). These genes are involved in regulating cell growth, division, and death. When they are mutated or altered, they can lead to uncontrolled proliferation and survival of abnormal cells.

To determine the extent and spread of PDAC, pathologists use a staging system called TNM, which stands for tumour, node, and metastasis (Kulkarni, Soloff et al. 2020). TNM describes the size and location of the primary tumour (T), the involvement of nearby lymph nodes (N), and the presence of distant metastases (M). Based on these factors, PDAC is classified into four stages: I, II, III, and IV (Wood, Canto et al. 2022). Stage I means that the tumour is confined to the pancreas and has not spread to nearby lymph nodes or distant organs. Stage II means that the tumour has grown outside the pancreas or has spread to nearby lymph nodes. Stage III means that the tumour has invaded major blood vessels around the pancreas. Stage IV means that the tumour has spread to other organs, such as the liver, lungs, or bones.

The unique physical and chemical conditions of the exocrine pancreas, such as low oxygen and changing pH, are commonly related to PDAC (Heinrich, Mostafa et al. 2021). However, current PDAC treatments do not take advantage of these special features (Ho, Jaffee et al. 2020). For example, the exocrine pancreas secretes a substantial amount of bicarbonate that goes into the ductal lumen; when hormones are released after a meal, the bicarbonate levels in the lumen can reach 150 mM (Ishiguro, Yamamoto et al. 2012). This means that the cells of the pancreas and its surrounding tissue face rapid pH changes with often episodes of acidic environment. An acidic environment makes cancer worse by favouring more aggressive cells that can spread more easily, but how this happens is not well understood (Peppicelli, Ruzzolini et al. 2022). PDAC is characterized by a desmoplastic reaction to the tumour, which is seen in both primary and metastatic tumours. Desmoplasia is a common feature in PDAC and consists of a dense layer of ECM and fibroblasts, more known as cancer-associated fibroblasts (CAF) (Cannon, Thompson et al. 2018). One of the cell types that can acquire this CAF phenotype are pancreatic stellate cells (PSC). These cells can contribute to the progression and metastasis of the tumour through secretion of cytokines and chemokines, through interstitial pressures and promotion of hypoxia (Provenzano and Hingorani 2013, Spivak-Kroizman, Hostetter et al. 2013, Norton, Foster et al. 2020). Desmoplasia creates a physical obstacle, blocking blood vessels and reducing the effectiveness of chemotherapy and immune cell infiltration. Previous studies suggested that desmoplasia helps the tumour grow (Yasuda, Torigoe et al. 2014, Zhao, Lin et al. 2017); however, this is not the whole picture. The current view is that desmoplasia has different aspects and that a more comprehensive strategy to target the stroma is needed. TRP channels can be sensitive to all those stimuli or even participate in their signalling cascades (Nielsen, Lindemann et al. 2014, Okada, Reinach et al. 2015).

1.7. Current therapeutic strategies for PDAC

The treatment options for PDAC depend on the stage of the disease, as well as the patient's overall health and preferences. The main types of treatment are surgery, chemotherapy, radiation therapy, targeted therapy, and immunotherapy (Wood, Canto et al. 2022).

Surgery is the only potentially curative treatment for PDAC, but it is only possible for about 15-20% of patients who have localized disease (Wood, Canto et al. 2022). Surgery involves removing part or all of the pancreas and surrounding tissues. The most common

type of surgery for PDAC is called pancreaticoduodenectomy or Whipple procedure (Giuliano, Ejaz et al. 2017). This surgery involves removing the head of the pancreas, part of the small intestine, part of the stomach, the gallbladder, and the bile duct. The remaining parts are then reconnected to allow digestion. Furthermore, surgery can have serious complications to the patients, with very nefarious secondary effects (Giuliano, Ejaz et al. 2017).

Chemotherapy is a treatment that uses drugs to kill cancer cells or stop them from growing. Chemotherapy can be given before surgery to shrink the tumour and make it easier to remove. It can also be given after surgery to reduce the risk of recurrence. Chemotherapy can also be given alone or in combination with other treatments for patients who cannot have surgery or have advanced disease. The most commonly used chemotherapy drug for PDAC is gemcitabine, although FOLFIRINOX (leucovorin, fluorouracil, irinotecan, oxaliplatin) and other combination therapies like gemcitabine with cisplatin are commonly used (Nishimoto 2022).

1.8. Ca^{2+} and ion channels in PDAC

The development of PDAC is also highly connected to Ca^{2+} signalling. Overall, Ca^{2+} has an important role in many cellular processes. The failure to regulate it can lead to known cancer hallmarks, like continued proliferation, tissue invasion and apoptosis resistance (Orrenius, Zhivotovsky et al. 2003, Wei, Wang et al. 2012, Pinto, Kihara et al. 2015). Ca^{2+} signalling can have a role in both cell proliferation and cell death. In proliferation, Ca^{2+} has a fundamental role for the initiation and progression of the cell cycle, as evidenced by the cell cycle arrest due to suppression of several Ca^{2+} channels (Borowiec, Bidaux et al. 2014).

The role of Ca^{2+} in apoptosis has also been assessed. Apoptosis can occur via the intrinsic or extrinsic pathway. Ca^{2+} plays an important role in the intrinsic pathway. In this pathway, there is an increase in the levels of Ca^{2+} inside the mitochondria which will lead to mitochondrial membrane permeabilization and the release of cytochrome c. This in turn will start a signalling cascade that culminates in the death of the cell (Varghese, Samuel et al. 2019). Cancer cells can find ways to avoid the Ca^{2+}-dependent apoptosis through modulation of Ca^{2+} levels inside the cell. For example, in breast cancer, overexpression of plasma membrane calcium-ATPase 2 helps controlling intracellular Ca^{2+} levels, conferring apoptosis resistance to the cells (VanHouten, Sullivan et al. 2010).

The migration processes are responsible for cancerous cell invasion into other tissues. Migrating cells exhibit Ca^{2+} gradients along their front–rear axis (Kim, Lee et al. 2016). They are instrumental for directional migration. This Ca^{2+} gradient is either due to the activity of Ca^{2+} permeable channels in the plasma membrane or through the mobilization of Ca^{2+} from internal cell stores (Chen, Chen et al. 2013). Furthermore, in order to migrate away from the primary tumour and invade surrounding tissues cells need to establish contacts with the ECM. Ca^{2+} signalling leads to the disassembly of cell adhesions, with the cleavage of several focal adhesion proteins, through the Ca^{2+} sensitive protease calpain (Storck, Hild et al. 2017). At the same time, Ca^{2+} signalling is also important for the formation of new adhesion points (D'Souza, Lim et al. 2020). Ca^{2+} signalling can induce focal degradation of the ECM, through the upregulation of different matrix metalloproteinases (Prevarskaya, Skryma et al. 2011, Iamshanova, Fiorio Pla et al. 2017). The control and modulation of these Ca^{2+}-dependent processes revolves around the TRP channels. They can be both the signaller and the target of Ca^{2+}-dependent processes and thus important players in Ca^{2+} modulated diseases (Hasan and Zhang 2018).

It is also known that PDAC cells exhibit abnormal Ca^{2+} signalling compared to normal pancreatic cells. For instance, even before achieving a malignant state, cells of KPC mice (mouse model of PDAC) present more irregular Ca^{2+} oscillations than normal cells (Stopa, Lozinski et al. 2023). Most of the signalling changes in Ca^{2+} can be explained by the increased expression and activity of various Ca^{2+} channels and pumps that mediate Ca^{2+} transport across the plasma membrane and the endoplasmic reticulum (ER). Some of these proteins include TRP channels, plasma membrane $Ca^{2\pm}$ATPases (PMCAs), sarco/endoplasmic reticulum $Ca^{2\pm}$ATPases (SERCAs), and inositol 1,4,5-trisphosphate receptors (IP3Rs) (Varghese, Samuel et al. 2019).

PMCAs are ATP-dependent pumps that extrude Ca^{2+} from the cytosol to the extracellular space. PMCAs are essential for maintaining low intracellular $Ca^{2\pm}$ concentration and preventing $Ca^{2\pm}$-induced cell death (James, Chan et al. 2013). However, PMCAs can also support tumour growth by enhancing cell survival and glycolysis (James, Chan et al. 2013). PMCAs are highly expressed in PDAC cells and are required for their viability. Inhibition of PMCAs leads to cytotoxic Ca^{2+} overload and apoptosis in PDAC cells (Richardson, Sritangos et al. 2020).

SERCAs are ATP-dependent pumps that transport Ca^{2+} from the cytosol to the ER lumen. SERCAs are responsible for refilling the ER Ca2+ stores after their depletion by IP3Rs or other channels (Chemaly, Troncone et al. 2018). SERCAs play a key role in regulating ER stress and apoptosis. SERCAs are also involved in tumour development and progression by modulating cell survival, growth, invasion, and angiogenesis (Chemaly, Troncone et al. 2018).

IP3Rs are ligand-gated channels that release Ca^{2+} from the ER to the cytosol in response to IP3, a second messenger generated by phospholipase C (PLC) (Taylor and Tovey 2010, Prole and Taylor 2019). IP3Rs also participate in tumour development and progression by modulating cell survival, growth, invasion, and metastasis (Foulon, Rybarczyk et al. 2022). In PDAC cells, after being stimulated by TGF-β1, IP3R channels changed their location in Panc-1 cells from cell-cell contact points to the front parts of moving cells (Okeke, Parker et al. 2016). This means that the IP3R channels go to the lamellipodia and the filopodia at the focal adhesion level. Furthermore, inhibition of IP3Rs led to lower migration levels in Panc-1 cells (Okeke, Parker et al. 2016).

As described in my review, TRPV6 has already been studied in pancreatic malignancies (Mesquita, Prevarskaya et al. 2021). TRPV6 channels have been described to regulate proliferation of INS-1E cells, which are a model of pancreatic β-cells, and BON-1 cells, which are a model of endocrine tumour cells (Skrzypski, Khajavi et al. 2015, Skrzypski, Kolodziejski et al. 2016). Regarding TRPV6 expression in PDAC, reports have presented contradictory information. While Zaccagnino et al. found a reduced expression of TRPV6 channels in micro-dissected PDAC samples (Zaccagnino, Pilarsky et al. 2016), Song et al. reported an overexpression in PDAC tissues (Song, Dong et al. 2018). However, both of these studies did not take into account whether the tissue samples were from invasive or non-invasive parts of the tumour. This is a relevant distinction, as a preponderance of TRPV6 expression was shown for the invasive parts of breast cancer (Dhennin-Duthille, Gautier et al. 2011). The silencing of TRPV6 in Capan-2 and SW1900 cells leads to decreased proliferation, increased apoptosis, lower levels of migration and invasion and cell cycle arrest. A phase I clinical trial for SOR-C13, a TRPV6 inhibitor, has been made with some positive results (Fu, Hirte et al. 2017). This trial had included 23 patients with different types of advanced solid tumours, two of whom had PDAC. Stable disease was observed in both patients. One of the patients had a 27% reduction from baseline in the sum of tumour diameters (by RECIST criteria), with a decrease of 55% in tumour marker CA19-9 (Fu, Hirte et al. 2017). TRPV6 levels also correlate with lower survival rates on patients with PDAC

(Song, Dong et al. 2018). Adding to the fact that TRPV6 is also linked to early onset chronic pancreatitis, a risk factor for the development of PDAC, makes it indispensable to undertake a more detailed analysis of TRPV6 channels in pancreatic cancer (Masamune, Kotani et al. 2020).

2. Project aims

PDAC is the fourth most common cause of cancer-related death. Although our knowledge on the genetics and epidemiology of PDAC has advanced last years, the molecular mechanisms that give rise to PDAC are far from being clear and have not yet delivered targeted therapies. Prevention is exceedingly difficult since patients rarely exhibit symptoms and currently no sensitive and specific tumour markers are available for early diagnosis at a curable stage. It is therefore mandatory to better understand the mechanisms responsible for both development and progression in order to provide new biomarkers and new therapeutic strategies for the clinicians to develop new efficient therapies.

On the other hand, Ca^{2+} signals, being pivotal molecular devices in sensing and integrating signals from the microenvironment, are emerging to be particularly relevant in cancer, where they mediate interactions between tumour cells and the tumour microenvironment to drive different aspects of neoplastic progression (e.g. cell proliferation and survival, cell invasiveness and pro-angiogenetic programs) (Monteith, Prevarskaya et al. 2017).

A possible piece that could connect Ca^{2+} and PDAC is TRPV6. This channel has a uniquely high Ca^{2+} selectivity within the TRP superfamily and makes this channel quite distinguishable, especially in Ca^{2+}-related intracellular pathways (Peng, Brown et al. 2003). In human pancreas, the expression of TRPV6 channel on the basolateral surface of acinar cells in addition to high levels of expression in the apical membrane was reported (Zhuang, Peng et al. 2002). Furthermore, when compared with normal tissue or cells, the expression of TRPV6 is substantially increased in prostate cancer tissue, and in human carcinomas of the pancreas, colon, breast, thyroid and ovary (Peng, Zhuang et al. 2001, Wissenbach, Niemeyer et al. 2001, Zhuang, Peng et al. 2002). The hypothesis presented in this thesis is that TRPV6 channel, being recognized as a proto-oncogene in many tumours, may play an important role in PDAC tumorigenesis.

To achieve that, 3 main goals have been set:

1 - Conduct a retrospective study regarding the correlation of the TRPV6 channel with the tumour grade as well as the patients' outcome.

2 - Study the role of the TRPV6 channel in pancreatic cancer cell proliferation, apoptosis resistance, migration and invasion *in vitro.*

3 - Clarify *in vivo* the role of the TRPV6 channel in the formation of pancreatic tumours, its role in tumour growth and progression.

In order to accomplish the first objective, a retrospective study on a PDAC cohort of 46 patients, with different stages of pancreatic cancer was performed. Staining was performed using an anti-TRPV6 antibody already validated at the Saint Vincent de Paul Hospital (Raphaël et al., 2014). This detailed study has enabled me to correlate the expression of the TRPV6 channel with the grade of the tumours as well as the differentiation and proliferation of the tumour cells within tissues.

For the second objective, I have prepared four stable clones, from Panc-1 cell lines, that either overexpress or knockdown TRPV6 (as well as the respective controls). This allowed me to study *in vitro* the potential role of TRPV6 in PDAC cells. The goal was to understand the function of the channels in proliferation, cell cycle progression, apoptosis and chemoresistance or migration. Pathways which might be affected by the changes of TRPV6 expression were also investigated, by performing an RNA-sequencing in these stable clones.

Lastly, the stable clones have been used to investigate the potential role of TRPV6 in the development of tumours *in vivo*. Subcutaneous injection was given to nude mice with the different stable clones. Tumour growth was then analysed throughout 10-13 weeks.

My main goal was to assess whether TRPV6 could be a potential marker of aggressiveness or therapeutic target in PDAC.

3. Materials

3.1. Chemicals

Table 1 – Overview of the chemicals used.

Chemical	**Manufacturer**
Ammoniumperoxodisulfat (APS)	SERVA Electrophoresis GmbH, Germany
Annexin Binding Buffer	Life Technologies GmbH, Germany
Annexin V - FITC	Life Technologies GmbH, Germany
BCA Protein Assay Kit	Thermo Fisher Scientific Inc., USA
Cell-titter	Promega, USA
Chloroform	Sigma-Aldrich, Germany
Cisplatin	Münster University Hospital, Germany
Clarity Max Western ECL Substrate	Bio-Rad Laboratories GmbH, Germany
Complete Tablets, Mini EDTA-free EASY	Roche Holding AG, Swizterland
D(+)-Glucose, water free	Merck KGaA, Germany
DMSO	Sigma-Aldrich, Germany
EGTA	Sigma-Aldrich, Germany
Ethanol	AppliChem, USA
FBS Superior	Biochrom GmbH, Germany
Fura-2-AM	Invitrogen AG, Carlsbad, USA
Glycerin	Carl Roth GmbH & Co. KG, Germany
Gemcitabine	Münster University Hospital, Germany

Geneticin (G418)	ThermoFischer, USA
HCl	Merck KGaA, Germany
HEPES	Sigma-Aldrich, Germany
Isopropanol	Carl Roth GmbH & Co. KG, Germany
KCl	Sigma-Aldrich, Germany
Laemmli 4x	Bio-Rad Laboratories GmbH, Germany
Lipofectamine 3000	ThermoFisher, France
Magic Marker	Invitrogen AG, USA
Matrigel	BD Biosciences, USA
Methanol	Carl Roth GmbH & Co. KG, Germany
MESA GREEN qPCR MasterMix Plus	Eurogentec, France
$MnCl_2$	Merck KGaA, Germany
MTS	Promega, USA
NaCl	Carl Roth GmbH & Co. KG, Germany
Page Ruler Plus	Thermo Scientific, USA
PBS	Sigma-Aldrich, Germany
Penicillin-Streptomycin	Pan-Biotech GmbH, Germany
Propidium Iodide	Sigma-Aldrich, Germany
PVDF Membrane	Merck KGaA, Germany
RIPA Buffer	Thermo Fisher Scientific Inc., USA

RPMI 1640	Sigma-Aldrich, Germany
RNAse A	Sigma-Aldrich, Germany
SDS	Carl Roth GmbH & Co. KG, Germany
TEMED	AppliChem, USA
Tris	Carl Roth GmbH & Co. KG, Germany
Trizol	Invitrogen AG, Carlsbad, USA
Trypsin	Pan-Biotech GmbH, Germany
Tween 20	Sigma-Aldrich, Germany
sh_Vectors	ClonTech, USA
β-actin antibody	Abcam, Germany
5-fluorouracil	Münster University Hospital, Germany

3.2. Devices and software

Table 2 - Overview of the devices and software used.

Device/Software	**Manufacturer**
Animal imaging system	Bruker, USA
BD FACSCalibur	BD Biosciences, USA
BioPhotometer	Eppendorf, Germany
Bio-Rad CFX Manager Software v2.0	Bio-Rad, USA

BioRad CFX96 Real-Time PCR Detection System	Bio-Rad, USA
CellQuest software	BD Biosciences, USA
ChemiDoc™ XRS+ Gel Imaging System	Bio-Rad Laboratories GmbH, Germany
CO_2 Incubator	Thermo Fisher Scientific Inc., USA
ImageJ software	National Institutes of Health, USA
Microscope: Apoptosis Nikon A1	Nikon, Japan
Microscope: Cell culture Axiovert S100	Carl Zeiss AG, Germany
Microscope: Migration Axiovert 1040	Carl Zeiss AG, Germany
MikroCamLab II software	Bresser, Germany
NIS Elemental software	Nikon, Japan
TriStar LB 94 Luminometer	Berthold technologies, USA
Superfusion System	Thermo Fisher Scientific Inc., USA
VisiChrome Polychromator	Visitron Systems GmbH, Germany
-80°C Freezer	Thermo Fisher Scientific Inc., USA

3.3. Human tissue data

Tumour and peri-tumoral tissues were obtained from patients with PDAC that was histopathologically confirmed by the medical staff of GHICL (Groupement des Hôpitaux de l'Institut Catholique de Lille) (TNM classification, 8th edition of the UICC 2016). The number of subjects is 46 and tissues were collected between January of 2014 and December of 2019 (RNIPH-2022-26). Immunohistochemistry of TRPV6 expression was analysed semiquantitatively in human tissue, with a scoring system ranging from 0 (no staining) to 3

(very intense staining). The analysis of the IHC was performed by Dr. Adriana Mihalache from the Saint Vicent de Paul Hospital. Staining intensity is based on the H-score, which results of the multiplication of the percentage of cells with score given (Fig.1A) (Fedchenko and Reifenrath 2014). The human tissues were divided in 2 groups for staging analysis: n=18 for early stages (T1 and T2) and n=28 for more advanced stages (T3 and T4). The second analysis distinguished between highly differentiated and poorly differentiated tissues. Highly differentiated tissues had n=12 slides and poorly differentiated tissues had n=22. Lastly, human tissues were separated by Ki67 staining. The groups were divided as following: 0-5% staining n=19; 5-25% staining n=9; 25-50% staining n=4; >50% staining n=3.

3.4. Medium

The medium used throughout the thesis was RPMI 1640 (Roswell Park Memorial Institute medium, Sigma-Aldrich). The following table describes the components added to the medium throughout all the experiments.

Table 3 – RPMI 1640 composition

Compounds	Quantities
RPMI 1640 medium (with L-glutamine and sodium pyruvate)	500mL
FCS-Superior (Fetal calf sérum)	10%
Penicillin-Streptomycin	1%
Geneticin (G418)	500µM

3.5. Animal experiments

Studies involving animals, including housing and care, method of euthanasia, and experimental protocol (APAFIS #22266), were conducted in accordance with the animal ethical committee (CEEA75) in the animal house (C59-00913) of the University of Lille.

For these experiments, the mice used were the Charles Rivers swiss-nude mice from Charles Rivers, aged 6-8 weeks. The mice were kept in a ventilated cabinet and all animal handling is performed under qualified personnel. Before starting the experiments, the animals had a week of quarantine to accommodate to the environment. Throughout the

study, the well-being of the animals was assessed daily. Human end-points were selected before the realization of the experiments. The observation of signs of pain or discomfort (prostration, coat condition, weight loss, aggressive behaviour with biting) would result in the animal being removed from the protocol and killed. One of the end-points was weight loss above 10% of initial body weight. Furthermore, when the tumour reaches the maximum permissible size of 2500mm3 the animal would be sacrificed. In our experiments, animals were sacrificed by cervical dislocation after isoflurane administration.

4. Methods

4.1. Meta analysis

A retospective analysis was made using SurvExpress (Aguirre-Gamboa, Gomez-Rueda et al. 2013). Clinical data was obtained from "The Cancer Genome Atlas Program". The only gene evaluated was TRPV6. The patients' data were divided in 2 groups: high risk or low risk. This was done by using a prognostic index estimation (PI). The PI is the linear part of the Cox model , $PI=\beta 1x1+ \beta 2x2+\ldots+\beta pxp$ where xi is the expression value and the βI are the risk coefficients from the Cox fitting.

4.2. Human tissue staining

For immunohistochemistry four micrometre-thick conventional whole tissue-sections were cut from formalin-fixed and paraffin-embedded (FFPE) tissue blocks. Immunohistochemical staining was performed using a BenchMark ULTRA system (Ventana Medical Systems Inc., AZ, USA) and a revelation kit (ultraView DAB Detection Kit (Roche Diagnostics)). Sections were pre-heated in citrate-based buffer (CCS1) several times before antibody incubation. Sections were then immunolabeled with anti-TRPV6 Clone Mab 82 antibody (Haustrate, Mihalache et al. 2022) or anti-Ki-67 by using heat-induced epitope retrieval in citrate-based buffer (CCS 2) at 91°C for 8 min followed by primary antibody incubation for 32 min. Haematoxylin was then applied to the samples for 16 minutes. This procedure is a benchmark protocol for IHC, done by the personnel of the Saint Vicent de Paul Hospital. Slides interpretation was made by Dr. Adriana Mihalache. Further analyses were made by and in cooperation with Dr. Adriana Mihalache.

4.2. Cell culture

Panc-1 and Capan-1 cells were incubated in a humidified atmosphere at 37 °C and 5% CO_2. The highly aggressive pancreatic adenocarcinoma cells were cultured in RPMI medium (Roswell Park Memorial Institute medium) (Table 1). When cells reached 70-80% confluence, a new passage was made. For this, they were washed with PBS and then 1 ml of trypsin (0.05% in EDTA) was pipetted to the cells. The cells were incubated for 3-5 min at 37°C and 5% CO^2. Detachment of the cells was monitored with a microscope. The reaction

was stopped with 10 ml of FCS-containing RPMI medium and the cells were divided into new cell culture dishes at the desired ratio (usually 1:10).

4.3. Cell Transfection

For transfection, the cells were seeded in 6-well plates at a density of 1 x 10^5 cells per well and incubated overnight. The next day, the cells were transfected with one of the following plasmids: vEF1ap-5'UTR-TRPV6_CMVp-mCherry-Vektor, vEF1ap-5'UTR_CMVp-mCherry or pSingle-tTS-shRNA-Vektor. The latter vector had Luciferase or TRPV6 as the shRNA sequence. The plasmids were diluted in Opti-MEM Reduced Serum Medium and mixed with Lipofectamine 3,000 Transfection Reagent according to the manufacturer's instructions. The transfection complexes were added to the cells and incubated for 24 h. The medium was then replaced with fresh RPMI with 500 μM of G418 in order to select transfected cells. After 2 weeks, a small group of cells (3-4 cells) was selected, and a new culture was prepared for each mixed clone. Continuous selection with G418 was done throughout the culture of stable clones. All the experiments were performed with the stable mixed clones.

4.4. RNA extraction

The total RNA from the four different stable clones were isolated using Trizol reagent and chloroform, and then used to perform RNA-sequencing and to transcribe into cDNA. Using 500 μL of Trizol, cells were lysed directly on 100 mm tissue culture dishes where they were grown until subconfluence. After adding 100 μL of chloroform to the cells and incubating them at room temperature for 5 min the solutions were centrifuged for 15 minutes at 12.000 x g and 4 °C. The supernatant with RNA was removed and 250 μL of isopropanol were added, then the solutions were centrifuged again for 10 min with the same settings. The resulting pellet was rinsed with 500 μL of RNAse-free ethanol (70%) and centrifuged once more at 7.500 g and 4 °C for 5 min. The final pellet with RNA was dissolved in 20 μL of RNAse-free water and the amount of RNA was measured with the BioPhotometer.

4.5. RNA sequencing

Each RNA sample was validated for RNA integrity using an 18S/28S ratio. 1μg of total RNA from each sample were used for library preparation. Library preparation was

realized following manufacturer's recommendations. Final samples pooled library prep were sequenced on ILLUMINA Novaseq 6000 with SP-200 cartridge (2x800Millions of 100 bases reads), corresponding to 2x26Millions of reads per sample after demultiplexing. This work benefited from equipment and services from the core genomics facility, at the Medical Faculty of the University of Münster (Münster, Germany). Results were then evaluated as fold change of the controls.

Quality of raw data was evaluated with FastQC. Poor quality sequences and adapters were trimmed or removed with Galaxy, with default parameters, to retain only good quality reads. GalaxyEU was also used to perform the analysis. Mapping on hg38 reference genome annotation gtf file was used. Data were normalized with DESeq2 prior to differential analysis with glm framework likelihood ratio test from DESeq2 workflow. Multiple hypothesis adjusted p-values were calculated with the Benjamini-Hochberg procedure to control FDR. Enrichment analysis was conducted with clusterProfiler R package with or Gene Set Enrichment Analysis, on gene ontology database, KEGG pathways and Hallmark gene sets.

4.6. qPCR

The quantitative real-time PCR of TRPV6 mRNA transcripts was done using MESA GREEN qPCR MasterMix Plus for SYBR Assay on the BioRad CFX96 Real-Time PCR Detection System. Preparations were made following manufacturer instructions. First the mix was made with the primers, 5 µg of RNA, dNTP mix and RNase free water. After the mix was heated for 65 °C for 5 min. After a brief centrifugation, cDNA buffer and RNase inhibitor were added and incubated for 3 minutes at 37 °C. Lastly, Mu-MLV RT was added and put on the thermocycler for 10 min 25 °C, 50 min 37 °C and 5 min at 95 °C. The GAPDH gene was used as an endogenous control to normalize sample difference and variability in RT efficiency. To quantify the results, the comparative threshold cycle method ΔΔCt and Bio-Rad CFX Manager Software v2.0 were used. To compare the knockdown and overexpression to the controls, fold change of TRPV6 relative expression between the stable clones. The primer sequences used for the qRT-PCR analysis are represented in table 4.

Table 1 - Primers for qPCR

Gene	Primer	Sequence
GAPDH	Forward	CTGTTGTGCTCTTGCTGGG
	Reverse	ACCCACTCCTCCACCTTTG
TRPV6	Forward	CCCAAGGAGAAAGGGCTAAT
	Reverse	TTGGCAGCTAGAAGGAGAGG

4.7. Western blot

Western blot protocol was followed like in Haustrate *et al.* (Haustrate, Mihalache et al. 2022). Cells used for western blotting were grown on 100mm culture dishes and kept on ice for the time of extraction. After rinsing with PBS, cells were lysed with RIPA buffer composed of: 1% Triton X-100 (non-ionic detergent), NaCl 150mM, PO4Na2/K 20 mM pH 7.2 (phosphate buffer), 1% sodium deoxycholate, 5mM EDTA and 0.1% SDS (sodium dodecyl sulfate, ionic detergent). A cocktail of protease inhibitors was added (10µL/mL). The lysates were then ultra-sonicated and centrifuged at 12,000g at 4°C for 10min to remove unlysed debris. Supernatants were recovered and quantified by the BCA method.

After BCA assay, 50µg of total proteins are recovered for SDS-PAGE (Sodium Dodecyl Sulfate-Polyacrylamide Gel Electrophoresis) electrophoresis. After adding Laemmli buffer to denature the proteins (Tris-HCl 125mM pH 6.8, SDS 4%, β-mercaptoethanol 5% (disulfide bridge reduction), glycerol 20%, bromophenol blue 0.01%), 10% acrylamide gel electrophoresis is performed. As the proteins have been denatured by the various buffers (and by heating at 95°c for 5 min) and negatively charged by SDS buffer (0.225 M Tris–Cl pH 6.8, 50% glycerol, 5% SDS, 0.25 M DTT, and 0.05% bromophenol blue), they can migrate through the polyacrylamide gel towards the positive pole (bottom of the gel). After migration, the proteins are transferred to a PVDF (Polyvinyldiene Fluoride) membrane by semi-dry electrotransfer, which has been permeabilized with methanol for 3 min. Once the transfer is complete, the non-specific sites on the membrane are saturated by incubating it for 1h at room temperature with TNT-milk 5% (Tris-HCl pH 7.4, NaCl 140mM, tween 20 0.05% and skimmed milk powder). The membrane is then incubated overnight at 4°C with the primary antibody (1:500 dilution for most of the antibodies used). After overnight incubation of the primary antibody, the membrane is rinsed 2 times with TNT solution, then incubated for 1 h at room temperature with the secondary antibody (anti-mouse or anti-rabbit, depending on the primary antibody used, at 1/100,000 dilution) coupled to HRP (HorseRadish Peroxidase) in 1% TNT-milk. After rinsing, the membrane is revealed by chemiluminescence using Clarity Max Western ECL Substrate solution

containing the luminol and hydrogen peroxide required by HRP for the chemiluminescence reaction. The bands on the membrane were visualized using enhanced chemiluminescence in ChemiDoc™ XRS+ Gel Imaging System. A densitometry calculation is performed Image J software to determine variations in the expression of our protein of interest of interest (TRPV6) relative to the housekeeping gene (β-actin) in different lines/conditions.

4.8. Mn^{2+} quench experiments

Mn^{2+} quench experiments were used to determine the Ca^{2+} influx into the cell. Panc-1 stable clones were stained with Fura-2-AM for 30 min at 37°C. Cells were superfused with HEPES-buffered Ringer's solution (without Ca^{2+}) for 3 min and then with the test solution (e.g., 0 Na^{+}) containing 400 μM $MnCl_2$ for 3-5 min. Mn^{2+} has a higher binding affinity to fura-2-AM and reduces fluorescence. By decreasing the fluorescence intensity, the Ca^{2+}- influx can be inferred.

The measurements were performed on an Axiovert 200 with a 40x oil objective. A superfusion system and a VisiChrome Polychromator were connected. The superfusion rate was performed at 1-1.5 ml/min. The excitation wavelength was 357 nm and fluorescence emission was measured at 510 nm. An image was acquired every 10 s with an exposure time of 100 ms. The experiments were performed at 37°C. For evaluation, the background intensity was first subtracted from the cell intensity. Then, the slope of each stable clone over 30 s for each time point during the Mn^{2+} influx was evaluated. The steepest slope over 30 s was determined and converted to the max Mn^{2+} influx per min.

4.9. Cell Count

Cell proliferation was assessed through cell count. Briefly, cells were plated in a T25 flask at a density of 30,000 cells per flask. Images of proliferating Panc-1 cells were acquired every other 30 min for 48 h, starting 2 hours after plating. Cell proliferation was also assessed through mitosis count. This allowed me to exclude cells migrating from other areas. Images were obtained in a Zeiss Axio1040 microscope, with controlled temperature. The pictures were taken using MikroCamLab II software.

4.10. Cell Cycle Assay

Cell cycle analysis was performed by means of flow cytometry of cell populations cultured in triplicate in culture dishes, as described in Lehen'kyi et al. 2011(Lehen'kyi, Raphael et al. 2011). Briefly, Panc-1 cells were washed with PBS and then trypsinized. After this procedure, they were fixed in cold methanol for 30 minutes at 4°C. After this step, cells were centrifuged and with PBS at 4°C, resuspended in 100 µl PBS, treated with 100 µl RNAse A (1 mg/ml), and stained with propidium iodide at a final concentration of 50 µg/ml. The stained cells were stored at 4°C in the dark and analysed within 2 h. Propidium iodide fluorescence was measured with a BD FACSCalibur. Data were acquired for 10,000 events, and red fluorescence was measured using a fluorescence detector 3 (FL3). The data were stored and analysed using CellQuest software to assess cell-cycle distribution patterns between the different phases: subG1 (apoptotic), G0/G1, S, and G2/M phases.

4.11. ATP quantification

For these experiments, cells were seeded in 96 well plates, at a density of 3×10^4 cells per well. The cells were maintained under normal cell culture conditions in 100 µl medium until the experiment, which occurred every day from day 0 (3 hours after plating) until day 4. In some experiments, individual plates were initially subjected to different treatments: gemcitabine (3µM), cisplatin (3µM), 5-fluoruouracil (3µM) or DMSO as negative control. To perform the experiment, 100 µL of CellTiter (Promega) were added to each well, followed by 2 min of agitation. The analysis was made 10 min after the addition of Cell-titter. Luminescence in the wells was measured by using the TriStar LB 94 Luminometer controlled by the Lumi Enhancer 2 software. In order to transform the luminescence values in ATP concentration values, a standard curve was created in parallel: 12 solutions with known concentrations of ATP (4000, 2000, 1000, 800, 650, 400, 200, 100, 80, 40, 20, 10 nM) were prepared and measured in the same 96-well plate in which the cells were seeded. All measurements were performed in duplicate. ATP concentration values are shown as mean of the duplicate (n=2 per condition for each N; N=3-6).

4.12. MTS assay

The Cell Titer 96 Aqueous Non-Radioactive Cell Proliferation Assay (MTS) is a colorimetric assay for the indirect measurement of cell viability. The assay uses tetrazolium salt (MTS) and phenazine methosulfate (PMS). These compounds are used to measure the activity of mitochondrial dehydrogenase present in metabolically active cells. Via $NAD+H^+$, the enzyme reduces MTS (in the presence of presence of PMS) to a coloured compound,

formazan. Thus, the quantity of formazan produced is indirectly indicative of cell viability and can be quantified using a plate-reading spectrophotometer at 490nm absorbance MTS+PMS were added directly to the medium for 1h in the dark at 37°C before absorbance is measured.

4.13. Annexin V staining

To determine apoptosis levels, Annexin V-FITC was used to stain and detect apoptosis in living cells after 24 h treatment. This assay is based on the fact that Annexin V has high affinity for the phosphatidylserine (PS) exposed on the outer leaflet of the plasma membrane of cells undergoing apoptosis.

For each condition 3 x 10^5 cells were seeded on a glass-bottom dish (pre-coated for 30 min at 37°C with 0.1% poly-L-lysin) and cultured overnight at 37 °C and 5% CO_2; the day after, individual dishes were subjected to different treatments: gemcitabine (3μM), cisplatin (3μM), 5-fluoruouracil (3μM) DMSO as negative control. After 24h treatment cells were first washed in PBS and then stained with 95 μL of annexin binding buffer 5x (50 mM HEPES, 700 mM NaCl, 12.5 mM CaCl2, pH 7.4) and 5 μL of Annexin-V coupled to Annexin V-FITC (excitation/emission 488/530 nm). After 15 min incubation at room temperature, the cells were then washed first in annexin binding buffer and then again in PBS before adding 1 ml of PBS as the final solution volume. The staining process was carried out in the dark.

The images for the detection of annexin V staining were taken using a FITC filter (488 nm excitation, 530 nm emission) at 20x magnification and an exposure time of 100 ms. Seven different fields for each dish were taken using a Nikon A1 confocal microscope with a filter set for FITC, with a 20x magnification controlled by NIS Elemental software (Nikon). Cells that bound Annexin V-FITC showed green staining on the plasma membrane. The images were acquired and processed using NIS-Elements software and after background subtraction, quantification of the cellular fluorescence intensity (arbitrary units) was performed on 10 cells per visual field.

4.14. Wound healing assay

Cells were cultured in RPMI supplemented with 10% FBS in glass bottom dishes, pre-coated with 0.01% poly-l-lysin, with a spacer until they reached confluence. The spacer was removed to create a cell-free gap and replaced the medium with fresh RPMI containing 20

mM HEPES and incubated the cells in a heating cabinet at 37°C for 2 h. The dishes were then transferred to a live cell imaging system (Zeiss Axio1040 microscope) and images of the wound area were captured every other 30 min for 20 h. Temperature was maintained at 37°C throughout the experiment. Cells moved to fill the gap, allowing me to study the speed at which the cells moved to each other. Images were analysed using NIS-elements software and the wound closure rate was assessed in μm^2 by determining the area newly covered by cells migrating into the wound during the course of the experiment.

4.15. Clustering assay

To take advantage of the migration experiment with the wound healing assay, I have used the videos of the images to study how the different stable clones are moving as a unit. The main goal of this experiment was to understand whether cells were moving as a cluster or making their own paths alone. This could make me understand whether cell-cell adhesion forces are playing a part in the motility of cells. To achieve this, the analysis was made using a main cell and four surrounding cells (Fig. 31). The distance of each surrounding cell to the main one (from nucleus to nucleus) was measured. Throughout the experiment I segmented the cells with AMIRA software, which allows me to analyse the distance between each cell at every time-point. To calculate the clustering of the cells, the difference of the distance between the main cell and the surrounding ones was taken at t=0h and at t=48h. The distance of each of the cells was used to average the distance in each experiment. Each experiment is compound of 4 replicates, and 3 experiments were made for each stable clone.

4.16. *In vivo* experiments

Mice were transplanted by subcutaneous injection of 2 million Panc-1 cells contained in 50% (vol:vol) matrigel containing growth factors to facilitate cell adhesion and prevent cell dispersion. Tumour growth was monitored every 2 days, using a calliper to establish a growth curve within a given time frame. After sacrificing the animals injected with Panc1-mCherry and Panc1-mCherry-TRPV6 tumour growth was analysed through mCherry intensity. To do that the mice were placed under a small animal imaging system, visualizing the fluorophore mCherry present in the cancer cell lines used. Each stable clone was injected in 10 mice. Mice were sacrificed after 10 weeks for the ones injected with Panc1-mCherry and Panc1-mCherry-TRPV6 and 13 weeks for Panc1-shLuciferase or Panc1-shTRPV6.

4.17. Statistical analysis

Experimental data are shown as mean ± SEM. The statistical analysis was performed in GraphPad Prism 8.0. ANOVA followed by Holm-Sidak test, with multiple comparisons between the different clones in different time points or with different concentrations. T-test was used for differences between two groups with one variable. In the graphs (*) denotes statistically significant differences with $p < 0.05$.

5. Results

The results obtained in this project are aimed at shedding a light in the possible roles of TRPV6 in the progression and aggressiveness of PDAC.

To understand how TRPV6 expression correlates with PDAC staging and progression a retrospective study was conducted to analyse in the literature different studies in which TRPV6 expression was present. This allowed me to determine how TRPV6 expression is correlated with patients' survivability.

After these analysis, PDAC patients' tissues were stained and marked for TRPV6 in order to establish a correlation between TRPV6 expression and PDAC staging and tissue differentiation and proliferation.

To understand the role of TRPV6 in an in vitro model, I have created four different stable clone models, based on two PDAC cell lines. An RNA sequencing was performed to investigate genes and full pathways modified by the overexpression or the knockdown.

The studies in human tissue and RNA sequencing allowed me to decide on which experiments to focus on. I've started by analysing proliferation and cell viability through via cell counting, MTS or ATP assay. Cell cycle was evaluated through DNA staining with propidium iodide.

I've also analysed chemotherapeutic resistance in Panc-1 cells. ATP assay and Annexin V staining were used to quantify cell viability and apoptosis in Panc-1 cells, in response to treatments like gemcitabine, cisplatin or 5-fluorouracil. Cell motility was analysed through wound healing assay.

Lastly, an in vivo study was made with the injection of Panc-1 stable clones into nude mice.

5.1. TRPV6 expression correlates with PDAC patients' survivability.

A retrospective study was conducted in order to understand how TRPV6 levels correlate with patients survivability to PDAC. First, generated risk groups were split by averaging the ordered PI (higher values for higher risk) by the number of risk groups leaving equal number of samples in each group (Fig.3A). The graph shows the Kaplan-Meier plots by risk group, the log-rank test of differences between risk groups and the hazard ratio (HR), which estimates the probability that subjects with a higher risk will experience the event after subjects with a lower risk (Bovelstad and Borgan 2011). Higher risk patients had an HR of 1.33 (p-value=0.1762). So, although the risk was higher in the high risk group, differences between the groups were not significant. TRPV6 expression was higher in the high risk group than in the lower risk group (3.9vs1.6) (Fig.3B).

A

B

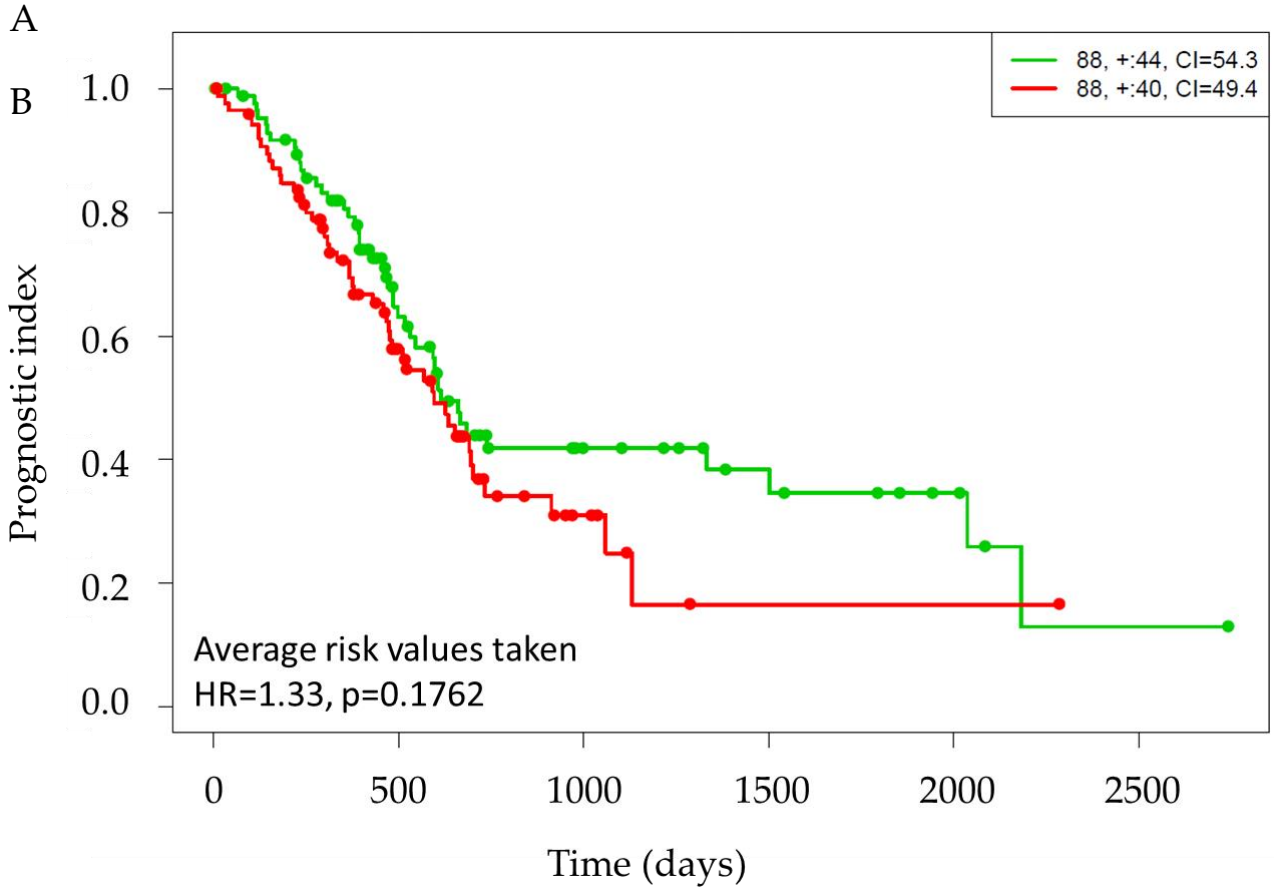

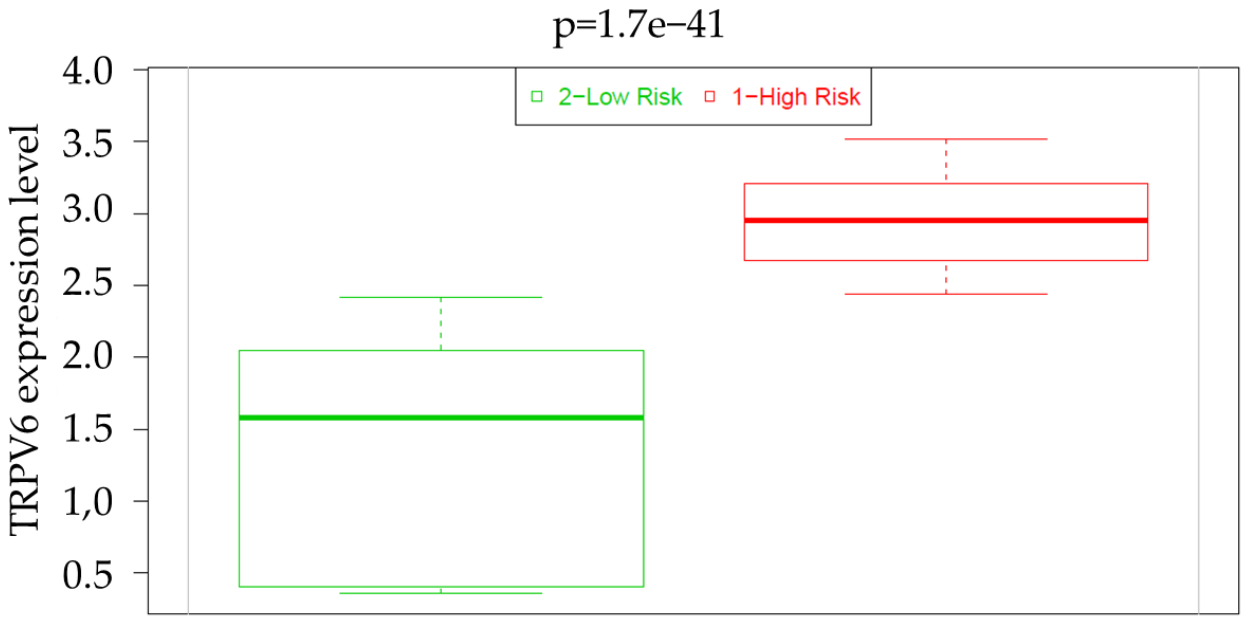

Figure 3 - **Risk analysis of PDAC patients by averaged risk groups and their TRPV6 expression**. A) This figure shows the results from a PDAC meta-base included in SurvExpress. Differential expression levels were calculated in the web-based tool SurvExpress by averaging two risk groups (high risk and low risk) by prognostic index median and Cox fitting. It shows a Kaplan-Meier curve for risk groups, HR and p-value of the log-rank testing equality of survival curves. B) Box plot across risk groups, including the p-value testing for difference using t-test.

To obtain a population significantly different from each other, risk groups have been maximized (Fig.4A). In brief, the 'Maximize Risk Groups' option in SurvExpress uses an algorithm that tests different cut-off points until it partitions the risk groups with the minimum p-value. In this plot, the high risk group had an HR of 2.12 (p-value=0.0129). TRPV6 expression was higher in the high risk group than in the lower risk group (2.5vs0.3) (Fig.4B). In this case, TRPV6 expression is even more dispersed between the higher and lower risk groups. The data obtained clearly shows a correlation between TRPV6 and patients' survivability. Low expression of TRPV6 in PDAC patients leads to better survivability rates, especially after 2 years of disease.

TRPV6 expression might then be an indicative of the aggressiveness and risk of PDAC.

A

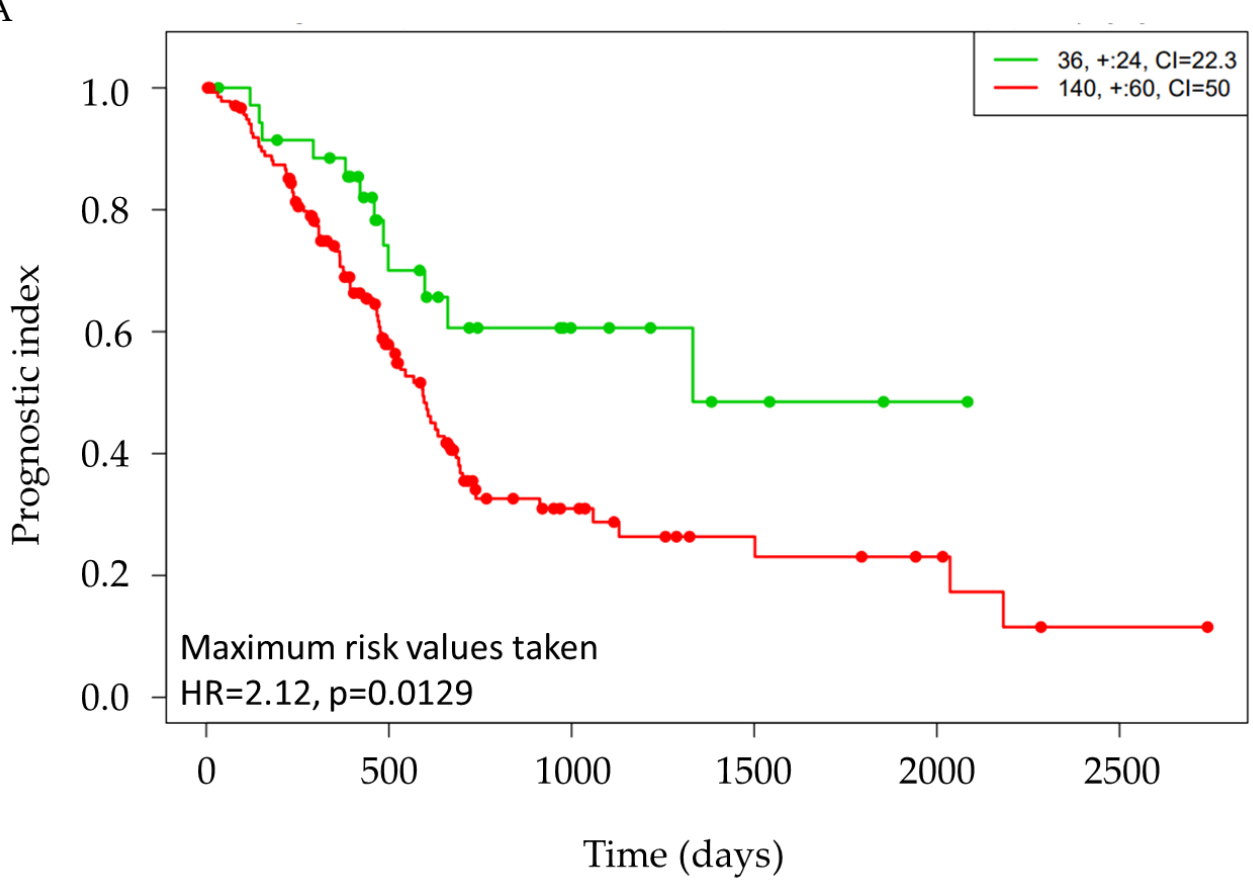
36, +:24, CI=22.3
140, +:60, CI=50
Prognostic index
1.0
0.8
0.6
0.4
0.2
0.0
Maximum risk values taken
HR=2.12, p=0.0129
0
500
1000
1500
2000
2500
Time (days)

B

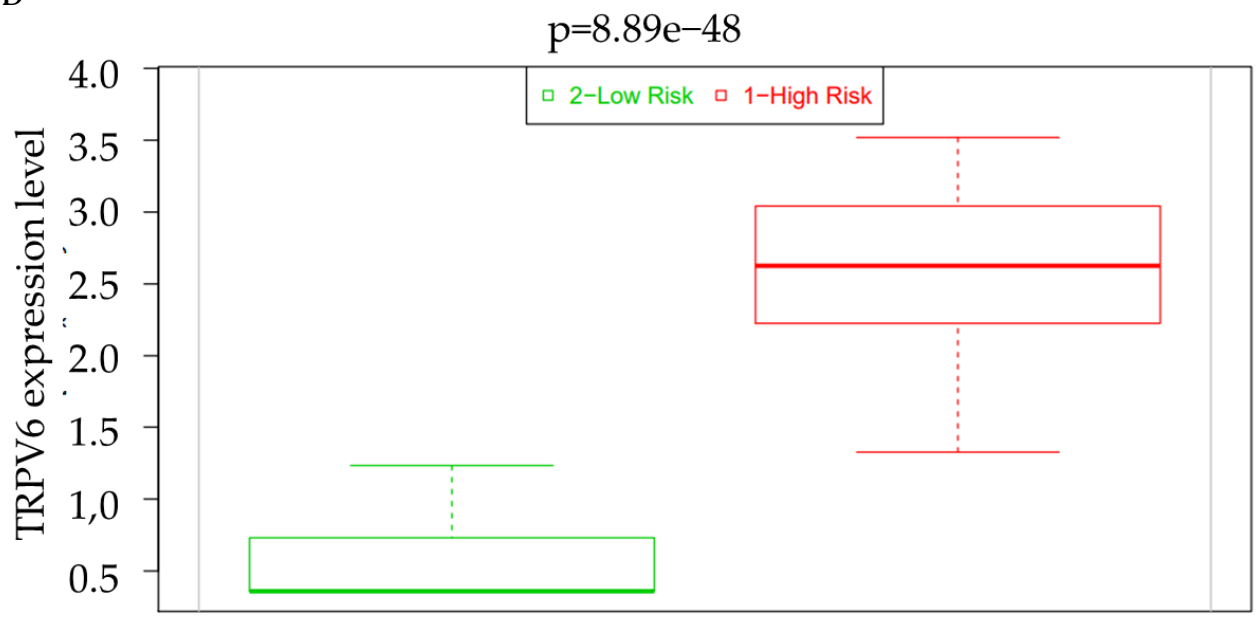
p=8.89e−48
2−Low Risk
1−High Risk
TRPV6 expression level
4.0
3.5
3.0
2.5
2.0
1.5
1,0
0.5

Figure 4 - **Risk analysis of PDAC patients by maximized risk groups and their TRPV6 expression.**A) This figure shows the results from a PDAC meta-base included in SurvExpress. Differential expression levels were calculated in the web-based tool SurvExpress by maximizing two risk groups (high risk and low risk) by prognostic index median and Cox fitting. It shows a Kaplan-Meier curve for risk groups, HR and p-value of the log-rank testing equality of survival curves. Box plot across risk groups, including the p-value testing for difference using t-test.

5.2. TRPV6 expression in PDAC tumour tissues correlates with tumour stage, differentiation and proliferation.

After analysing the current known studies through SurvExpress, TRPV6 appears to be a good prognosis indicator for PDAC. To further investigate it, expression of TRPV6 was analysed in tissue samples from 46 patients with PDAC in different stages. This work was made in collaboration with the Hospital of Saint Vicent de Paul in Lille. TRPV6 staining was made using Mab82, a specific monoclonal antibody for TRPV6, validated by Dr. Aurélien Haustrate during his PhD thesis with Dr. Vyache'slav Lehen'kyi. The staining intensity of TRPV6 was compared in tumour tissues against peri-tumoural tissues (as the control) and graded according to the H-scoring system ranging from 0 (no staining) to 3 (very intense staining) (Fig.5). The H-score indicates that the score given corresponds to the staining intensity within a certain percentage of cells in the tissue.

Figure 5 - **TRPV6 staining score.** TRPV6 expression was analysed semiquantitatively with immunohistochemistry using the TRPV6 antibody Mab82. The expression was scored according to its intensity, ranging from 0 (no staining) to 3 (very intense staining).

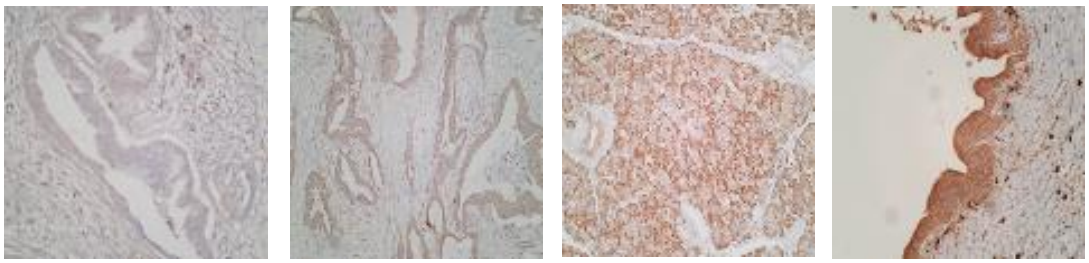

We used the TMN to categorize tumour tissues into lower disease progression (T1/T2) or higher disease progression (T3/T4) (Fig.6). As indicated in the Introduction chapter, the staging of a tumour is an important tool in clinics to differentiate resectable tumours, from those that need chemotherapeutics to help tumour reduction. Late-stage cancers are very hard to cure because they have already spread to other parts of the body from the original site. This means that the cancer cells have invaded the blood vessels or lymph nodes and travelled to other organs, where they can form new tumours. These metastatic tumours are often resistant to the standard treatments, such as chemotherapy or radiation, and may require more aggressive or targeted therapies. It was observed that TRPV6 expression increased with the tumour stage, from the early stages (stages I and II) to the later ones (stages III and IV) (Fig.9A). TRPV6 staining intensity increased by 67.9 ± 23.1% for tumour tissues and 18.3 ± 10.5% for peri-tumoural tissues between early and late stages.

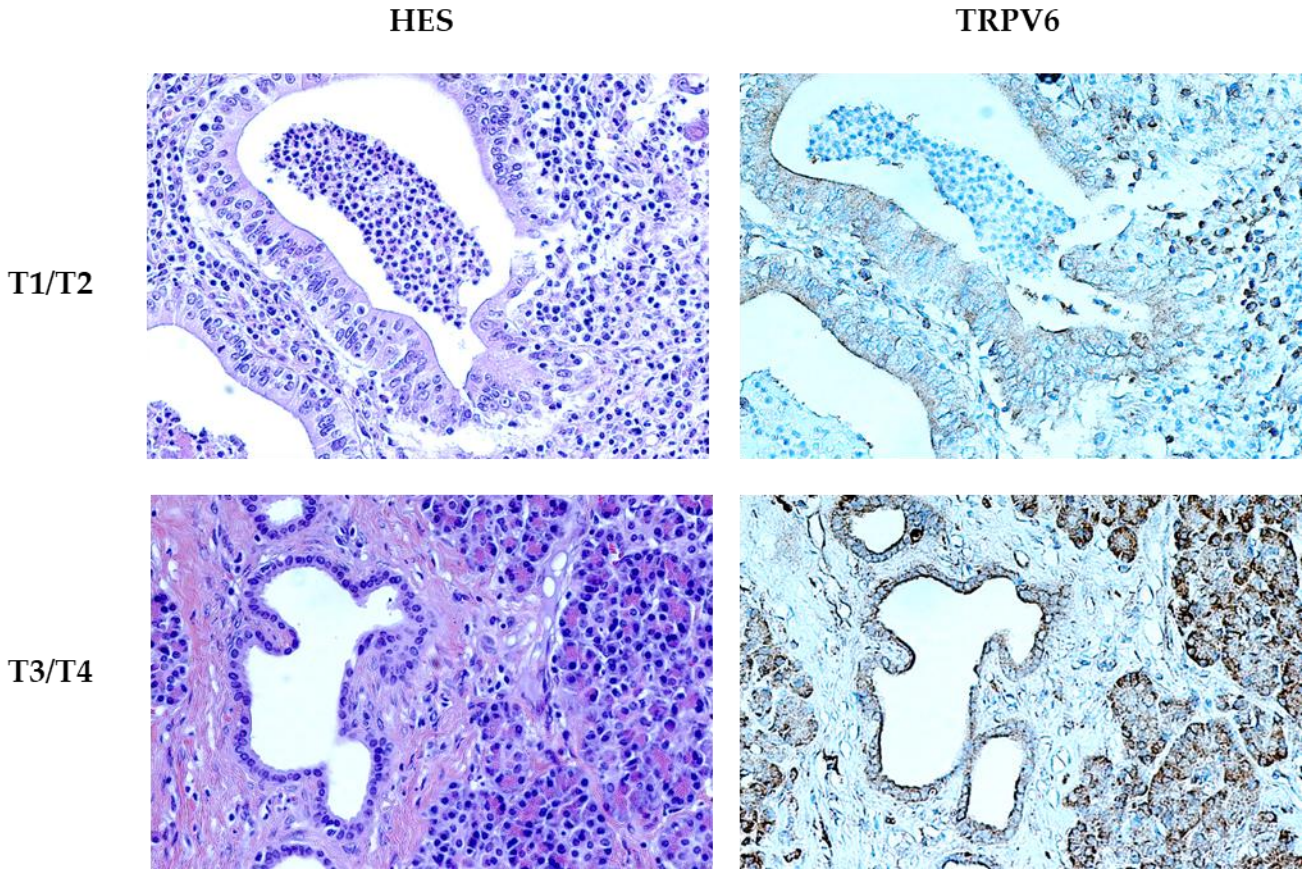

Figure 6 - **TRPV6 is more expressed in tissues on the later stages of PDAC.** PDAC tissue from patients in different stages of the cancer. The images represent tissues from patients in the early stages (top) or late stages (bottom). HES staining can be found in the left columns. TRPV6 staining is shown in the right columns, Scale bars indicate 50 μm.

We also classified the tumour tissues as highly differentiated or poorly differentiated based on histopathological features (Fig.7). Tissue differentiation is important in cancer because it reflects how abnormal the cancer cells are compared to the normal cells of the same tissue type. The more abnormal the cancer cells are, the more likely they are to grow and spread faster and resist treatment. This is why poorly differentiated or undifferentiated cancers have a worse prognosis than well differentiated or moderately differentiated cancers (Jogi, Vaapil et al. 2012). In this study, poorly differentiated tumour tissues were found to have higher TRPV6 expression than highly differentiated ones (Fig.9B). Poorly differentiated tissues showed a TRPV6 staining intensity of 126.9 ± 16.2. Well differentiated tissues had a staining intensity of 81.7 ± 10.1, which is a 32% reduction in staining compared to poorly differentiated tissues.

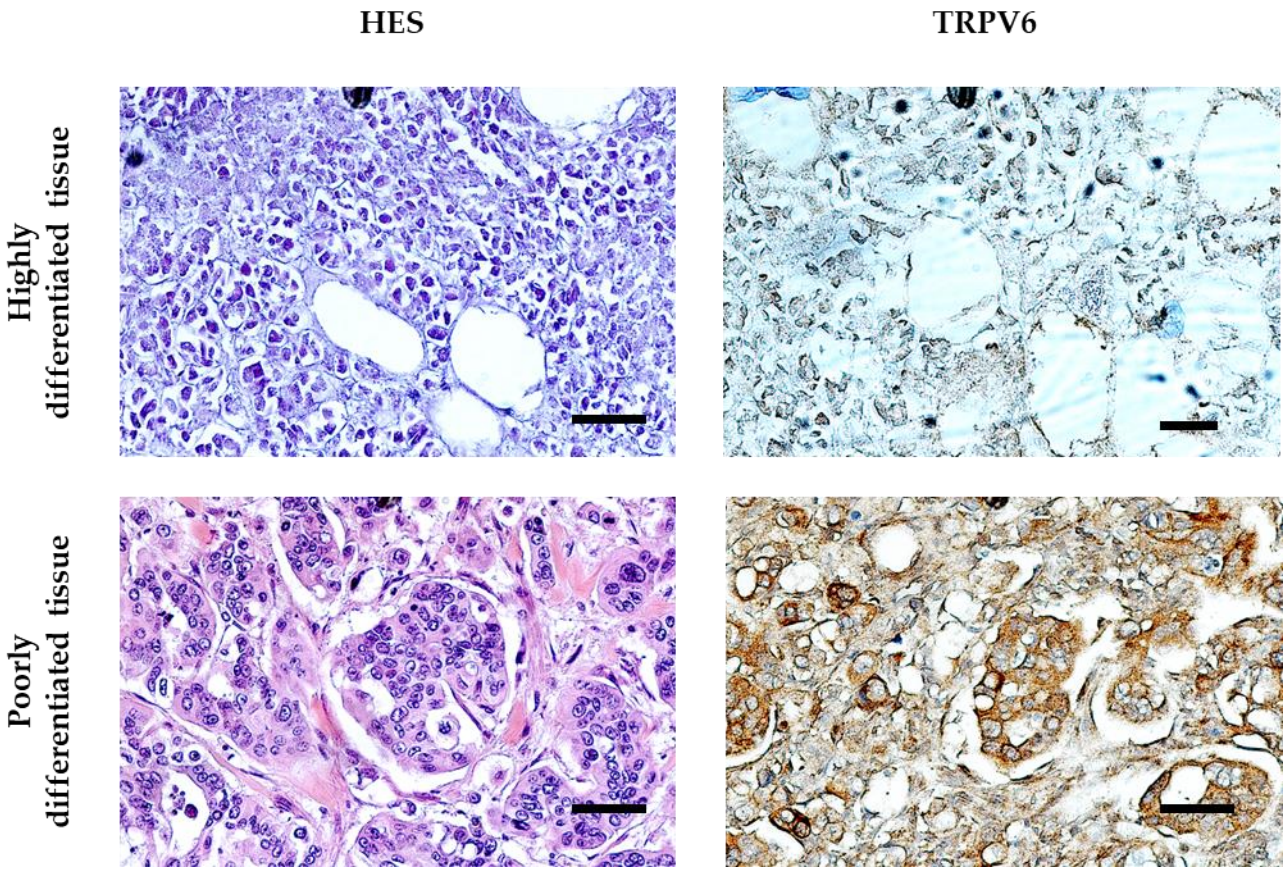

Figure 7 - **TRPV6 is more expressed in poorly differentiated tissues in PDAC patients.** PDAC tissue from patients with different differentiation levels. The images represent tissues from patients with highly differentiated tissue (top) or poorly differentiated tissue (bottom). HES staining can be found in the left columns. TRPV6 staining is represented in the right columns, Scale bars indicate 50 μm.

Moreover, the association between TRPV6 expression and cell proliferation in PDAC tumour tissues was examined, using the Ki-67 marker. Tumour tissues were divided into four groups, depending on the percentage of Ki-67 positive cells: 0-5% (lower proliferation), 5-25%, 25-50%, and >50% (higher proliferation). TRPV6 staining intensity in relation to Ki-67 expression was then analysed (Fig.8).

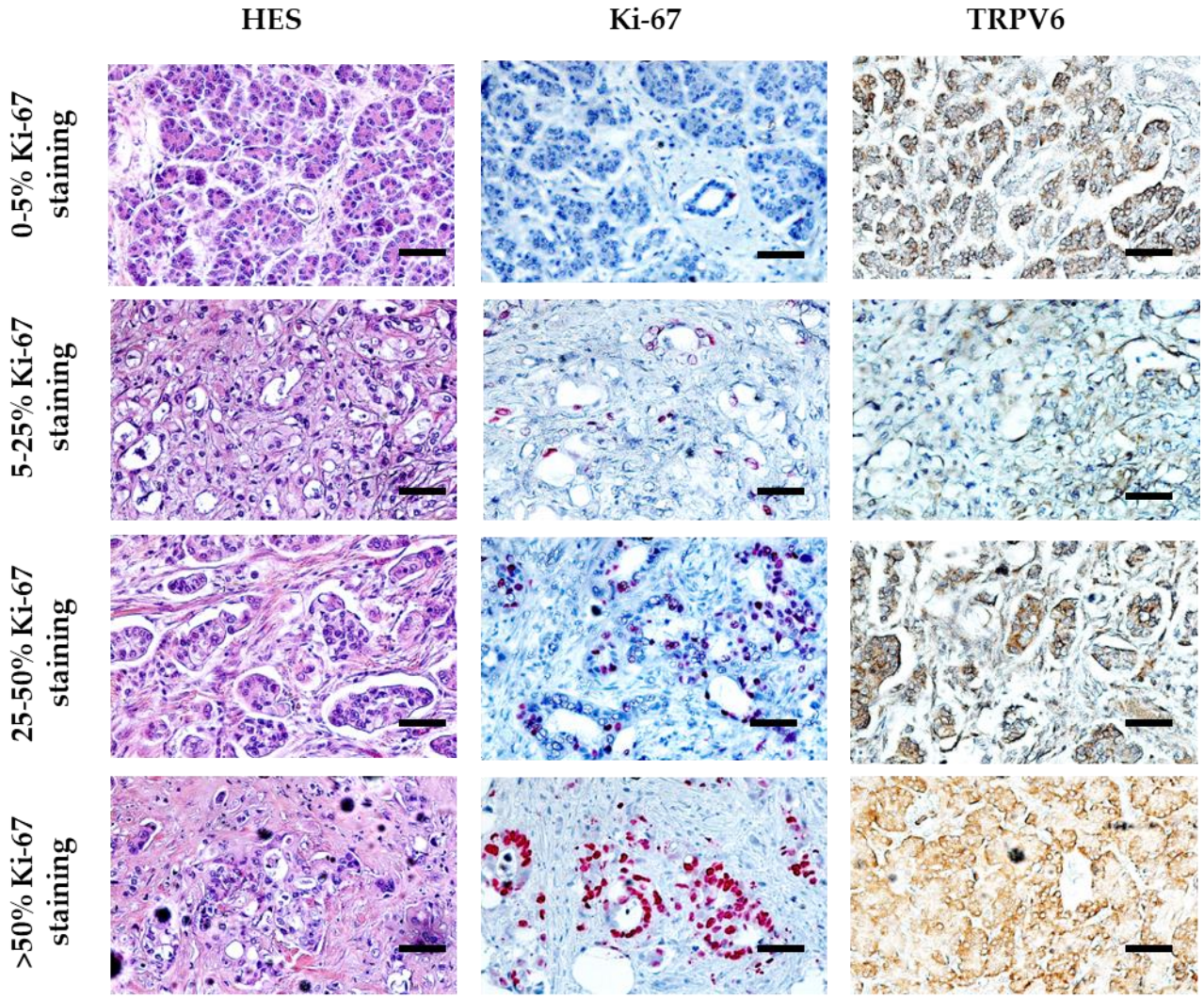

Figure 8 - **TRPV6 expression correlates with high Ki-67 staining.** PDAC tissue from patients with different proliferation levels. HES staining can be found in the left columns. TRPV6 staining is represented in the right columns, Middle column indicates Ki-67 staining. Rows are separated by different cell percentage with Ki-67 stainining. From top to bottom: 0-5%, 5-25%, 25-50% and >50%. Scale bars indicate 50 μm.

A trend was noticed for a rise in TRPV6 expression with increasing Ki-67 positivity (Fig.9C). It was significant for the group with >50% Ki-67 positive cells. The mean TRPV6 staining intensity for each group was as follows: 61.3 ± 9.7 for 0-5%, 72.2 ± 16.5 for 5-25%, 93.7 ± 16.2 for 25-50%, and 230 ± 30 for the group with >50% of Ki-67 positive cells. This suggests that TRPV6 expression is higher in highly proliferative PDAC tumour cells.

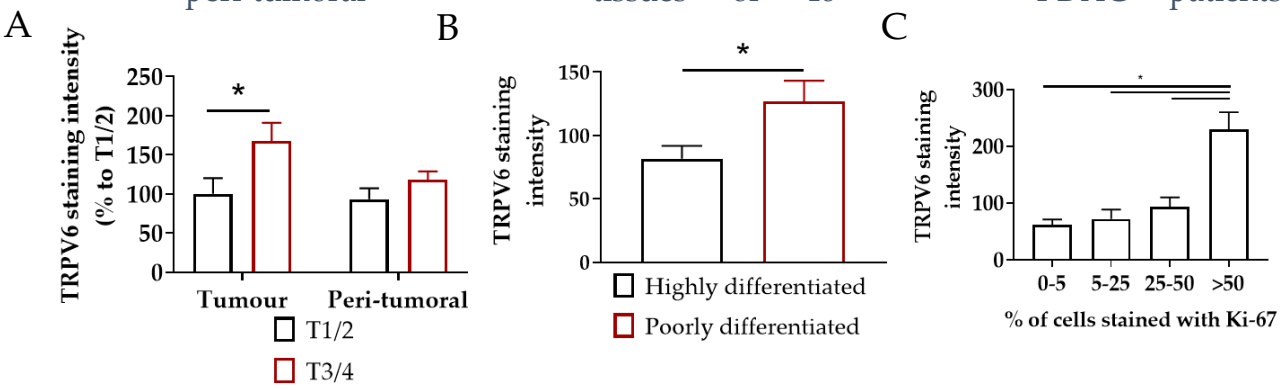

Figure 9 - **Quantification of TRPV6 staining in PDAC patients' tissues.** A) Tumoral and peri-tumoral tissues of 46 PDAC patients were divided into two groups according to their pathological stage (early T1/2 or late T3/4). TRPV6 staining intensities were normalized to the mean values of those found in stage I and II specimen. Error bars represent standard error of the mean of at least 3 independent tissues. Statistical significance was determined using t-test. $p<0.05$. B) Tissues were divided into two groups according to their differentiation. Data represents the TRPV6 staining analysis of the two groups. Error bars represent standard error of the mean of at least 3 patient tissues. Statistical significance was determined using an unpaired t-test. $p<0.05$. C) TRPV6 staining intensity as a function of the expression of the proliferation marker Ki-67. Error bars represent standard error of the mean of at least 3 independent tissues. Statistical significance was determined using one-way ANOVA, with Holm-Sidak method. $p<0.05$.

5.3. Characterization of Panc-1 and Capan-1 cells with altered TRPV6 expression.

Before starting my *in vitro* work, a TRPV6 scanning of different cell lines was used to understand TRPV6 expression in them. Western Blot was made in the following cell lines: BxPC-3, Panc-1, Capan-1, Colo357, MiaPaca-2, Aspc-1 and Capan-2 (Fig.10).

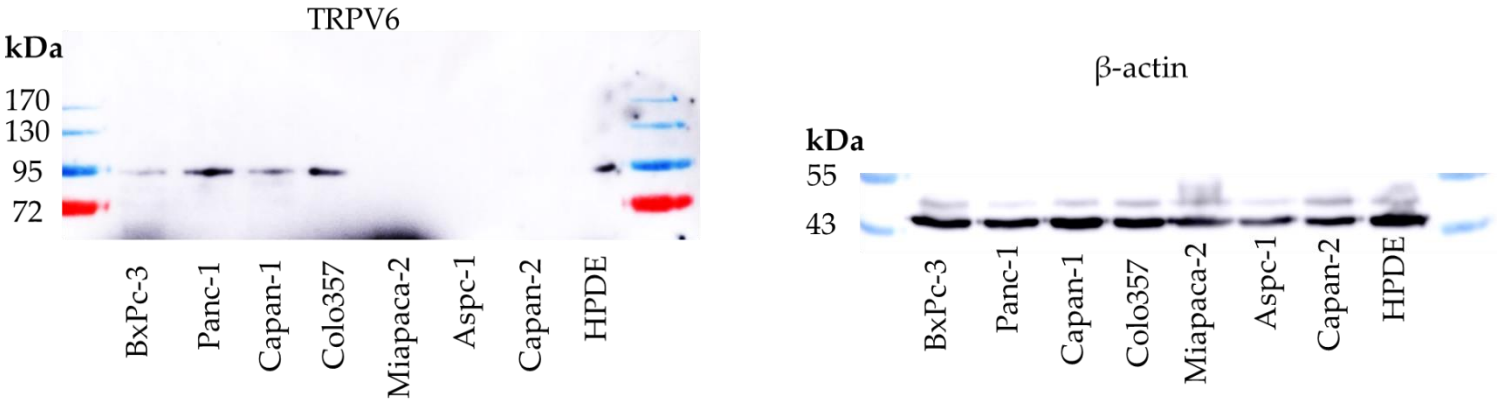

Figure 10 – **TRPV6 protein expression in different.** PDAC cell lines. The representative immunoblotting of the total lysates of the BxPc-1, Panc-1, Capan-1, Colon357, MiaPaca-2, Aspc-1, Capan-2 and HPDE cells revealed with mouse monoclonal anti-TRPV6 antibody Mab82 (left) and with mouse monoclonal anti-β-actin antibody (right).

I observed TRPV6 protein expression in four of the seven cell lines. The choice of cell lines to develop the *in vitro* studies was made in agreement with having TRPV6 expressed plus being known and commonly published cell lines. Panc-1 and Capan-1 were the cells chosen. In order to investigate the role of TRPV6 channels in mechanistic studies two groups of stable clones of both Panc-1 and Capan-1 cells were created: one with a knockdown of TRPV6 expression (Panc-1-shTRPV6 or Capan-1-shTRPV6) and one with an overexpression of TRPV6 (Panc-1-mCherry-TRPV6 or Capan-1-mCherry-TRPV6) (Fig.11). Each group had a control clone with normal TRPV6 expression (Panc-1[Capan-1]-shLuciferase or Panc-1[Capan-1]-mCherry) (Fig.11).

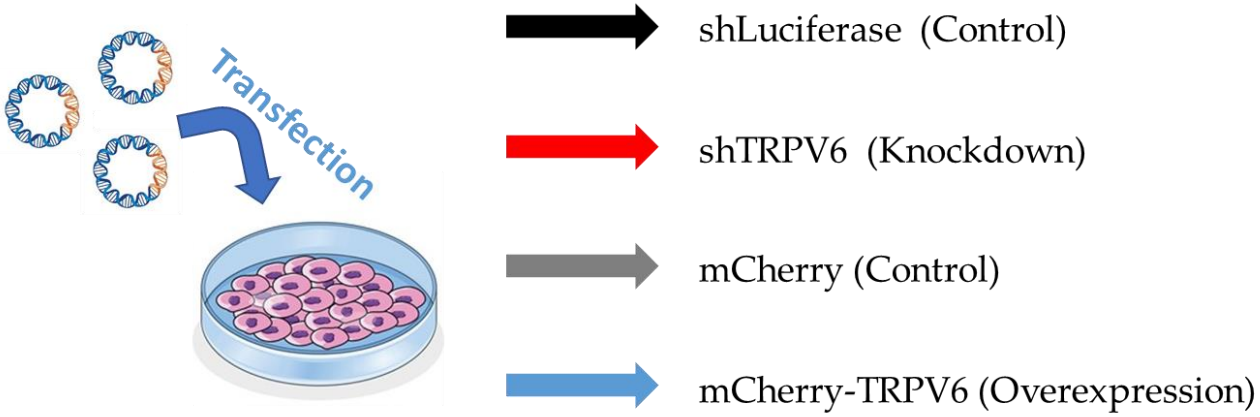

Figure 11 **- Representation of the different stable clones.** In order to investigate the role of TRPV6 channels in mechanistic studies two groups of stable clones of both Panc-1 and Capan-1 cells were created: one with a knockdown of TRPV6 expression (Panc-1-shTRPV6 or Capan-1-shTRPV6) (red colour) and one with an overexpression of TRPV6 (Panc-1-mCherry-TRPV6 or Capan-1-mCherry-TRPV6) (blue colour). Each group had a control clone with normal TRPV6 expression (Panc-1[Capan-1]-shLuciferase (black colour) or Panc-1[Capan-1]-mCherry (grey colour)).

The altered expression of TRPV6 channels was assessed in multiple ways. RNA sequencing analysis revealed the expected difference of the respective mRNA levels in Panc-1 cells. In here, Panc-1-shTRPV6 cells had a 60 fold decrease in TRPV6 expression compared to the control, whilst Panc-1-mCherry-TRPV6 had an increase of 8 fold comparing to the control (Fig.12A). Western blot demonstrated that the protein levels of the stable clones do translate to changes in protein level in Panc-1 cells (Fig.12B). Again here, Panc-1-shLuciferase cells had 40% less TRPV6 protein expression, while on the contrary, Panc-1-mCherry-TRPV6 had a 30% increase, when compared to the respective controls.

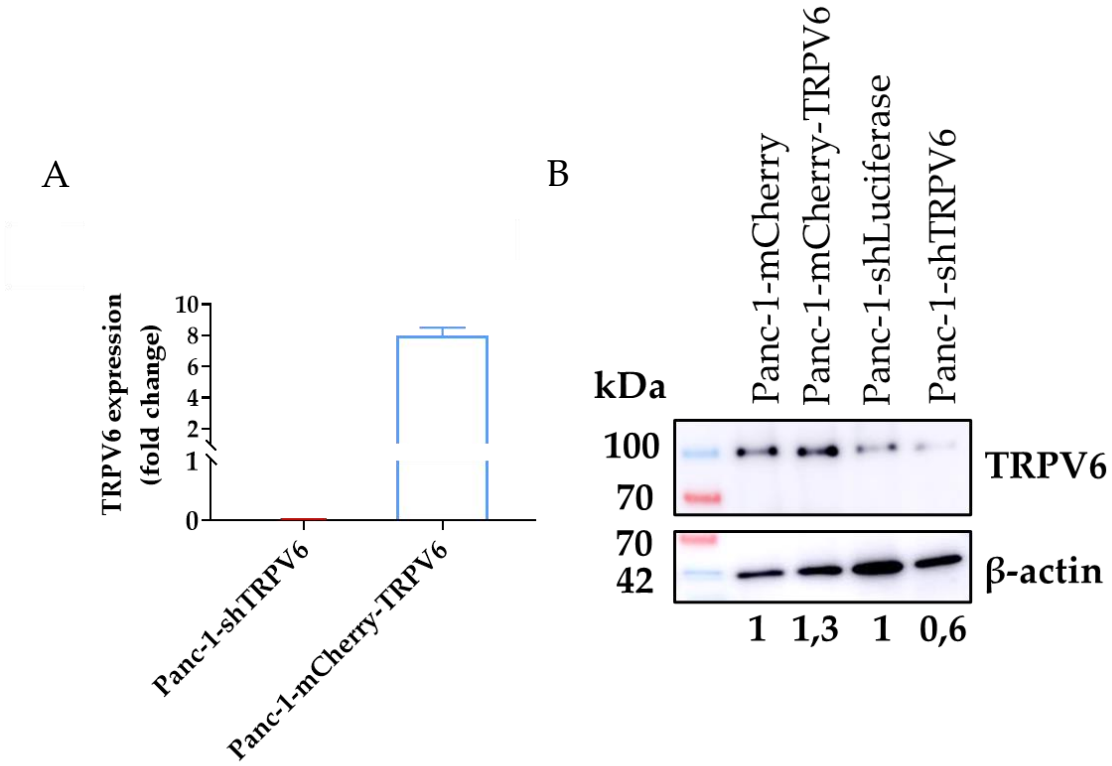

Figure 12 - **TRPV6 expression in the different Panc-1 stable clones.** A) Change of TRPV6 mRNA expression in the knockdown (red) and overexpression (blue) Panc-1 clones as determined by RNA sequencing. Changes were normalized to the respective control cell lines and results presented as fold-change. B) Representative immunoblot of whole cell lysates obtained from the stable Panc-1 clones. Channel expression is revealed with a mouse monoclonal anti-TRPV6 (top) or β-actin (bottom) antibody.

Moreover, the impact of altered TRPV6 expression on the Ca^{2+} influx into Panc-1 cells was assessed with the Mn^{2+} quench technique (Fig.13). It is based on the principle that Mn^{2+} enters the cells through similar pathways as Ca^{2+} and quenches the fluorescence of the Ca^{2+}-sensitive dye Fura2.

TRPV6 knockdown impairs the Ca^{2+} influx into Panc-1 cells, as the Mn^{2+}-induced decline of Fura2 fluorescence intensity occurs more slowly in Panc-1-shTRPV6 cells (0.05 $\Delta F/F_0$/min) than in control cells (0.34 $\Delta F/F_0$/min) (Fig.13C). No differences were found in the quench rate between the Panc-1-mCherry-TRPV6 (0.24 $\Delta F/F_0$/min) and the Panc-1-mCherry cells (0.27 $\Delta F/F_0$/min) suggesting that overexpressed TRPV6 channels are apparently not able to significantly impact the Ca^{2+} influx (Fig.13D).

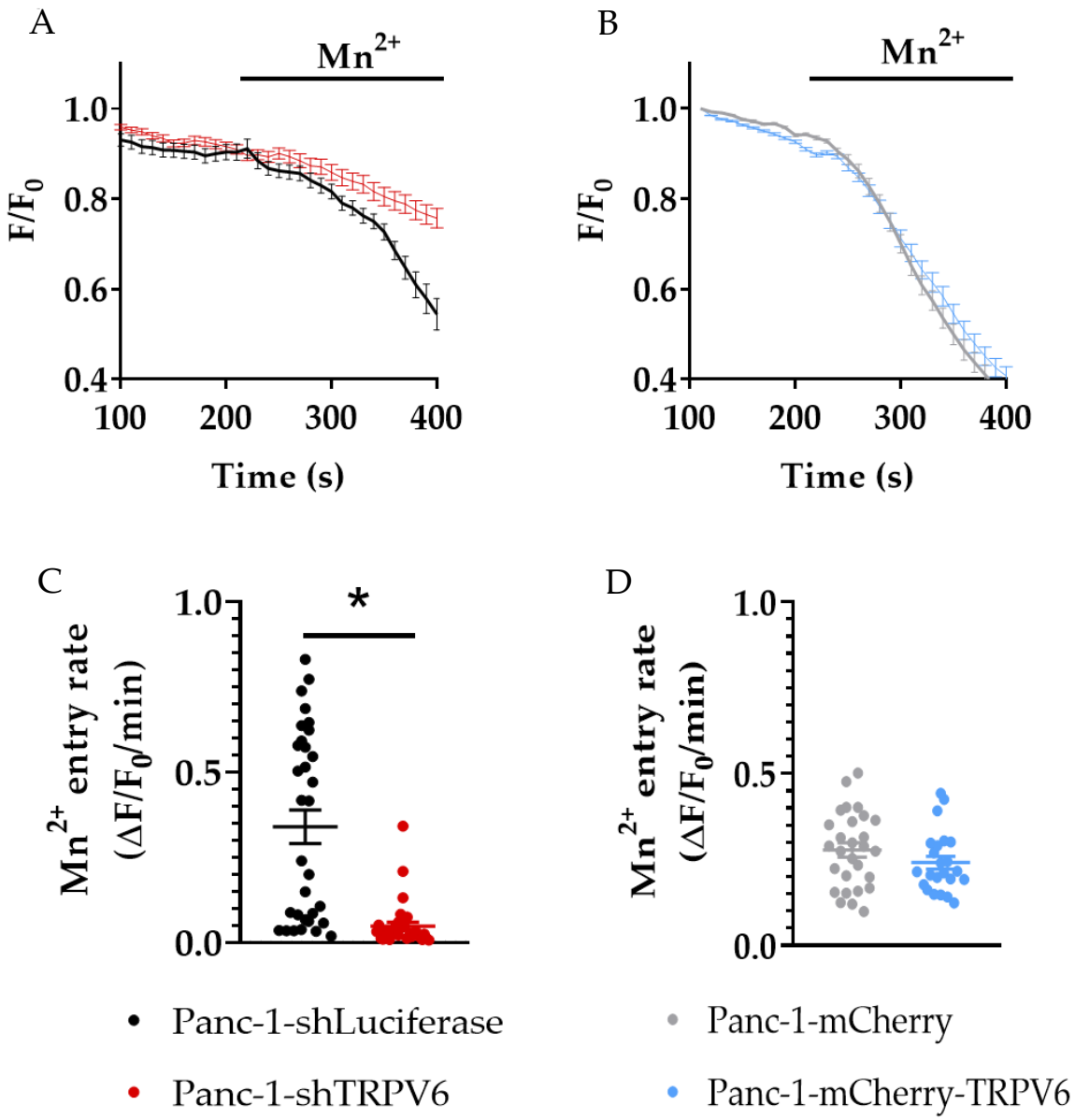

Figure 13 – **TRPV6 knockdown impairs calcium influx.** A and B) Graphical representation of Mn^{2+} quench experiments, evaluated as the fraction of the initial Fura2 fluorescence intensity. D) Panc-1-shLuciferase (black) and Panc-1-shTRPV6 (red); F) Panc-1-mCherry (grey) and Panc-1-mCherry-TRPV6 (blue). C and D) Summary of the Mn^{2+} quench experiments. The Mn^{2+} entry rate is calculated as the ratio of the slope of Fura2 fluorescence decline under control conditions and in the presence of Mn^{2+}. Error bars represent standard error of the mean of 3 replicates. Statistical significance was determined using an unpaired t-test. $p<0.05$.

TRPV6 levels in Capan-1 cells were assessed via RT-PCR (Fig.14). Similarly, to Panc-1 cells, in Capan-1-shTRPV6 cells TRPV6 expression is reduced 60 fold. On the other hand, the increase in expression of Panc-1-mCherry-TRPV6 was more than 50 fold. The results clearly demonstrate the strength of the chosen model. In both cell lines, stable transfection led to the knockdown or overexpression of TRPV6 confirmed in the desired groups. Furthermore, the impact of the knockdown of TRPV6 induced reduced Ca^{2+} channel activity in Panc-1-shTRPV6 cells.

Figure 14 - **TRPV6 expression in Capan-1 stable clones.** Change of TRPV6 mRNA

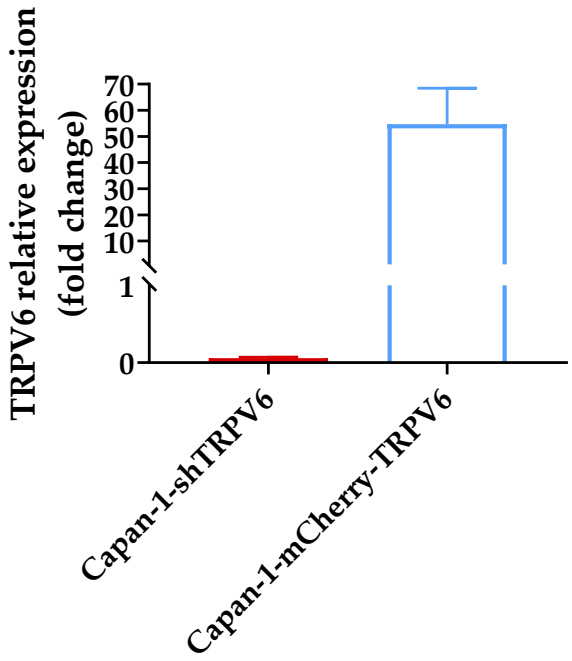

expression in the knockdown and overexpression Capan-1 clones as determined by qPCR. Fold change was obtained by comparing relative expression of TRPV6 between Capan1-shTRPV6 (red) and its control or Capan1-mCherry-TRPV6 (blue) and its control. Relative expression was calculated by 2-ΔΔCt after normalizing TRPV6 ct values to the ct values of the housekeeping gene GAPDH.

5.4. RNA sequencing of the stable clones

To elucidate the differences in the transcriptome on the different clones of Panc-1 an RNA sequencing was made. RNA sequencing (RNA-Seq) uses the capabilities of high-throughput sequencing methods to provide insight into the transcriptome of a cell. Using

Galaxy workflow, I've analysed and identified gene and pathways modified between the knockdown and overexpression groups and the respective controls. The ratio of the specific gene reads to the total reads in the sample indicated how much the gene was expressed.

Principal component analysis of RNA-seq data showed that the transcriptome differs significantly between Panc-1-shLuciferase and Panc-1-shTRPV6 (Figure 15A), and between Panc-1-mCherry and Panc-1-mCherry-TRPV6 (Figure15B).

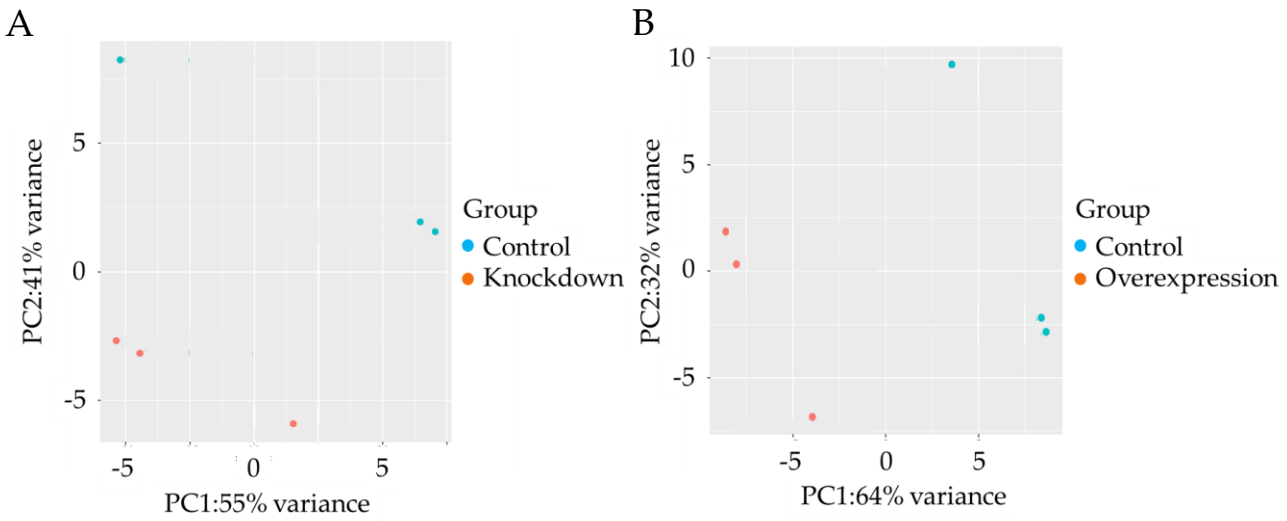

Figure 15 – **Principal component analysis between the stable clones.** Principal component analysis showing the overall transcriptomic similarity between A) Panc-1-shLuciferase (Control) and Panc-1-shTRPV6 (Knockdown) or B)Panc-1-mCherry (Control) and Panc-1-mCherry-TRPV6 (Overexpression).

The differential expression analysis was performed to determine transcriptomic changes induced by TRPV6-expression modulation in the different stable clones. Figure 16 represents the volcano plots of the transcripts with $|Log2FC| \geq 1$ (q value ≤ 0.05) in Panc-1-shLuciferase versus Panc-1-(PC1: 55% variance and PC2:41% variance) as well as in Panc-1-mCherry versus Panc-1-mCherry-TRPV6 (PC1:64% variance and PC2: 32% variance), demonstrating a clear differential transcriptome between the stable clones.

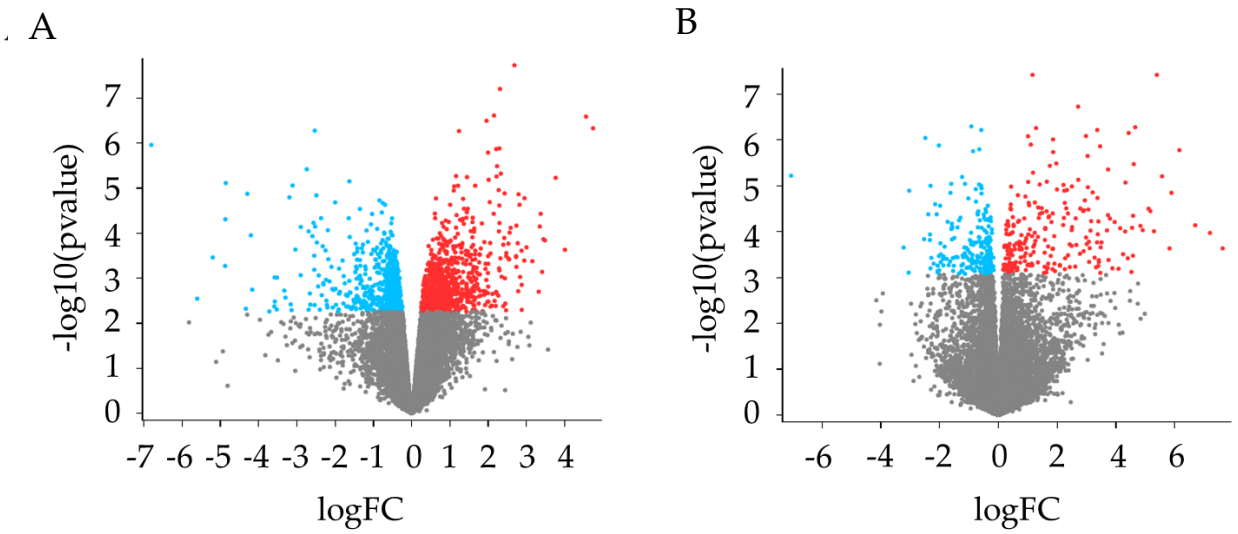

Figure 16 - **Representation of the volcano plots between the stable clones.** Volcano plots showing the differentially expressed genes (DEGs; Log2FC > 1 or < −1, false discovery rate adjusted p-value <0.05) between A) Panc-1-shLuciferase and Panc-1-shTRPV6 and between B) Panc-1-mCherry and Panc-1-mCherry-TRPV6.

The heatmaps of Figure 17 demonstrate the transcriptome changes between the different stable clones. A total of 1492 differentially expressed genes were found between Panc-1-shLuciferase and Panc-1-shTRPV6 (Fig.17A) and 476 between Panc-1-mCherry and Panc-1-mCherry-TRPV6 (Fig.17B). It does appear that transcriptome changes are more significant when knocking down TRPV6 instead of overexpressing it.

A

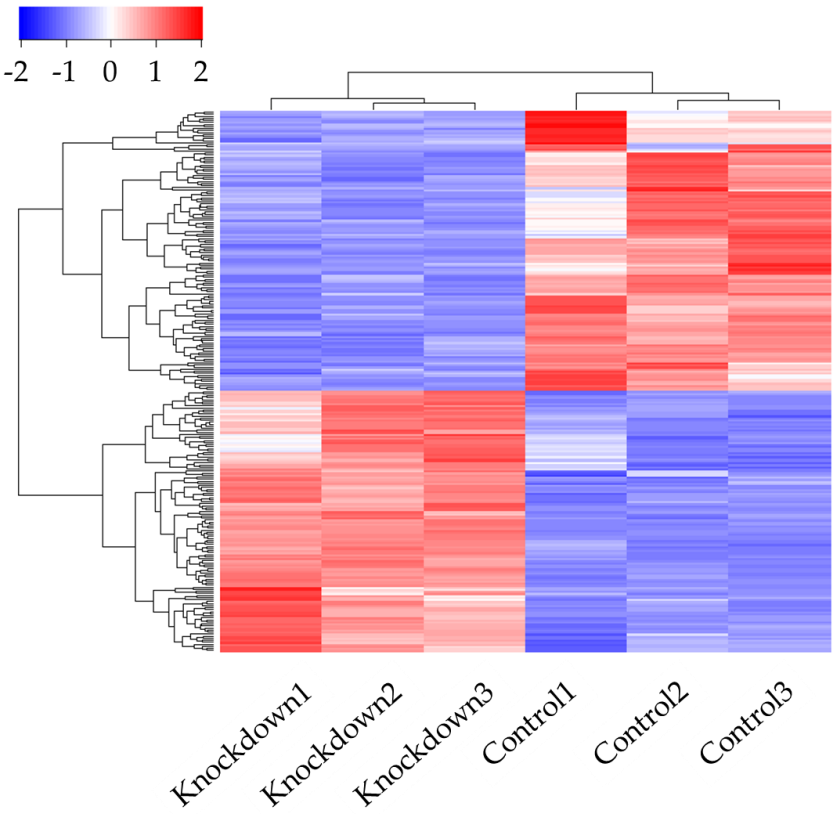
-2 -1 0 1 2
Knockdown1
Knockdown2
Knockdown3
Control1
Control2
Control3

B

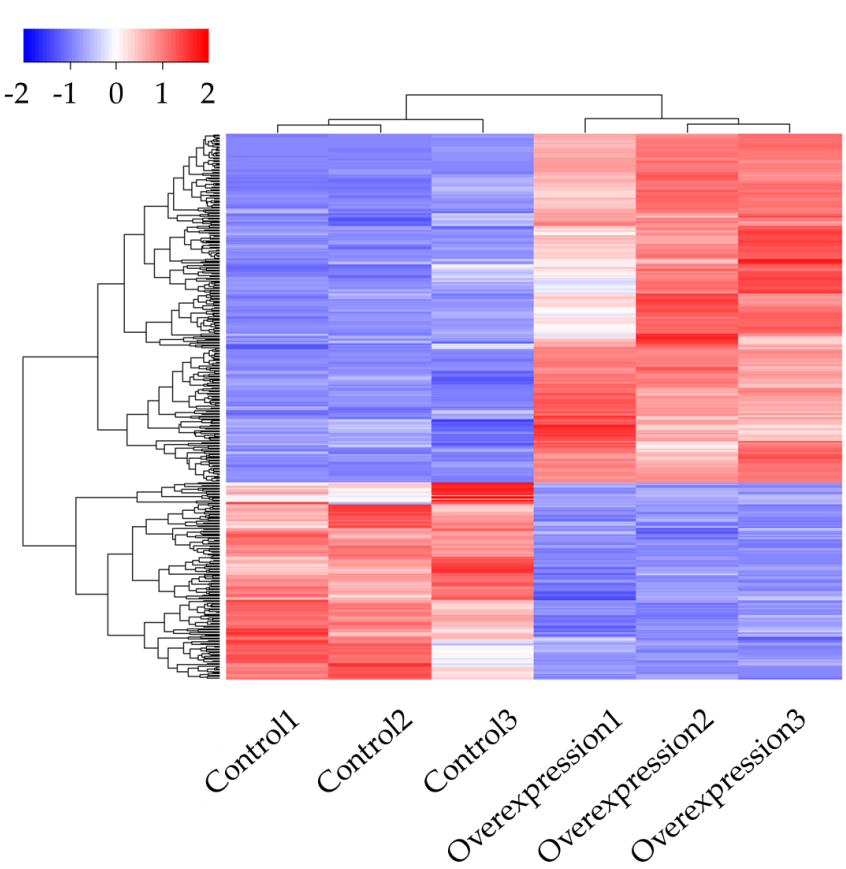
-2 -1 0 1 2
Control1
Control2
Control3
Overexpression1
Overexpression2
Overexpression3

Figure 17 – **Heatmaps showcasing the differential transcriptomics between the stable clones.** Heatmap indicating transcriptome changes between the 3 replicates of A) Panc-1-shLuciferase (Control) and Panc-1-shTRPV6 (Knockdown) or B)Panc-1-mCherry (Control) and Panc-1-mCherry-TRPV6 (Overexpression).

Pathways and Gene Ontology (GO) categories significantly modulated by TRPV6 overexpression or knockdown were identified. On the top over-represented categories for the knockdown versus control cells, we could find cell adhesion, cell migration, locomotion, between some extracellular categories and cell development (Fig.18A). On the other hand, in the overexpression group against the control, we can observe that the top most represented categories revolve around extracellular structures and vesicles (Fig.18B).

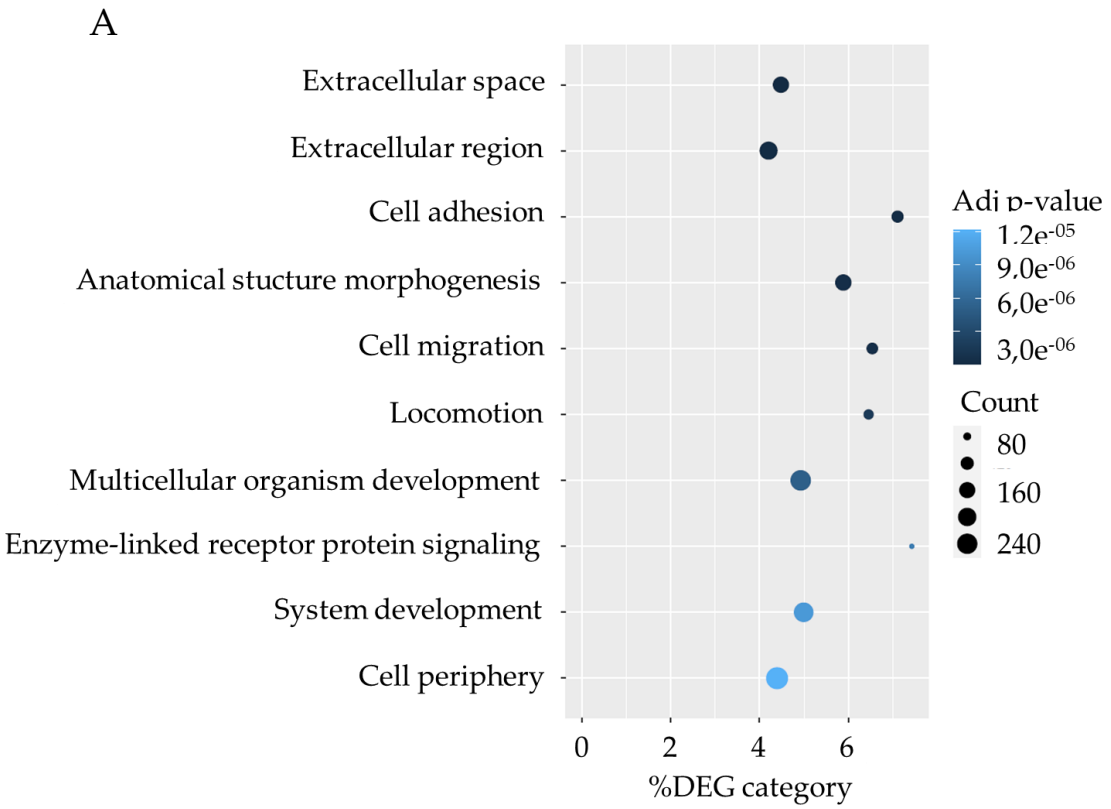

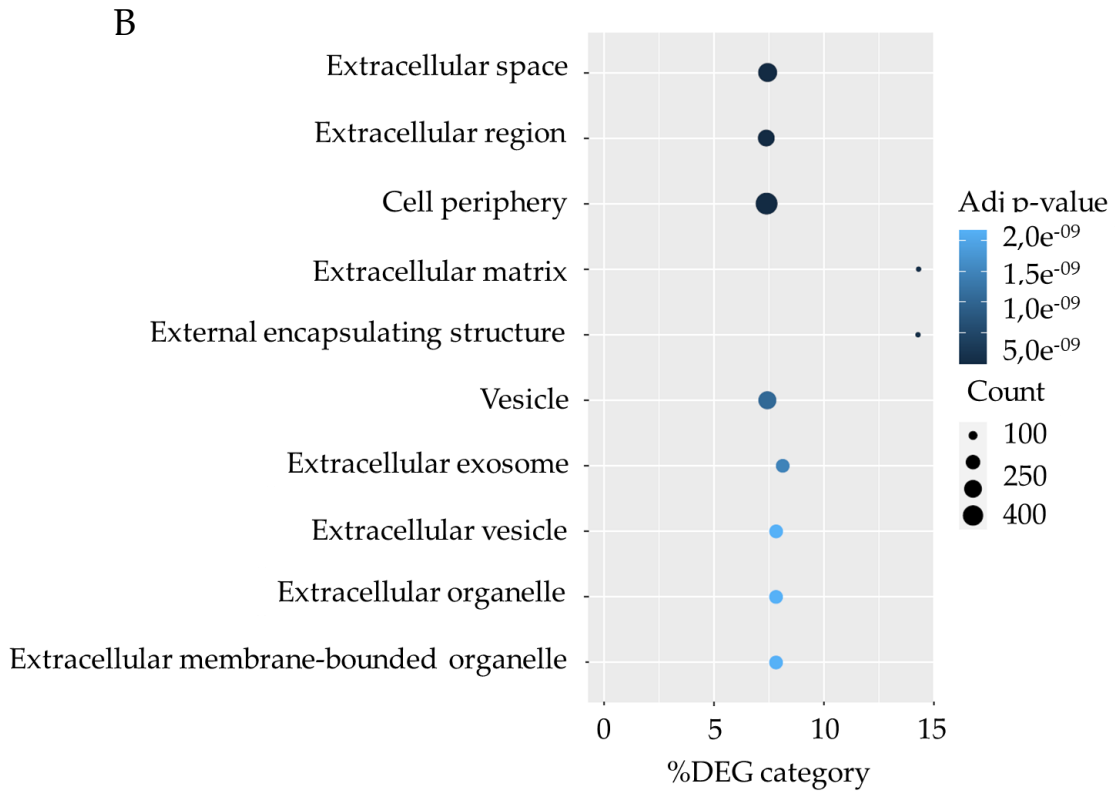

Figure 18 – **Functional enrichment analysis of the stable clones.** Functional enrichment analysis of the differentially expressed genes (terms of the top 10 over-represented categories) A) between Panc-1-shLuciferase and Panc-1-shTRPV6 or B) between Panc-1-mCherry and Panc-1-mCherry-TRPV6 Gene Ontology categories studied were Cellular Component, Biological Process and Molecular Function.

The hallmark signatures of Panc-1-shLuciferase versus Panc-1-shTRPV6 were examined (Fig.19A). Of interest, Panc-1-shTRPV6 has an up-regulation of genes down-regulated by KRAS activation. On the other hand, it was observed that genes responsible for angiogenesis are down-regulated. Other main differentiated hallmark genes were down-regulated genes in response to UV, genes involve in metabolism of bile acids and salts and genes defining early response to oestrogen. From the most differentiated cluster of genes (genes down-regulated by KRAS activation) a significant up-regulation could be seen in the knockdown group to the expression of *tfcpl1*, *edn1*, *htr1d*, *kcnd1* and *fggy* (Fig.19B). There was also a down-regulation in the expression of *fgfr3*, *wnt16*, *cyp39a1*, *slc16a7* and *thrb*.

A

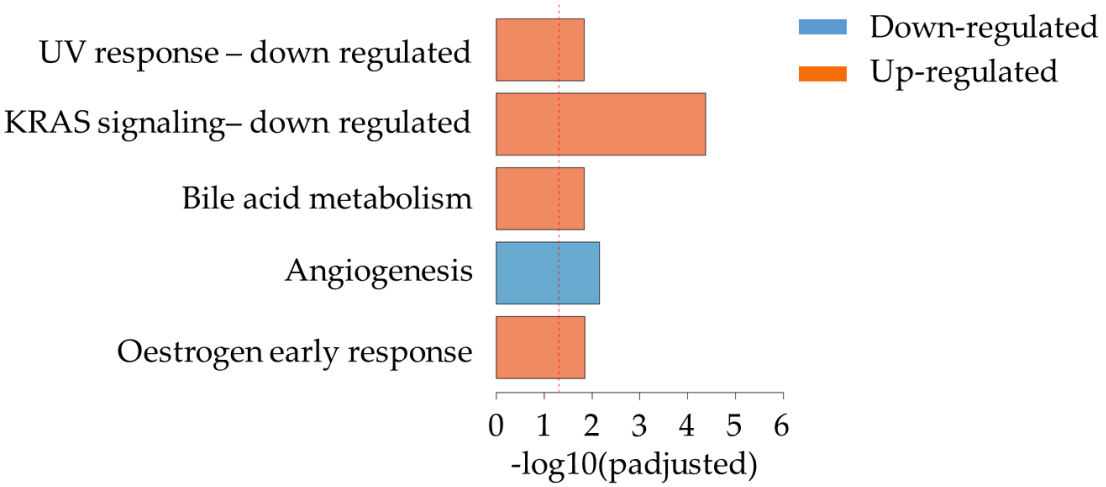

B

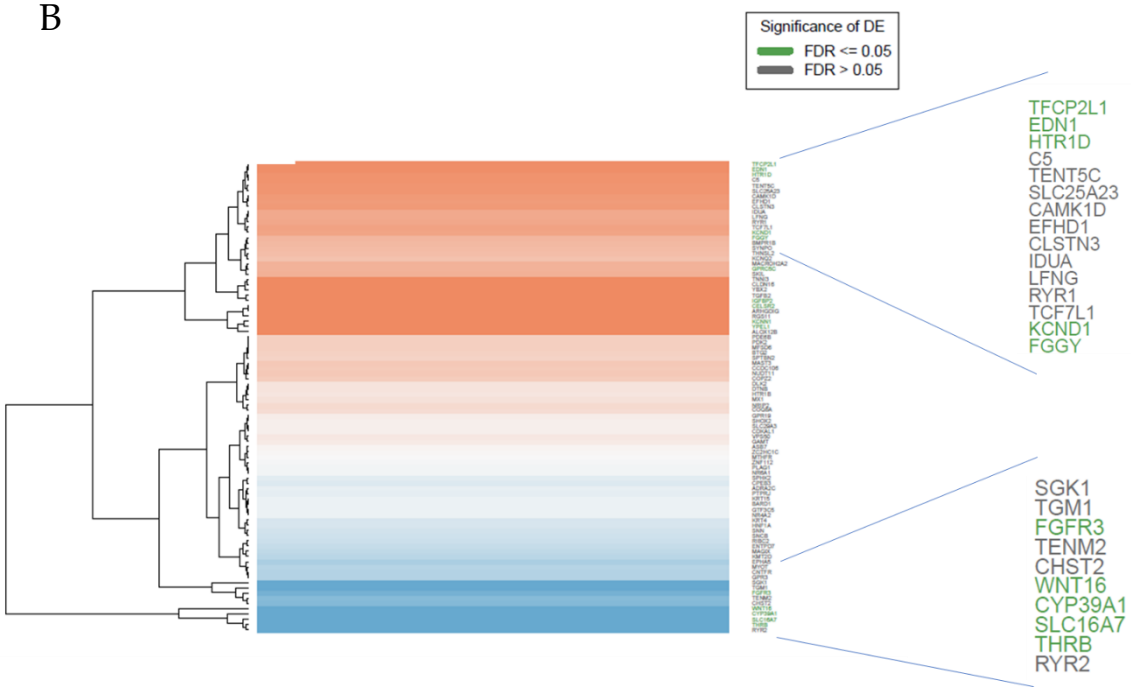

Figure 19 – **Hallmark signatures of functional clustering of genes for the knockdown group and the respective heatmap of KRAS signalling – down regulated genes.** A) Hallmark signatures of functional clustering of genes that were up or down regulated between Panc-1-shLuciferase and Panc-1-shTRPV6. B) Main genes involved in the epithelial-mesenchymal transition in Panc-1-shLuciferase and Panc-1-shTRPV6.

After analysing the knockdown group, it was the turn of Panc-1-mCherry and Panc-1-mCherry-TRPV6 (Fig.20A). The most up-regulated hallmark gene clusters are the ones involved in EMT. Opposite to the knockdown, overexpression led to an up-regulation of genes responsible for angiogenesis. Other main differentiated hallmark genes were genes up-regulated in response to interferon alpha and gamma. From the most differentiated cluster of genes (genes involved in EMT), it could be observed a significant up-regulation in the overexpression group to the expression of *postn*, *col4a2*, *col4a1*, *col3a1*, *mmp1*, *edil3*, *dpysl3*, *crlf1*, *col5a2*, *ptx3*, *nid2*, *igfbp2*, *gja1*, *prrx1*, *bdnf*, *lama2*, *col11a1*, *tnfrsf11b* and *mmp14* (Fig.20B). There was also a down-regulation in the expression of *mylk*, *sparc*, *thbs1*, *tnc*, *fstl1*, *loxl1*, *tfgbi*.

A

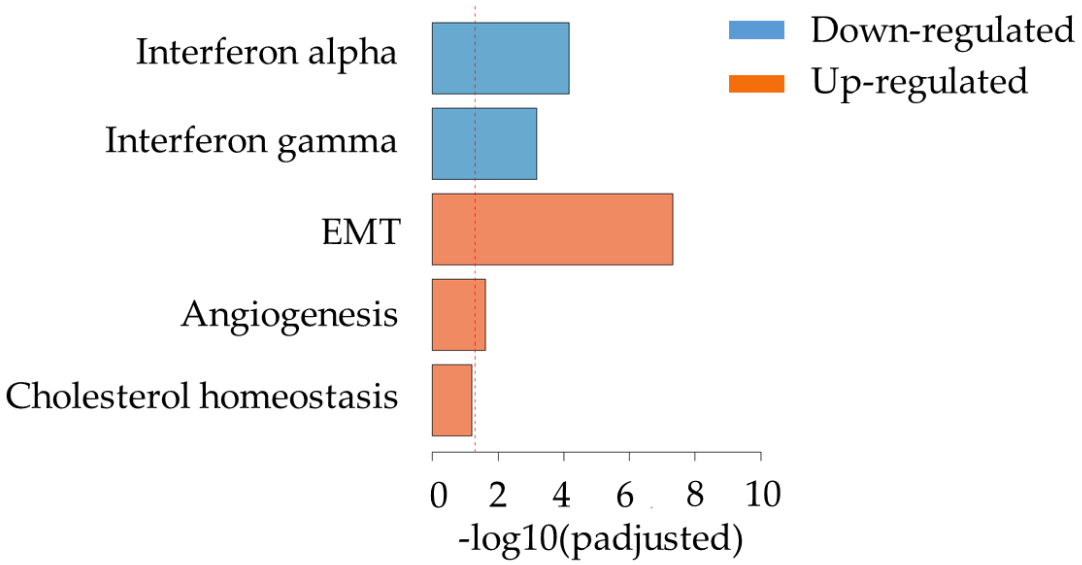

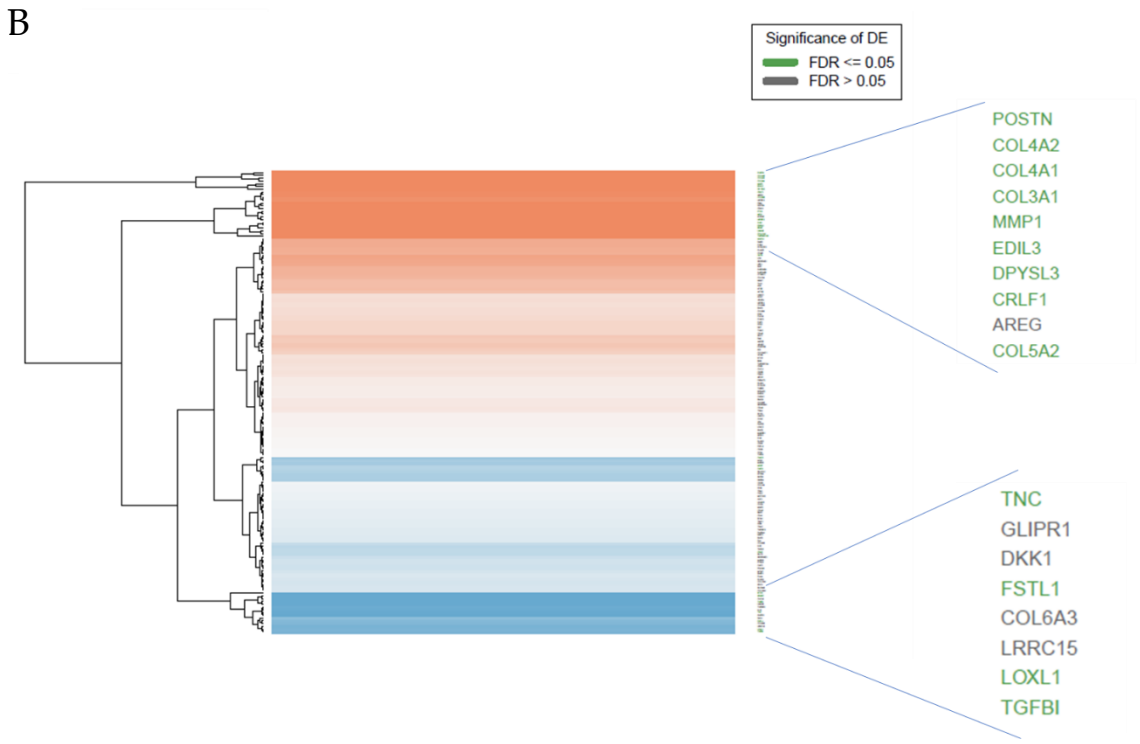

Figure 20 - **Hallmark signatures of functional clustering of genes for the overexpression group and the respective heatmap of EMT involved genes.** A) Gene Ontology (GO) functional clustering of genes that were up or down regulated between Panc-1-mCherry and Panc-1-mCherry-TRPV6. B) Main genes involved in the epithelial-mesenchymal transition in Panc-1-mCherry and Panc-1-mCherry-TRPV6.

5.5. TRPV6 knockdown impairs proliferation, cell survival and cell cycle progression of Panc-1 and Capan-1 cells.

The effect of TRPV6 expression on the proliferation of Panc-1 cells was assessed by counting the cell numbers at t = 0h, 24 h and 48 h after seeding. Panc-1-shTRPV6 cells grew more slowly than Panc-1-shLuciferase cells (186 ± 2.6% vs. 217 ± 6.5% at t = 48 h) (Fig.21A). Conversely, Panc-1-mCherry-TRPV6 grew faster than the Panc-1-mCherry cells (215 ± 10.4% vs. 155 ± 20.7% at t = 48 h) (Fig.21B). To ensure that these results are not affected by cell death or cell migration, the cumulative mitosis that occurred during the experiment were counted

(Fig.21C and D). These results indicate that TRPV6 expression enhances the proliferation of Panc-1 cells.

Figure 21 - **TRPV6 regulates Panc-1 proliferation.** A and B) Proliferation of stable Panc-1

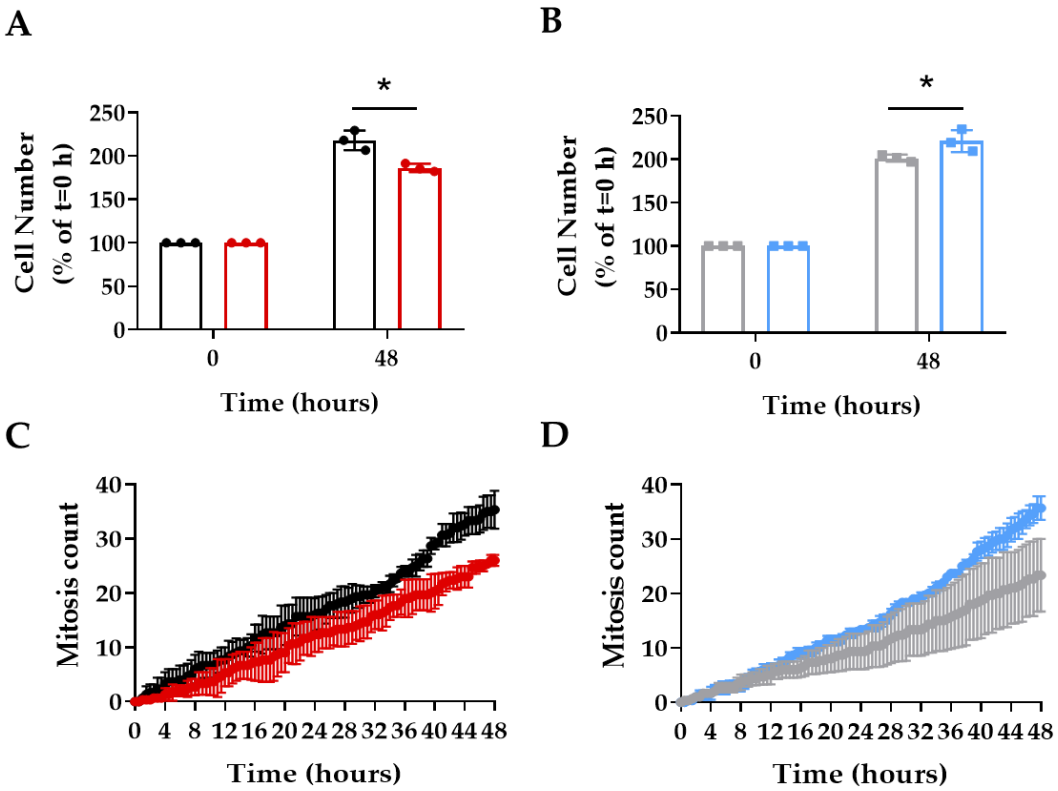

cell clones Panc-1-shLuciferase (black) and Panc-1-shTRPV6 (red), Panc-1-mCherry (grey) and Panc-1-mCherry-TRPV6 (blue), 48 hours after seeding. Data are expressed as percentage of cell number compared to initial seeding density. Error bars represent standard error of the mean of three replicates. Statistical significance determined using an unpaired t-test *$p < 0.05$. C and D) Mitosis count throughout 48 hours between stable Panc-1 cell clones Panc-1-shLuciferase (black) and Panc-1-shTRPV6 (red), Panc-1-mCherry (grey) and Panc-1-mCherry-TRPV6 (blue).

I have also assessed whether the differences in TRPV6 expression influence cell viability, by measuring its impact on the intracellular ATP concentration of our Panc-1 cell lines using CellTiter-Glo assay at 24, 48, 72, and 96 h after seeding. Panc-1-shTRPV6 cells had significantly lower ATP levels than the Panc-1-shLuciferase cells after 48 h and throughout the remaining of the experiment (Fig.22A). On the other hand, there was no difference in ATP levels between the Panc-1-mCherry-TRPV6 group and the Panc-1-mCherry group at any time point (Fig.22B).

Figure 22 - **Knockdown of TRPV6 leads to lower viability levels in Panc-1.** Cell viability

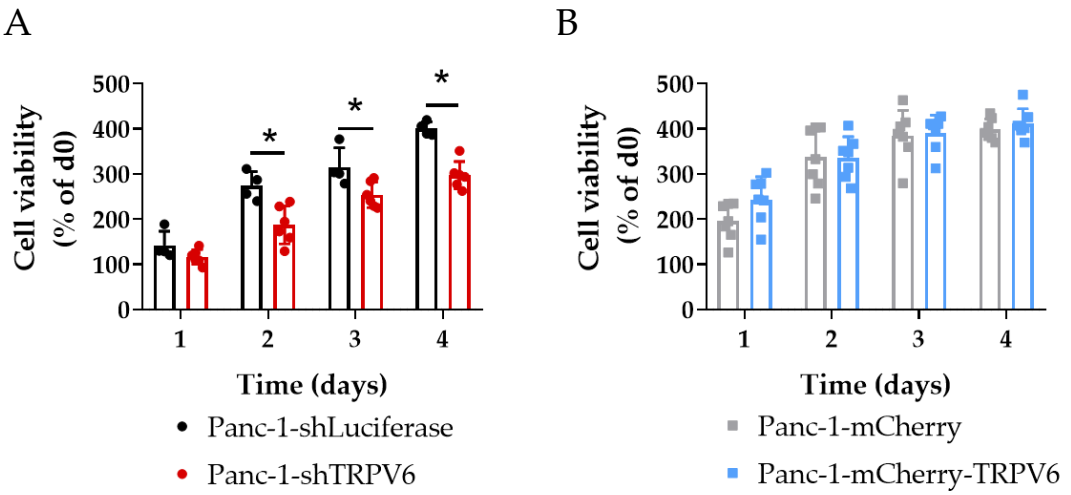

through ATP concentration between A) Panc-1-shLuciferase (black) and Panc-1-shTRPV6 (red) or B) Panc-1-mCherry (grey) and Panc-1-mCherry-TRPV6 (blue) at 24, 48, 72, and 96 hours after seeding measured by CellTiter-Glo assay. Data are expressed as percentage of daily luminescence from CellTitter, normalized to the initial luminescence values. Error bars represent standard error of the mean of 4-6 replicates. Statistical significance determined using using 2-way-ANOVA with Holm-Sidak method *$p < 0.05$.

These results were also similar in Capan-1 cells. Proliferation levels were dependent on TRPV6 expression. Similarly to Panc-1 cells, in Capan-1 cells, knockdown of TRPV6 led to lower proliferation rates (321 ± 35% vs 194 ± 28%), as opposed to the overexpression of TRPV6 that generated higher proliferation rates (185 ± 20% vs 279 ± 20%) (Fig.23A and B). Furthermore, cell viability was also impacted by TRPV6 expression. Capan-1-shTRPV6 had significantly lower viability levels from the third day onwards (Fig.23C and D).

Figure 23 - **TRPV6 regulates Capan-1 proliferation and viability.** A and B) Proliferation of

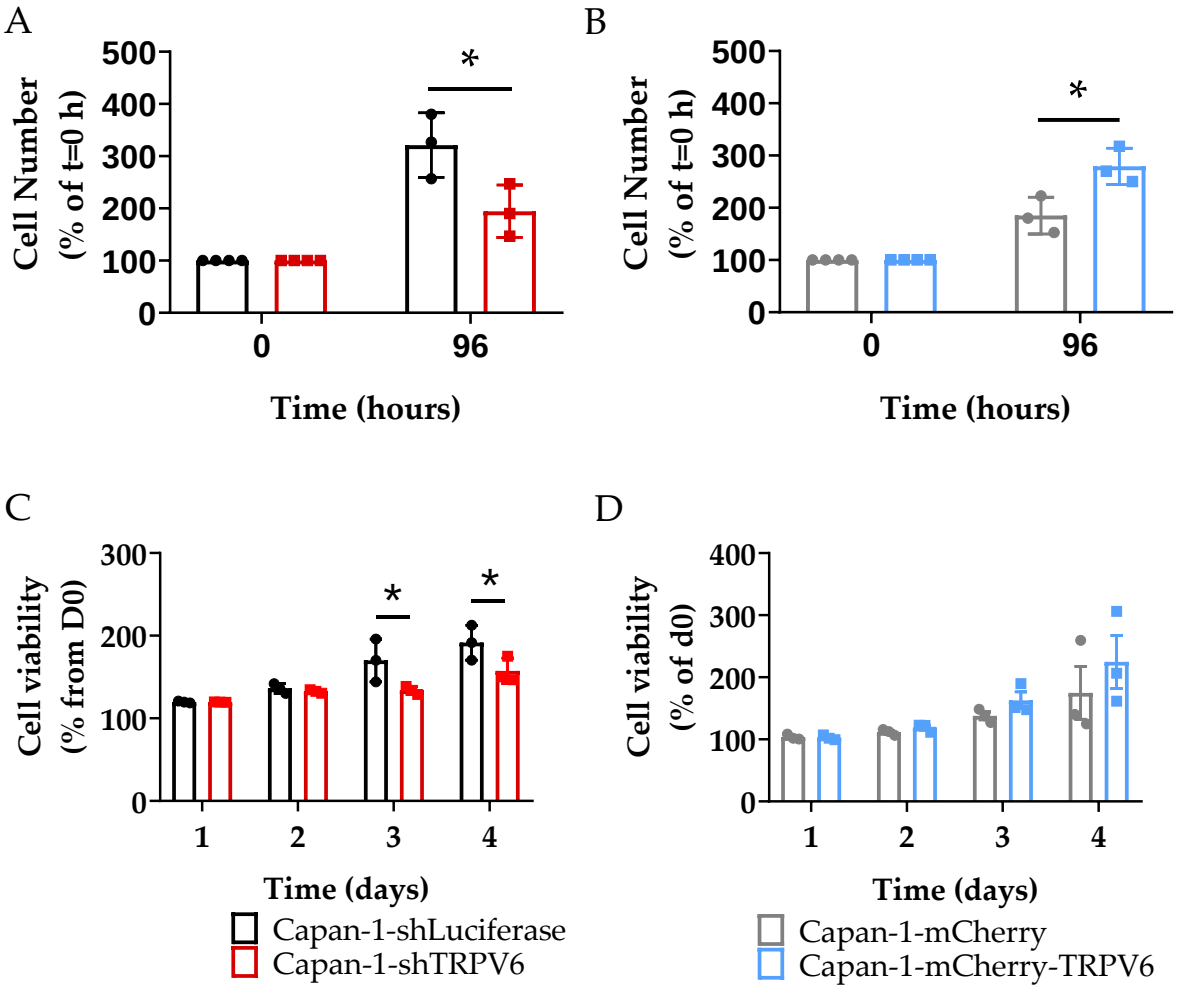

stable Capan-1 cell clones Capan-1-shLuciferase (black) and Capan-1-shTRPV6 (red), Capan-1-mCherry (grey) and Capan-1-mCherry-TRPV6 (blue), 48 hours after seeding. Data are expressed as percentage of cell number compared to initial seeding density. Error bars represent standard error of the mean of three replicates. Statistical significance determined using an unpaired t-test *$p < 0.05$. Cell viability through MTS of the four stable clones at 24, 48, 72, and 96 hours after seeding. Data are expressed as percentage of daily absorbance from MTS reaction, normalized to the initial luminescence values. Error bars represent standard error of the mean of three replicates. Statistical significance determined using unpaired t-test *$p < 0.05$.

The effects of TRPV6 channel expression on cell cycle progression were assessed, by using propidium iodide staining and flow cytometry, in Panc-1 cells. The main focus of this experiment was on the sub-G1 phase of the cell cycle, which corresponds to the fraction of cells with fragmented DNA indicating cell death (Fig.24).

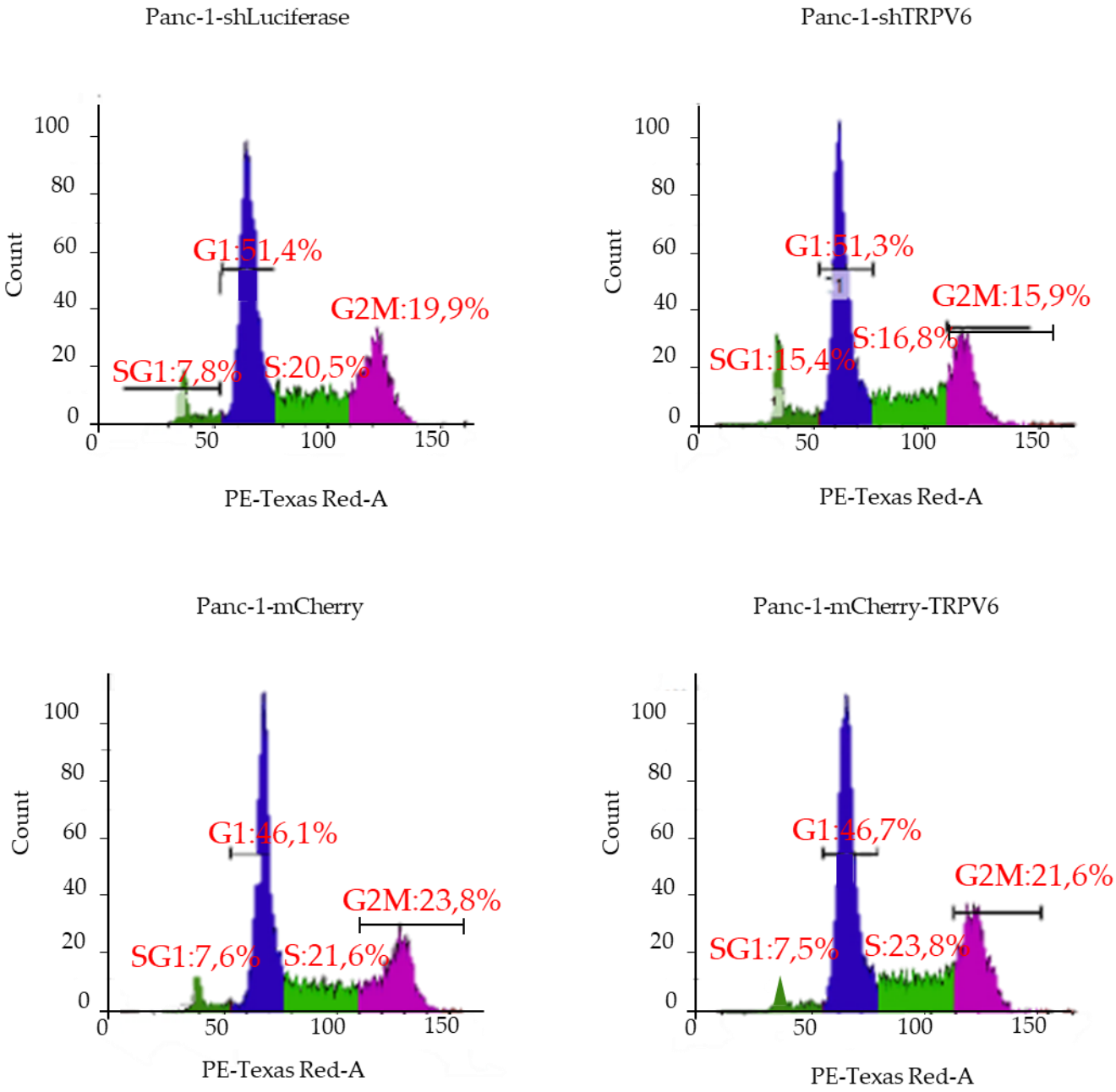

Figure 24 - **Cell cycle assay of the stable clones.** Representative histogram depicting the cell cycle phases of Panc-1-shLuciferase (top left) and Panc-1-shTRPV6 (top right), Panc-1-mCherry (bottom left) and Panc-1-mCherry-TRPV6 cells (bottom right) determined with propidium iodide staining and flow cytometry. Histograms are divided into four groups: SG1 (sub G1), G1, S and G2M (G2 and M phases). Y axis indicates the number of cells whilst X axis indicates staining intensity (DNA quantity).

There was a higher percentage of Panc-1-shTRPV6 than Panc-1-shLuciferase cells in the sub-G1 phase (10.8 ± 1.1% vs. 7.8 ± 0.3%) (Fig.25A). This suggests that TRPV6 knockdown triggers apoptosis of Panc-1 cells. Conversely, there was no difference in the sub-G1 phase between Panc-1-mCherry-TRPV6 and Panc-1-mCherry cells (6.5 ± 0.8% vs. 6.6 ± 0.4%) (Fig.25B) indicating that TRPV6 overexpression does not affect cell cycle progression of Panc-1 cells.

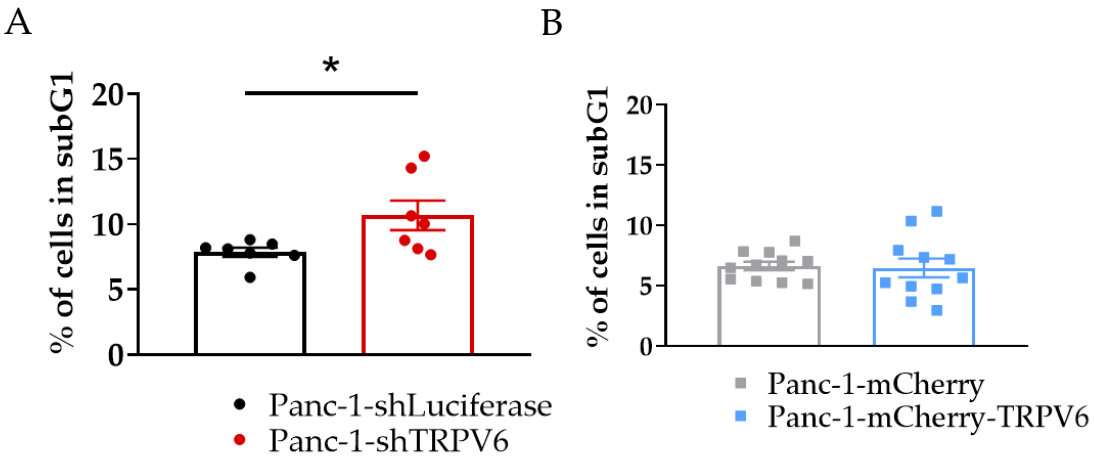

Figure 25 - **Knockdown of TRPV6 leads to cell cycle arrest.** Quantification of cells in the sub-G1 phase, which represents apoptotic cells, between A) Panc-1-shLuciferase (black) and Panc-1-shTRPV6 (red) or B) Panc-1-mCherry (grey) and Panc-1-mCherry-TRPV6 (blue). Error bars represent standard error of the mean of 7-11 replicates. Statistical significance was determined with unpaired t-test *p < 0.05.

5.6. TRPV6 increases Panc-1 resistance to chemotherapeutics.

Observing the low viability and high percentage of cells in the sub-G1 phase in Panc-1-shTRPV6, knockdown of TRPV6 makes cells more susceptible to cell death. This can be an interesting factor in chemoresistance. PDAC chemotherapeutical treatments are usually ineffective, mostly due to the dense stroma covering the tumour (Tiwari and Kumar 2018). To study the effect of TRPV6 expression in chemoresistance, ATP assay to assess cell viability and Annexin V to investigate apoptosis have been performed. I tested the effect of TRPV6 expression on the resistance of Panc-1 cells to gemcitabine, cisplatin and 5-

fluorouracil (5-FU). These drugs are often used in the therapy of pancreatic cancer. Cells were exposed to different concentrations of these agents for 96 h for ATP assay and 24 hours for annexin V.

First, the intracellular ATP concentration of the clones was assessed as a measure of cell viability (Fig.26). It was observed that TRPV6 knockdown makes Panc-1 cells more sensitive to 5-FU treatment, as the Panc-1-shTRPV6 cells have lower ATP levels than the control cells (Panc-1-shLuciferase) after treatment with 1 (234 ± 29 versus 165 ± 30) and 10 μM (222 ± 29 versus 133 ± 20) of 5-FU for 96 h (Fig.23C). This indicates that TRPV6 may provide resistance to 5-FU in pancreatic cancer cells. On the other hand, there was no difference in ATP levels between the TRPV6 overexpressing cells (Panc-1-mCherry-TRPV6) and the control cells (Panc-1-mCherry) under any treatment given. Furthermore, there was a trend for the Panc-1-shTRPV6 cells to have lower ATP levels than the Panc-1-shLuciferase group after 96 h of treatment with higher concentrations of gemcitabine (10μM – 235 ± 24 versus 182 ± 44) or cisplatin (10μM – 172 ± 52 versus 101 ± 26). This suggests that TRPV6 knockdown might also affect the resistance of Panc-1 cells to gemcitabine or cisplatin.

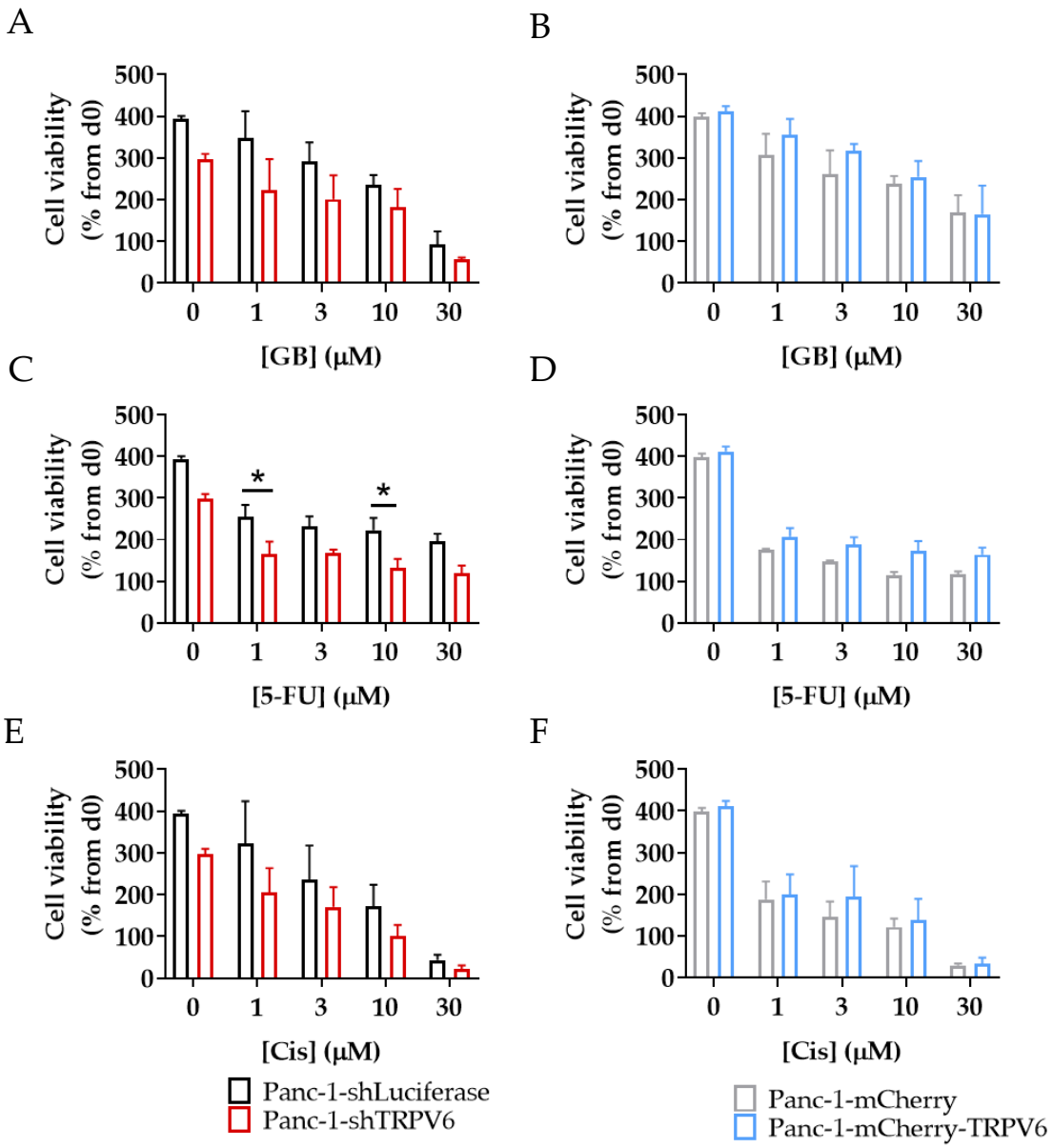

Figure 26 - **TRPV6 knockdown sensitizes Panc-1 cells to 5-FU.** ATP concentration of Panc-1-shLuciferase (black) and Panc-1-shTRPV6 (red), Panc-1-mCherry (grey) and Panc-1-mCherry-TRPV6 cells (blue) after 96 h of treatment with chemotherapeutics, measured by CellTiter-Glo assay. Stable clones were treated with different concentrations (1, 3, 10 and 30 μM) of A and B) gemcitabine (GB), C and D) 5-fluorouracil (5-FU) and E and F) cisplatin (Cis). Error bars represent standard error of the mean of 4-6 replicates. Statistical significance determined using 2-way ANOVA with Holm-Sidak method *$p < 0.05$.

To investigate whether the expression level of TRPV6 channels affects apoptosis of Panc-1 cells induced by chemotherapeutic agents, Annexin V assay was used. Annexin V binding was measured to detect the early apoptosis of the cells that were exposed to gemcitabine, cisplatin and 5-FU for 24 h. The acquired images were processed and after

background subtraction, quantification of the cellular fluorescence intensity on FITC channel (arbitrary units) was performed on 10 cells per visual field (Fig. 27).

Figure 27 - **Annexin V assay done to the stable clones.** Representative images of Annexin

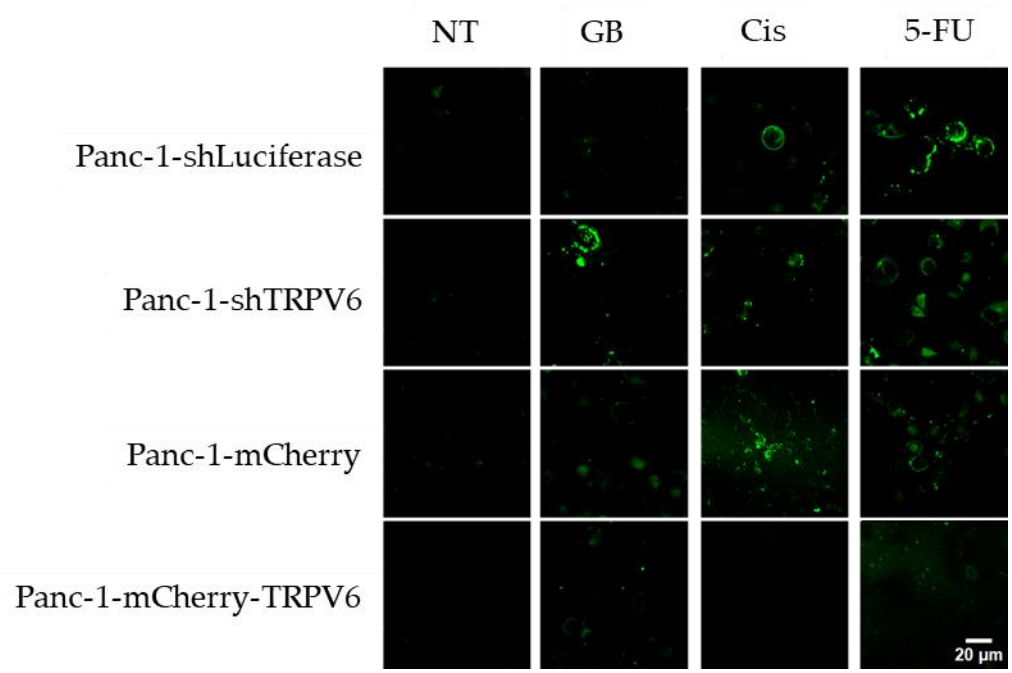

V staining for the stable clones without treatment (NT) and treated with 3 µM of gemcitabine (GB), cisplatin (Cis) or 5-FU, after 24 hours. Scale bar represents 20 µm.

It was observed that TRPV6 knockdown enhances apoptosis of Panc-1 cells in response to 5-FU and gemcitabine treatment as Panc-1-shTRPV6 cells bind more annexin V than the Panc-1-shLuciferase cells, when comparing to the non-treated group (GB: 49 ± 10 versus 169 ± 32% and 5-FU: 226 ± 23% versus 316 ± 35%) (Fig28A). This supports the idea that TRPV6 may confer resistance to 5-FU and, possibly, gemcitabine in pancreatic cancer cells. It was not seen any increase in annexin V binding in TRPV6 overexpressing cells under any of the treatments (Fig.28B). Taken together, these results indicate that TRPV6 expression might modulate chemotherapeutics impact in PDAC treatment. Interestingly, overexpression of TRPV6 did not affect the impact of chemotherapeutics in Panc-1 cells.

Figure 28 - **Chemotherapeutics efficiency increases with TRPV6 knockdown.** Differences in annexin V staining between stable Panc-1 cell clones Panc-1-shLuciferase (black) and Panc-1-shTRPV6 (red), Panc-1-mCherry (grey) and Panc-1-mCherry-TRPV6 (blue). Data are expressed as the percentage of annexin staining intensity, compared to the non-treated

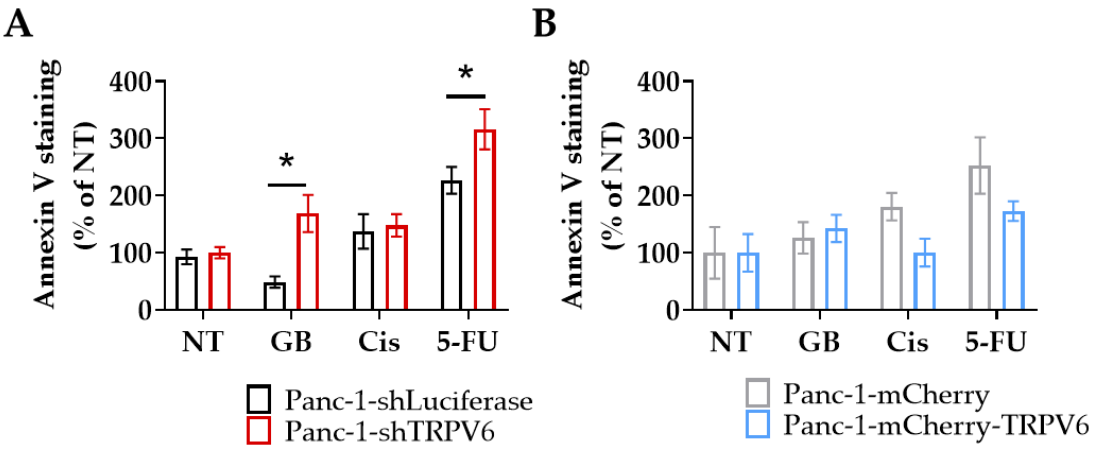

group. Each replicate has the mean value of 10 cells per field in 7 fields evaluated. Error bars represent standard error of the mean of 3 replicates. Statistical significance was determined using 2-way ANOVA with Holm-Sidak method. *p < 0.05.

5.7. (Collective) migration of Panc-1 cells depends on TRPV6 channel expression.

Since several alterations in migration related genes were observed, in the RNA-seq, I focused on understanding what the effects of TRPV6 expression modulation are in the migration of Panc-1 cells.

I have then tested the effect of TRPV6 expression on the migration of Panc-1 cells, by using wound healing assays and tracking the closure of the cell layer during a 20 h period (Fig.29).

Figure 29 -

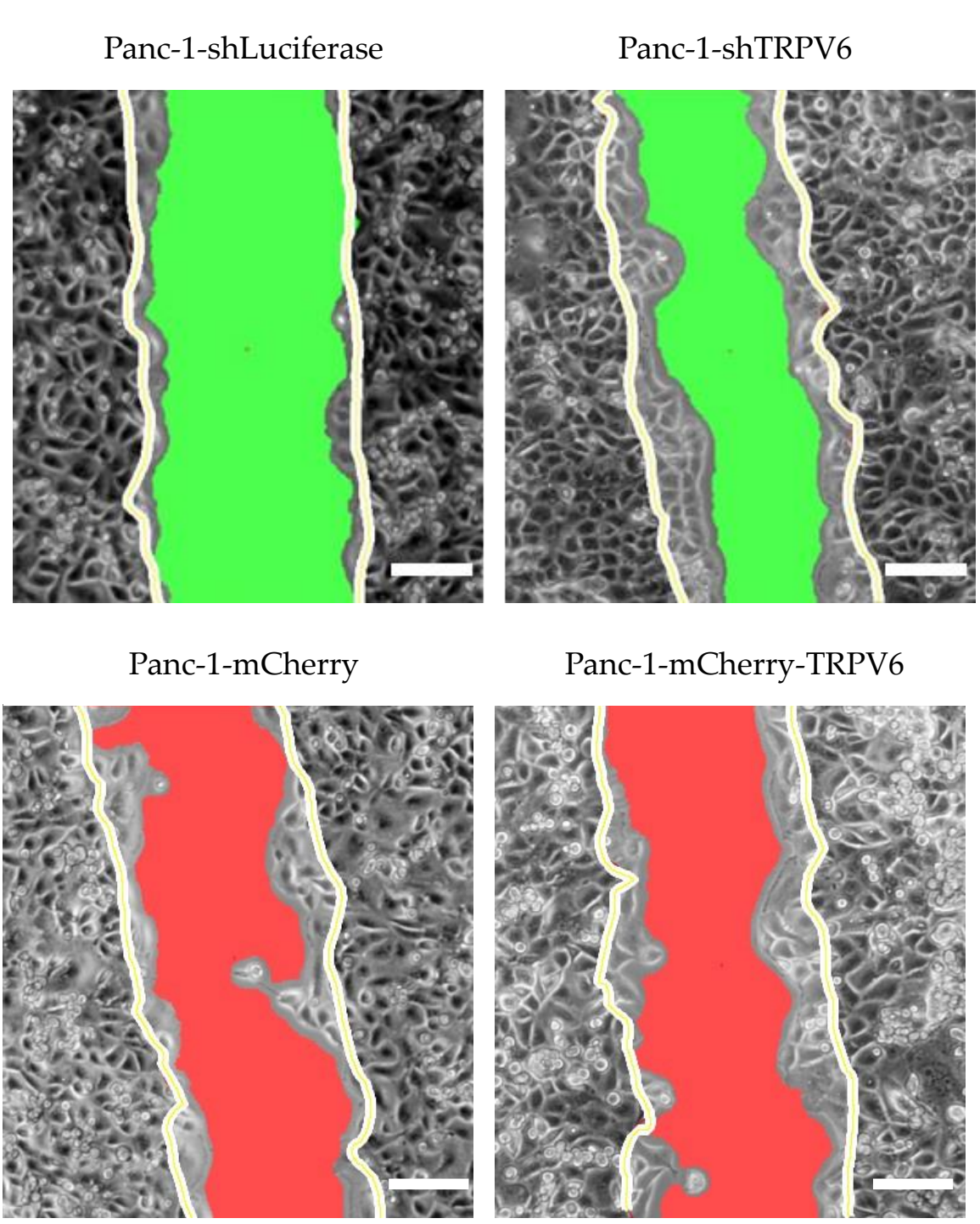

Representation of the wound healing assay done with the stable clones. A wound healing assay was performed and analysed during a time period of 20 h. The figure shows representative images of the wound closure of Panc-1-shLuciferase, Panc-1-shTRPV6, Panc-1-mCherry and Panc-1-mCherry-TRPV6 cells. Images depict the differences in area from t=0 h (represented by the white line) and t=20h (represented by either the green (Panc-1-shLuciferase and Panc-1-shTRPV6) or red (Panc-1-mCherry and Panc-1-mCherry-TRPV6) area. Scale bars represent 50 μm.

It was discovered that TRPV6 expression inhibits the migration of Panc-1 cells. Therefore, TRPV6 knockdown improves the migration of Panc-1 cells, as Panc-1-shTRPV6 cells close the wound faster than the Panc-1-shLuciferase cells (Fig.30A). On the other hand, TRPV6 overexpression hinders the migration of Panc-1 cells, as the Panc-1-mCherry-TRPV6 closes the wound slower than Panc-1-mCherry cells (Fig.30B).

Figure 30 – **Panc-1 cells' motility is regulated by TRPV6 expression.**

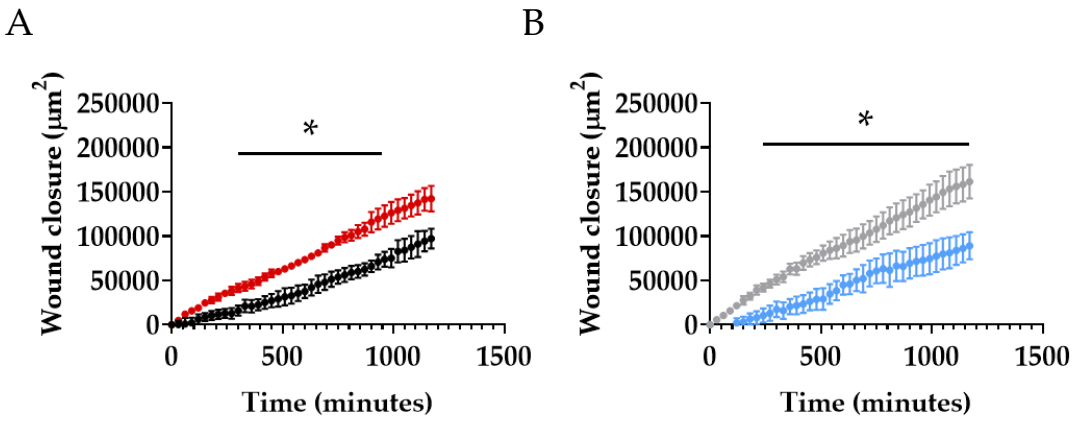

Quantification of wound closure in μm² during the course of the experiment A) Panc-1-shLuciferase (black) and Panc-1-shTRPV6 (red) or B) Panc-1-mCherry (grey) and Panc-1-mCherry-TRPV6 (blue). Error bars represent standard error of the mean of 4 replicates. Statistical significance was determined using multiple t-test. *$p < 0.05$.

The dynamics of the collective movement during the wound closure by measuring the average distance between four neighbouring cells and a central cell during the experiment were also analysed (Fig.31).

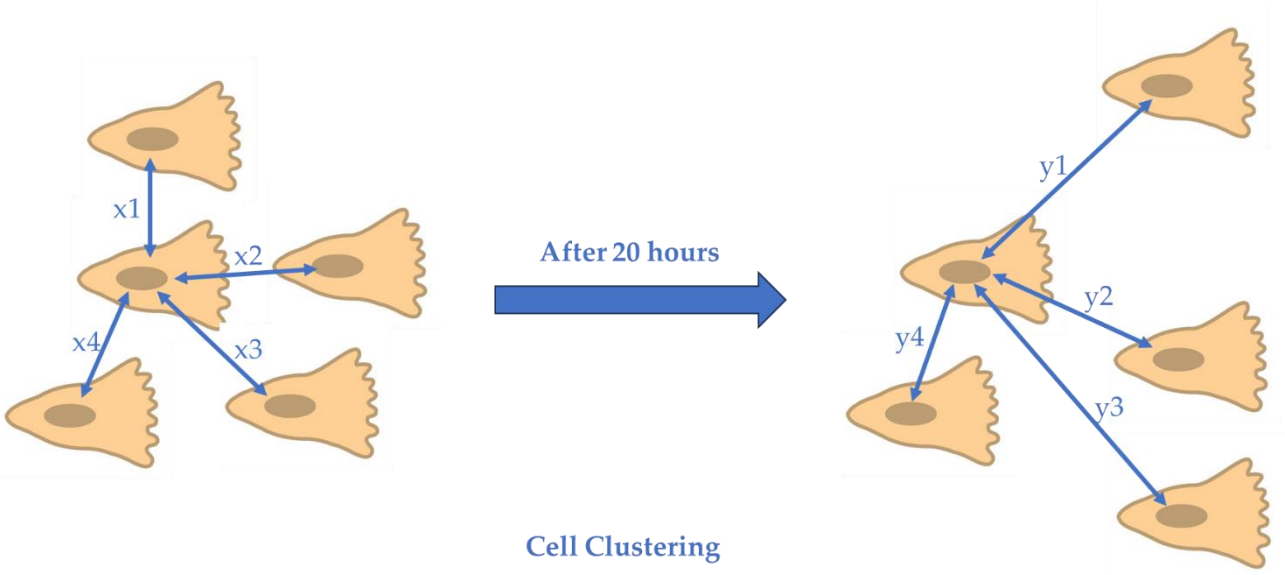

$$\frac{(y1 - x1) + (y2 - x2) + (y3 - x3) + (y4 - x4)}{4} = \text{average distance from main cell}$$

Figure 31 – **Representation of the clustering assay.** Representation of the clustering calculation. Distance between cells and "main" cell was assessed on the beginning and end of the experiment and for each n of the experiment. For each experimental replicate, 3 main cells were used.

TRPV6 channel knockdown fosters the clustering and a more cohesive movement of Panc-1 cells. The average distance between Panc-1-shTRPV6 cells is much lower than between the Panc-1-shLuciferase cells (Fig.32A). The average distance between cells is also lower in the Panc-1-mCherry-TRPV6 cells than the control cells (Fig.32B). However, this does not mean that TRPV6 overexpression also supports a more cohesive movement of Panc-1 cells. The data collected shows that cells overexpressing TRPV6 have nearly half of wound area closed than the control group. This would normally result in more proximity between the cells, hence ruling out the possibility that the overexpression of the channels is responsible for this effect.

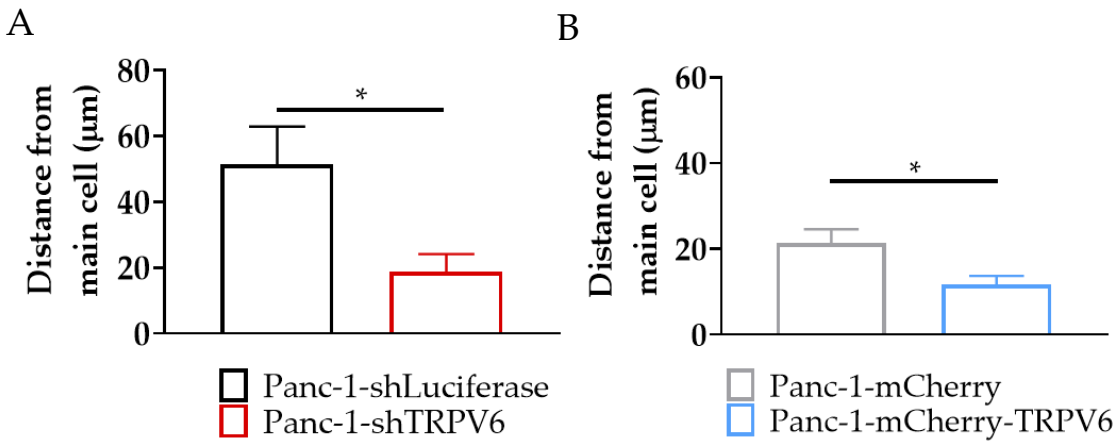

Figure 32 – **Knockdown of TRPV6 leads to higher cell aggregation in Panc-1 cells.** A and B) Clustering of cells was analysed by determining the distance (µm) of 4 neighbouring cells to a "central" cell during the course of the experiment. Results represent the average distance gained throughout the experiments from the neighbouring cells to the "main" cell between A) Panc-1-shLuciferase (black) and Panc-1-shTRPV6 (red) or B) Panc-1-mCherry (grey) and Panc-1-mCherry-TRPV6 (blue). Error bars represent standard error of the mean of 3 replicates. Statistical significance was determined using an unpaired t-test. *$p < 0.05$.

5.8. TRPV6 dysregulation inhibits tumour formation in vivo.

So far, this manuscript describes a correlation between TRPV6 staining and tumour aggressiveness in patient samples which could, by and large, be recapitulated in *in vitro* experiments. To lend further support to this view, the effect of TRPV6 expression on tumour growth in vivo in a mouse model was explored. The four Panc-1 cell lines were injected subcutaneously into nude mice. Tumour size was tracked weekly for 10 weeks, either by using a calliper to measure the tumour volume or by measuring mCherry intensity in the tumour area (for Panc-1-mCherry or Panc-1-mCherry-TRPV6 cells) (Fig.33).

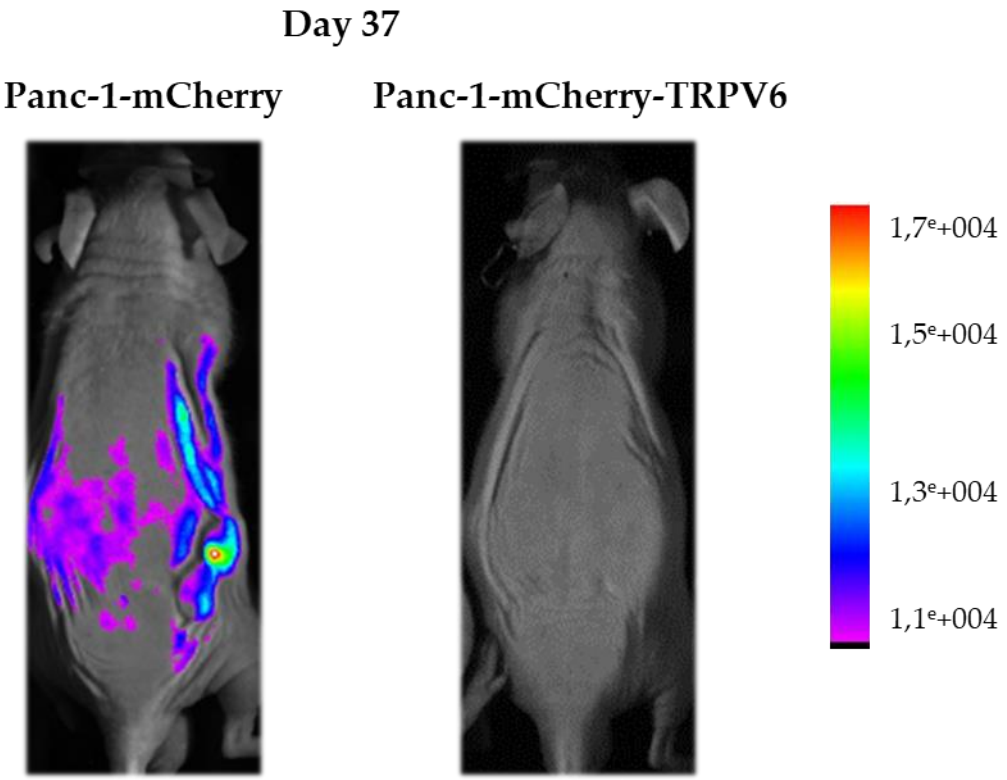

Figure 33 - **Representative images of the mChery imaging taken during the in vivo experiment.** Nude mice were injected subcutaneously with the four different Panc-1 stable clones. Tumour growth was measured through mCherry imaging. Representative image comparing the control group (Panc-1-mCherry) with the overexpression of TRPV6 group (Panc-1-mCherry-TRPV6).

Unexpectedly, it was observed that both control clones form larger tumours than Panc-1-shTRPV6 and Panc-1-mCherry-TRPV6 cells (Fig.34A and 34B). The mean tumour volume at 10 weeks is 525 ± 132 mm^3 for Panc-1-mCherry cells, 410 ± 118 mm^3 for Panc-1-shLuciferase, 194 ± 30 mm^3 for Panc-1-shTRPV6 cells and 137 ± 55 mm^3 for Panc-1-mCherry-TRPV6 cells. These results indicate that TRPV6 expression influences tumour growth in Panc-1 cells and that both low and high levels of TRPV6 channel expression are strongly inhibitory in our setting.

A

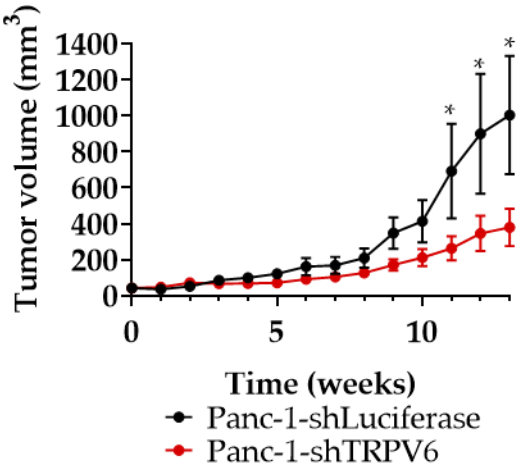

B

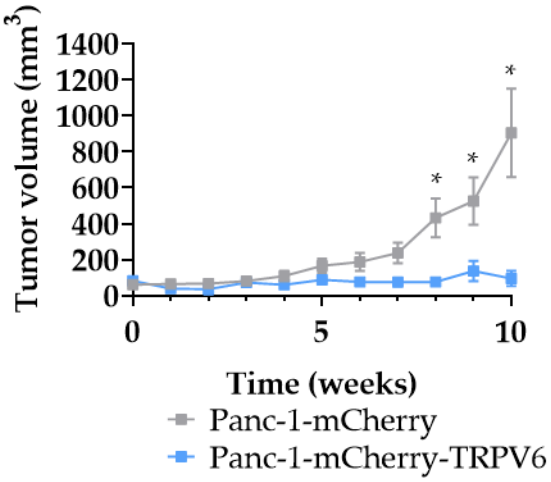

Figure 34 - **Dysregulation of TRPV6 leads to halt in tumour growth.** A) Panc-1-shLuciferase (black) and Panc-1-shTRPV6 (red) B) Panc-1-mCherry (grey) and Panc-1-mCherry-TRPV6 (blue). Tumour growth was evaluated for 10 weeks by measuring and calculating its volume (mm3). Error bars represent standard error of the mean of 10 mice. Statistical significance was determined using unpaired t-test method between each modulated group and its control. *$p < 0.05$.

Mice weights did not show any significant differences throughout the experiment (Fig.35A and B). Only 2 mice were sacrificed due to human end-points, on the 11th week of experimentation (Fig.36 Cand D). Both mice were from the Panc-1-shLuciferase group.

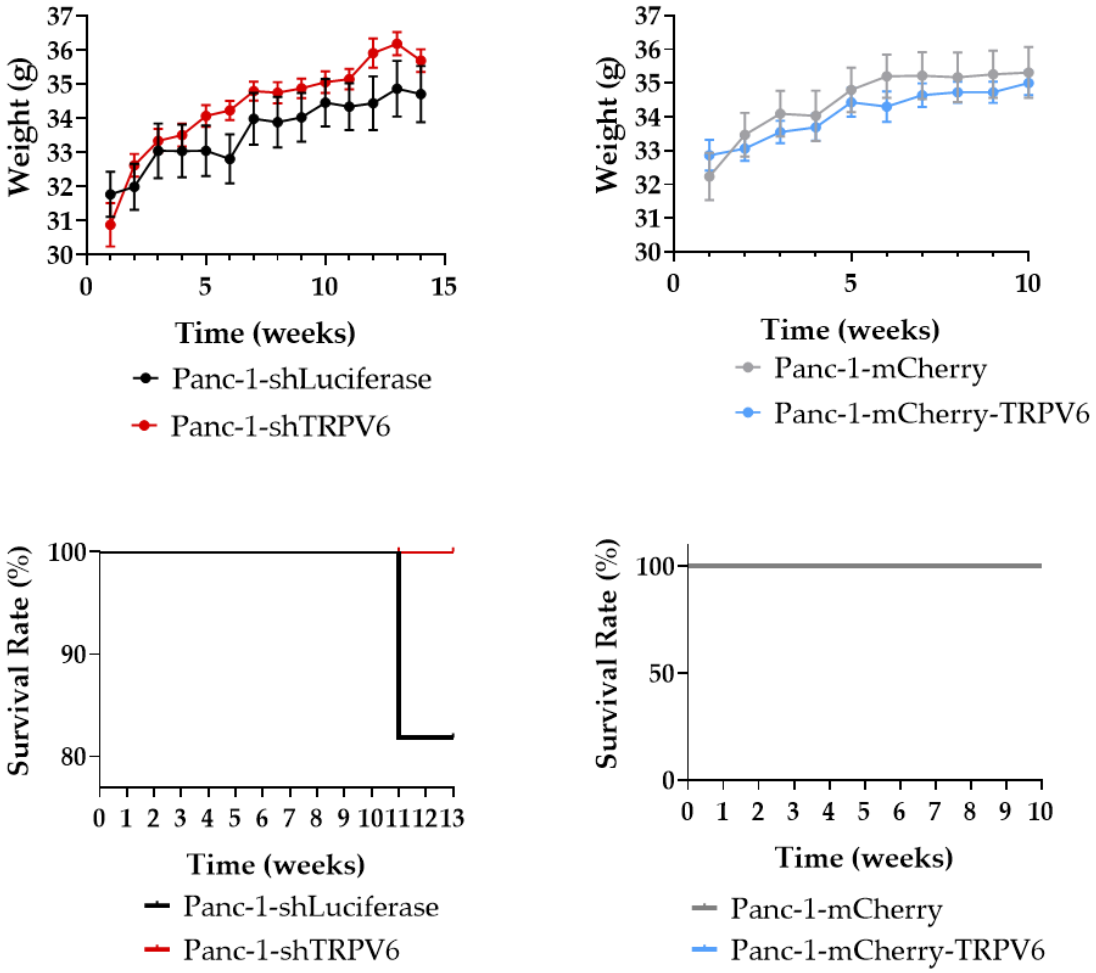

Figure 35 – **Animal survival curve and weight.** Weight of the mice, A) Panc-1-shLuciferase (black) and Panc-1-shTRPV6 (red) or B) Panc-1-mCherry (grey) and Panc-1-mCherry-TRPV6 (blue), was measured every week throughout the experiments. C) Survival curve of the Panc-1-shLuciferase (black) and Panc-1-shTRPV6 (red) or D) Panc-1-mCherry (grey) and Panc-1-mCherry-TRPV6 (blue).

A preliminary study was already made in order to investigate aggressiveness markers present in the tumours from the different stable clones (Fig 36). The markers chosen for this were CxCR4 and K18. The first is associated with an increase in liver and lung metastasis derived from PDAC, whilst Ck18 expression is a common occurrence in PDAC, participating in several signalling pathways, such ERK-MEK or PI3K-Akt. The preliminary observations that could be done, were that both control groups had a higher expression of the aggressiveness markers when comparing to the knockdown or overexpression groups.

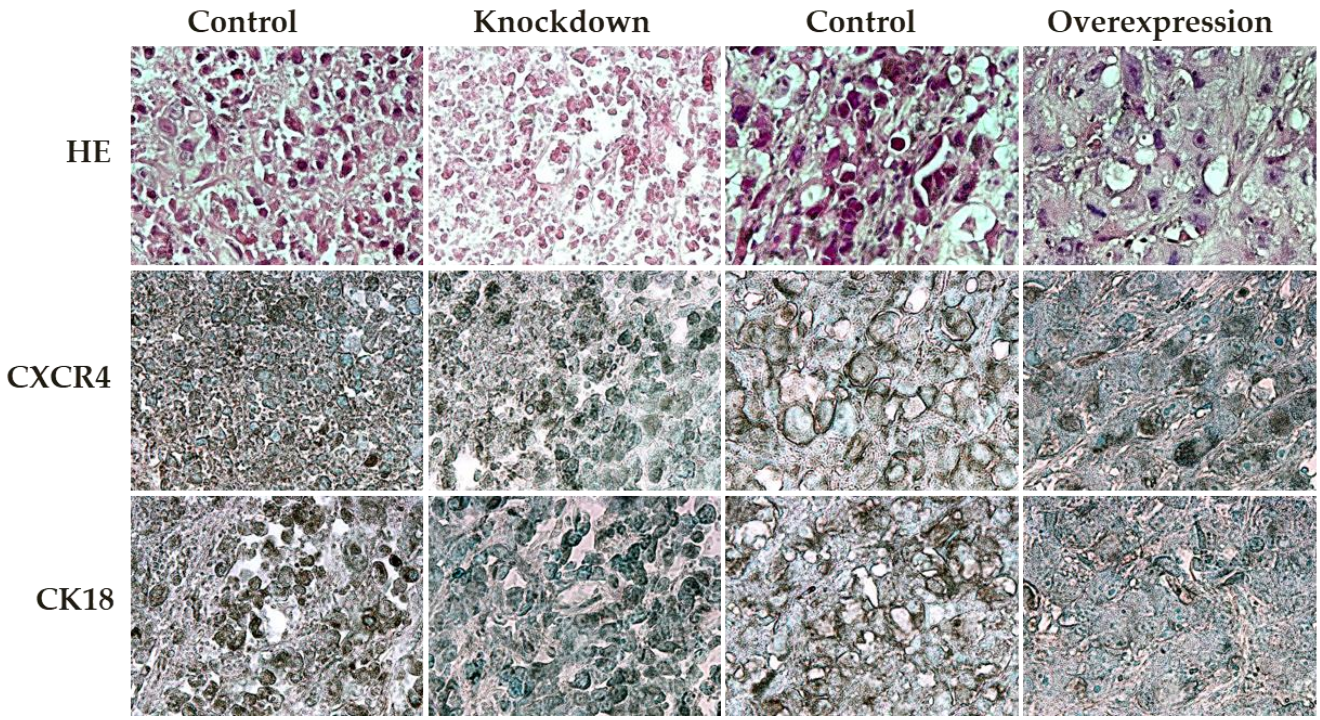

Figure 36 – **Preliminary data of aggressiveness markers in the tumours of the different stable clones.** PDAC tissue from mice injected with different stable clones. The images represent tissues with HE staining (top row), CXCR4 (middle row) and CK18 (bottom row).

6. Discussion

Pancreatic cancer is a type of cancer that originates in the pancreas and is one of the most lethal cancers, with a 5-year survival rate of only 9% (Rawla, Sunkara et al. 2019). The most common type is pancreatic ductal adenocarcinoma, which accounts for about 90% of all cases (Kleeff, Korc et al. 2016).

The unique physical and chemical conditions of the exocrine pancreas, such as low oxygen, high pressure, and changing pH, are commonly related to PDAC (Heinrich, Mostafa et al. 2021). PDAC is characterized by a desmoplastic reaction to the tumour, which is seen in both primary and metastatic tumours. Desmoplasia is a common feature in PDAC and consists of a dense layer of ECM and fibroblasts, more known as CAF (Cannon, Thompson et al. 2018). Desmoplasia creates a physical obstacle, blocking blood vessels and reducing the effectiveness of chemotherapy and immune cell infiltration. The treatment options for PDAC depend on the stage of the disease, as well as the patient's overall health and preferences. The main types of treatment are surgery, chemotherapy, radiation therapy, targeted therapy, and immunotherapy (Wood, Canto et al. 2022).

The development of PDAC is also highly connected to Ca^{2+} signalling. Overall, Ca^{2+} has an important role in many cellular processes. The failure to regulate it can lead to known cancer hallmarks, like continued proliferation, tissue invasion and apoptosis resistance (Orrenius, Zhivotovsky et al. 2003, Wei, Wang et al. 2012, Pinto, Kihara et al. 2015). Several studies have shown that PDAC cells exhibit abnormal Ca^{2+} signalling compared to normal pancreatic cells. For instance, PDAC cells have higher basal [Ca^{2+}] and more frequent Ca^{2+} oscillations than normal cells (Stopa, Lozinski et al. 2023). These changes are associated with increased expression and activity of various Ca^{2+} channels and pumps that mediate Ca^{2+} transport across the plasma membrane and the endoplasmic reticulum (ER).

Taking this into consideration and adding to the fact that TRPV6 mRNA and protein levels are high in many human cancers (Schwarz, Wissenbach et al. 2006, Lehen'kyi, Raphael et al. 2012, Stewart 2020), a study analysing the impact of TRPV6 in PDAC at different levels was needed.

The work developed during my thesis tries to shed a light on the potential of TRPV6 in PDAC, at human tissue, *in vitro* and in *in vivo* levels. Several key points can be taken from this dissertation and will be discussed in the following chapters. The key takeaways are:

1. TRPV6 is overexpressed in patients with lower survivability.
2. TRPV6 is more expressed in later PDAC stages and correlates with poor tissue differentiation and high proliferation.
3. TRPV6 knockdown and overexpression promote significant transcriptomic changes
4. TRPV6 impacts proliferation in Panc-1 cells *in vitro*.
5. TRPV6 knockdown sensitizes Panc-1 cells to chemotherapeutic treatments.
6. Cell migration is affected by TRPV6 expression.
7. TRPV6 dysregulation impairs tumour growth.

6.1. TRPV6 is overexpressed in patients with lower survivability.

Before starting our experiments, a meta-analysis was made to understand how TRPV6 expression is correlated with PDAC patients' survivability. The analysis was made with 176 samples collected from TCGA, using SurvExpress. This analysis highlighted that patients with higher expression of TRPV6 are more at risk to PDAC. More in detail, TRPV6 expression is connected to survivability and the significance between high and low patient risk is achieved with higher difference of TRPV6 expression. Furthermore, the correlation between the overexpression and poor cancer prognosis has already been observed in breast cancer (Xu, Li et al. 2021). Besides the poor prognosis, overexpression of TRPV6 was found in metastatic tissue and correlated with primary breast cancer cell migration.

6.2. TRPV6 is more expressed in later PDAC stages and correlates with poor tissue differentiation and high proliferation.

The expression of TRPV6 channels in tissue samples from 46 patients with PDAC of different stages was analysed. It was shown that TRPV6 expression increased with the tumour stage and dedifferentiation status. Our results show that TRPV6 expression is upregulated in PDAC tumour tissues, but only in the later stages and especially in poorly differentiated ones. This suggests that TRPV6 may be involved in the progression and aggressiveness of PDAC. Previous studies have shown that TRPV6 is overexpressed in various cancers, such as prostate, breast, colon, and ovarian cancers (Zhuang, Peng et al. 2002, Raphael, Lehen'kyi et al. 2014, Xue, Wang et al. 2018, Xu, Li et al. 2021). In PDAC, there are contradictory studies (Zaccagnino, Pilarsky et al. 2016, Song, Dong et al. 2018). In our cohort, it appears that TRPV6 is prominent in the later more aggressive stages. It should be stated that the tumour has generally metastasized to neighbouring tissues in later stages. Furthermore, poorly differentiated tissues are connected to higher tumour progression (Rhim, Oberstein et al. 2014, Shinkawa, Ohuchida et al. 2022). Similarly to other tumours, TRPV6 appears to correlate with the aggressiveness of PDAC. Accordingly, the presence of the proliferation marker Ki-67 in patient samples correlates with increased TRPV6 expression. This effect was already demonstrated in prostate cancer tissues (Raphael, Lehen'kyi et al. 2014).

6.3. TRPV6 knockdown and overexpression promote significant transcriptomic changes

In order to investigate the function of TRPV6 channels in PDAC cell behaviour I generated four stable Panc-1 or Capan-1 cell lines with different levels of TRPV6 expression: a knockdown of TRPV6 expression (Panc-1-shTRPV6 or Capan-1-shTRPV6) and an overexpression of TRPV6 (Panc-1-mCherry-TRPV6 or Capan-1-mCherry-TRPV6) and a control clone with normal TRPV6 expression (Panc-1[Capan-1]-shLuciferase or Panc-1[Capan-1]-mCherry). These cell lines were used for *in vitro* and *in vivo* experiments to assess the effect of TRPV6 expression on the viability, proliferation, resistance, migration, and tumour growth in nude mice.

Through an RNA-seq, a clear differential transcriptome could be seen in these cell lines. Interestingly, the knockdown of TRPV6 promoted an increased number of differentially expressed genes when compared to the overexpression. The functional enrichment analysis

of the differentially expressed genes showed that several modules related to migration were dysregulated. This goes in line with our findings in migration assays with the knockdown group. Further discussion is done below.

Functional clustering of genes and functional enrichment analysis indicated that TRPV6 knockdown over-regulates genes down-regulated by KRAS activation. Changes in the KRAS pathway of the knockdown group could be crucial to control PDAC aggressiveness. Activation of KRAS leads to the binding of GTP, leading to further activation of RAL, RAF-MEK-ERK, and PI3K-AKT pathways (Kim, Lee et al. 2021). These pathways control cells growth, proliferation, and differentiation (Bryant, Mancias et al. 2014, Leung, Luo et al. 2018, Ogawa, Walters et al. 2019). From this pathway, DEGs like *tfcp2l1*, *edn1* or *fgfr3* might be of importance for the development of PDAC. TFCP2L1 has been the object of several studies in cancer, although its role is not fully understood. In clear cell renal cell carcinoma, TFCP2L1 loss leads to EMT and osteogenic differentiation, which leads to the cancer development (Kotarba, Krzywinska et al. 2018). On the other hand, neutralization of TFCP2L1 can lead to reduced angiogenesis and better prognosis in colorectal cancer (Hsu, LaBella et al. 2023). EDN1 was also studied in the context of PDAC. EDN1 was observed to be overexpressed in tumour tissue compared to healthy tissue (Cook, Brais et al. 2015). Cells with mutated EGFR that had EDN1 overexpressed ectopically showed reduced drug uptake and slower growth *in vivo*, but not *in vitro*. Furthermore, drug delivery to tumours and blood circulation in tumour-related blood vessels improved when EDN1 was reduced (Pulido, Ollosi et al. 2020). Lastly, FGFR3 was also studied in PDAC cell lines Capan-2, BxPC-3, MiaPaca-2 and Panc-1 (Lafitte, Moranvillier et al. 2013). The results obtained were quite interesting. Although FGFR3 overexpression led to higher proliferation in Capan-2 and BxPC-3, the opposite effect was observed in MiaPaca-2 and Panc-1. This is similar to our results where the knockdown group had lower levels of proliferation when compared to the control.

Functional clustering of genes and functional enrichment analysis indicated that TRPV6 overexpression over-regulates genes impacting EMT whilst, contrary to TRPV6 knockdown, up-regulating genes participating in angiogenesis.

The most differentiated cluster of genes and functional enrichment analysis for the overexpression group belongs to genes involved in EMT. This process is a crucial step in cancer progression for those of epithelial origin and can activate different pathways that

lead cells to acquire motile characteristics and an ability to degrade and reorganize the extracellular matrix (Palamaris, Felekouras et al. 2021). As we observed on human tissue, TRPV6 is present in later stages of PDAC, when the tumour has developed into a more invasive form. This indicates a possible role for TRPV6 in the progression and aggressiveness of PDAC, supported by the RNA-seq. The relation between TRPV6 and EMT was studied in MCF10A epithelial cell line of the breast in which TRPV6 correlated with EMT markers at protein level (Karki, Rajakyla et al. 2020). TRPV6 overexpression clearly up-regulates several collagen genes, like *col4a1*, *col4a2*, *col3a1* or *col5a2*. This type of up-regulation leads to excessive collagen turnover products. Of notice, in colorectal cancer patients, these products are associated with cancer progression being more significantly present in later stages of the tumour (Kehlet, Sanz-Pamplona et al. 2016). *tgfb1* is the most significantly down-regulated gene of the cluster of genes involved in EMT. TGF-β1 low expression was already associated with poor prognosis on PDAC patients (Glazer, Welsh et al. 2017). Furthermore, low TGF-β1 also correlated with higher tissue proliferation. This corroborates the findings in this thesis, in which higher TRPV6 levels correlated with higher tissue proliferation.

6.4. TRPV6 impacts proliferation in Panc-1 cells in vitro.

The stable clones allowed me to confirm several of the findings *in vitro* that were made in patient tissue. It was noted that TRPV6 knockdown reduces the cell proliferation and cell viability in Panc-1 and Capan-1 cells, and cell cycle progression of Panc-1 cells. Conversely, TRPV6 overexpression enhances proliferation. Capan-1 cells were only used to confirm *in vitro* data of cell proliferation and viability, which is one of the major findings in our article. In addition to the proliferation and viability results, TRPV6 knockdown induces apoptosis in Panc-1 cells, as indicated by the increased percentage of cells in the sub-G1 phase. The lack of differences between the overexpression and the control in this experiment can be explained due to 3-5% of the cells being naturally in the sub-G1 phase. These results indicate that TRPV6 is involved in survival and growth of PDAC cells, and that its inhibition may trigger cell death. The mechanisms by which TRPV6 regulates these processes are not fully understood but may involve at least in part the modulation of Ca^{2+}-dependent signalling pathways. For example, calmodulin, a Ca^{2+}-dependent TRPV6 inhibitor, can control the

KRas4B pathway that can impact proliferation(Prior, Lewis et al. 2012, Singh, McGoldrick et al. 2018). Inhibition of calmodulin can lead to effects such as lower proliferation levels, inability to progress in the cell cycle or higher cell death rates (Berchtold and Villalobo 2014, O'Day, Mathavarajah et al. 2020). Moreover, store operated Ca^{2+} channels (SOCE) can act on Akt/mTor or NF-κB pathways modulating proliferation (Bettaieb, Brule et al. 2021). In prostate cancer, an interaction between SOCE and TRPV6 was already described and could in principle occur in PDAC as well (Raphael, Lehen'kyi et al. 2014). TRPV6 was shown to increase proliferation, and lead cells to a more aggressive phenotype in prostate cancer cell lines.

6.5. TRPV6 sensitizes Panc-1 cells to chemotherapeutic treatments.

Evaluation of the effect of TRPV6 expression on the resistance of Panc-1 cells to chemotherapeutic drugs was made with the use of 3 known treatments of PDAC: gemcitabine, cisplatin, and 5-FU. These drugs are commonly used in the treatment of pancreatic cancer, but often fail to achieve satisfactory outcomes due to the development of drug resistance (Wang, Yang et al. 2014, Sohn, Yuh et al. 2015, Mezencev, Matyunina et al. 2016, Koltai, Reshkin et al. 2022). A founding was made, that TRPV6 knockdown sensitizes Panc-1 cells to 5-FU treatment. On the other hand, it was shown that TRPV6 overexpression does not affect the sensitivity of Panc-1 cells to 5-FU. It is known that 5-FU makes use of Ca^{2+} as a second messenger to induce apoptosis of HCT116 colon carcinoma cells (Can, Akpinar et al. 2013). Furthermore, calmodulin inhibition, e.g. by a reduction of the intracellular Ca^{2+} concentration, can impair this process. 5-fluorouracil treatment of T47D breast carcinoma cells can increase TRPV6 expression after 48 and 96 hours (Bolanz, Hediger et al. 2008). Another important pathway that might be in play in 5-fluorouracil action is NFAT-P-glycoprotein (encoded by *abcb1*). This pathway contributes to 5-fluorouracil resistance. In breast cancer and human colorectal cells, the abolishment of *abcb1* expression reverted chemotherapeutic resistance (Ma, Cai et al. 2012, Wang, Chen et al. 2015). TRPV6 enhances calcium entry into the cell, which activates the calcium binding protein calmodulin. This complex then activates calcineurin that de-phosphorylates and activates Nuclear Factor of Activated T-cells (NFAT), a gene transcription factor involved in multiple oncogenic processes. It was observed that, in prostate cancer cells, TRPV6 can impact proliferation by modulating NFAT-dependant pathways (Lehen'kyi, Flourakis et al.

2007). It may be possible that this function is also impacting chemotherapeutics in PDAC. Our experiments with Gemcitabine are in line with the role of TRPV6 as a Ca^{2+} channel. Gemcitabine toxicity is activated by the blockage of calmodulin pathways (Principe, Aissa et al. 2022). The knockdown of TRPV6 can lead to lower levels of calmodulin activation and thereby increase the cytotoxicity of gemcitabine action in PDAC cells (Singh, McGoldrick et al. 2018). The lack of differences found in the overexpression group when compared to the control, in both chemoresistance and Ca^{2+} influx, might be an indication that TRPV6 overexpression does not necessarily translate into higher TRPV6 expression on the membrane. Recently, Kogel *et al.* indicated that in HEK293 cell line TRPV6 has a very short membrane period before a rapid endocytosis (Kogel, Fecher-Trost et al. 2022). This internalization of TRPV6 might be impacting Ca^{2+} signalling inside the cells. Thus, TRPV6 could be impacting intracellular homeostasis more than membrane homeostasis. This should be a subject for further studies.

6.6. Cell migration is affected by TRPV6 expression.

The effect of TRPV6 expression on the migration of Panc-1 cells was assessed, using a wound healing assay. It could be observed that TRPV6 overexpression negatively regulates the migration of Panc-1 cells. Hence, TRPV6 knockdown enhances the migration of Panc-1 cells, while TRPV6 overexpression impairs it. This effect was quite interesting, seeing that the overexpression of TRPV6 improves proliferation rates, whilst the knockdown gives preference to the migration of the cells. Even though the selection of these phenotypes in the tumour requires different specifications, it was shown that cells can interchange from a more proliferative phenotype to a more migratory one, as it was suggested in different works previously (De Donatis, Ranaldi et al. 2010, Gallaher, Brown et al. 2019). Indeed, TRPV6 might rise as a promoter or a switch for these changes. TRPV6 knockdown cells have an increased number of cells in the sub-G1 phase, which clearly demonstrates a deviation from the proliferative phenotype, whilst it could be observe that the overexpression of TRPV6 decreases cell motility despite the higher proliferation levels. I also found that in particular TRPV6 knockdown promotes the clustering and a more cohesive movement of Panc-1 cells. On the other hand, TRPV6 knockdown impacted negatively both cell migration and cell-cell adhesion, in breast, prostate and ovarian cancer cell lines (Jiang, Gou et al. 2023). This effect was observed in TRPV6 expressing cell lines, treated with different concentrations of lidocaine. This compound downregulated TRPV6 and led to lower

viability of the cells, and less migration and invasion. The mechanisms that led to these effects are suggested to be the inactivation of MEK/ERK and NF-kβ pathways (Jiang, Gou et al. 2016).

6.7. TRPV6 dysregulation impairs tumour growth.

Lastly, the results obtained in the *in vivo* experiments show that TRPV6 expression modulates tumour growth. Surprisingly, we found that both control cell lines form larger tumours than Panc-1-shTRPV6 and Panc-1-mCherry-TRPV6 cell lines. These results suggest that TRPV6 expression has a biphasic effect on tumour growth in Panc-1 cells and that both low and high levels of TRPV6 can impact tumour development. This finding is unexpected, as the *in vitro* results indicated a positive correlation between TRPV6 expression and cell proliferation. One possible explanation is that TRPV6 expression may affect other aspects of tumour biology, such as angiogenesis, inflammation, or immune response, which are not captured by the in vitro assays (Pulido, Ollosi et al. 2020). Finally, we cannot dismiss the possibility that yet to be identified properties of the tumour microenvironment increases the susceptibility of Panc-1 cells to alterations of their TRPV6 expression.

7. Conclusion and perspectives

The main conclusion taken from the work performed in this thesis is that PDAC aggressiveness is modulated by TRPV6. This conclusion comes from the role of the calcium channel in aiding cell proliferation, as seen both in human tissue and *in vitro*. Furthermore, knockdown of TRPV6 sensitizes cells to the effects of gemcitabine and 5-fluorouracil. These findings indicate TRPV6 as a potential target for PDAC treatment. On the same note, a phase I study was made with SOR-C13, a TRPV6 inhibitor, had a promising activity against pancreatic cancer tumour growth (Fu, Hirte et al. 2017).

Despite the intensive work done on this thesis, some loose ropes were left. There is a need for confirmation of this data on a KO cell model, which would be a better model than just a knockdown of the channel. The use of inhibitors could also be a hypothesis, but no specific inhibitors are available commercially to the date. Further studies on which pathways are being modulated by TRPV6 are also important. As discussed in **6.3**, KRAS pathway, one of the most important in the development of PDAC, is significantly impacted by TRPV6 knockdown. With the rising of targeted therapies for cancer this could be an interesting focus to increase the ability of known chemotherapeutics to effectively impair tumour growth and metastasis.

Due to the lack of difference in calcium influx on the overexpression cells, compared to the control, it would be of interest to understand whether the changes observed between those groups are because of the channel activity of TRPV6 or if it is a reaction to higher protein expression. To do that, a pore-mutated TRPV6 could be created. This would provide us information on if TRPV6 can modulate cell behaviour independently of Ca^{2+}.

Another interesting study would be how these stable clones perform in a pancreatic-like organoid. This would give us a better idea on how TRPV6 control migration and invasion, on a 3D model, as well as, how proliferation is impacted on a cell cluster with different levels of TRPV6. Lastly, a more deepened analysis on *in vivo* studies is essential. Although TRPV6 modulation *in vitro* led to either higher proliferation, on cells with an overexpression of the channel, or higher motility, in cells with a knockdown, the results of animal studies were distinct showcasing the inability of these clones to promote tumour

growth in a mouse model. Future studies developed on TRPV6 and immune system should also be considered, in order to have a comprehensive understanding of TRPV6 dysregulation in cancer tissues.

8. Annexes

cancers

MDPI

Article

TRPV6 Channel Is Involved in Pancreatic Ductal Adenocarcinoma Aggressiveness and Resistance to Chemotherapeutics

Gonçalo Mesquita [1,2], Aurélien Haustrate [1], Adriana Mihalache [3], Benjamin Soret [1,2], Clément Cordier [1], Emilie Desruelles [1], Erika Duval [3], Zoltan Pethö [2], Natalia Prevarskaya [1], Albrecht Schwab [2,*] and V'yacheslav Lehen'kyi [1,*]

1 Laboratory of Cell Physiology, INSERM U1003, Laboratory of Excellence Ion Channel Science and Therapeutics, Department of Biology, Faculty of Science and Technologies, University of Lille, 59650 Villeneuve d'Ascq, France; emilie.desruelles@univ-lille.fr (E.D.); natacha.prevarskaya@univ-lille.fr (N.P.)
2 Institute of Physiology II, University of Muenster, Robert-Koch-Str. 27b, 48149 Muenster, Germany; pethoe@uni-muenster.de
3 Service d'Anatomie et de Cytologie Pathologiques, Groupement des Hôpitaux de l'Institut Catholique de Lille (GHICL), 59000 Lille, France; mihalache.adriana@ghicl.net (A.M.); duval.erika@ghicl.net (E.D.)
* Correspondence: aschwab@uni-muenster.de (A.S.); vyacheslav.lehenkyi@univ-lille.fr (V.L.)

Simple Summary: Pancreatic ductal adenocarcinoma (PDAC) is a highly aggressive cancer with limited treatments and poor prognosis. TRPV6, a calcium-permeable channel overexpressed in cancers, holds potential as an influencer of cancer cell behavior. This study investigates TRPV6 expression in PDAC, analyzing 46 patient tissue samples of varying stages and grades. We manipulated TRPV6 expression (knockdown, overexpression) in the human PDAC cell lines Panc-1 and Capan-1. We then revealed the impact of TRPV6 expression on Ca^{2+} influx, proliferation, apoptosis, migration, chemoresistance, and tumor growth both in vitro and in vivo. Notably, TRPV6 expression correlated with tumor stage and grade, relating it to PDAC proliferation. Knockdown decreased Ca^{2+} influx. This was paralleled by reduced proliferation, enhanced apoptosis, and sensitization of cells to chemotherapeutic drugs. Conversely, TRPV6 overexpression yielded opposing effects. Strikingly, both knockdown and overexpression curtailed tumor formation in vivo. These findings underscore an intricate role of TRPV6 channels in PDAC progression, highlighting its potential as a therapeutic target.

Abstract: Pancreatic ductal adenocarcinoma (PDAC) stands as a highly aggressive and lethal cancer, characterized by a grim prognosis and scarce treatment alternatives. Within this context, TRPV6, a calcium-permeable channel, emerges as a noteworthy candidate due to its overexpression in various cancers, capable of influencing the cell behavior in different cancer entities. Nonetheless, the exact expression pattern and functional significance of TRPV6 in the context of PDAC remains enigmatic. This study scrutinizes the expression of TRPV6 in tissue specimens obtained from 46 PDAC patients across distinct stages and grades. We manipulated TRPV6 expression (knockdown, overexpression) in the human PDAC cell lines Panc-1 and Capan-1. Subsequently, we analyzed its impact on multiple facets, encompassing Ca^{2+} influx, proliferation, apoptosis, migration, chemoresistance, and tumor growth, both in vitro and in vivo. Notably, the data indicate a direct correlation between TRPV6 expression levels, tumor stage, and grade, establishing a link between TRPV6 and PDAC proliferation in tissue samples. Decreasing TRPV6 expression via knockdown hampered Ca^{2+} influx, resulting in diminished proliferation and viability in both cell lines, and cell cycle progression in Panc-1. The knockdown simultaneously led to an increase in apoptotic rates and increased the susceptibility of cells to 5-FU and gemcitabine treatments. Moreover, it accelerated migration and promoted collective movement among Panc-1 cells. Conversely, TRPV6 overexpression yielded opposing outcomes in terms of proliferation in Panc-1 and Capan-1, and the migration of Panc-1 cells. Intriguingly, both TRPV6 knockdown and overexpression diminished the process of tumor formation in vivo. This intricate interplay suggests that PDAC aggressiveness relies on a fine-tuned TRPV6 expression, raising its profile as a putative therapeutic target.

check for updates

Citation: Mesquita, G.; Haustrate, A.; Mihalache, A.; Soret, B.; Cordier, C.; Desruelles, E.; Duval, E.; Pethö, Z.; Prevarskaya, N.; Schwab, A.; et al. TRPV6 Channel Is Involved in Pancreatic Ductal Adenocarcinoma Aggressiveness and Resistance to Chemotherapeutics. *Cancers* **2023**, *15*, 5769. https://doi.org/10.3390/cancers15245769

Academic Editor: Arpad Szallasi

Received: 12 October 2023
Revised: 20 November 2023
Accepted: 29 November 2023
Published: 8 December 2023

Keywords: PDAC; TRPV6; calcium; therapy; resistance

1. Introduction

Pancreatic ductal adenocarcinoma (PDAC) is the most common type of pancreatic cancer, accounting for about 90% of all cases [1]. It is one of the most lethal malignancies, with a 5-year survival rate of only approximately 10% [2]. The poor prognosis of PDAC is mainly due to its late diagnosis, aggressive invasion, metastasis and resistance to conventional therapies [3]. Therefore, there is an urgent need to develop alternative therapeutic concepts for this disease.

TRPV6 is a Ca^{2+}-permeable channel that belongs to the transient receptor potential (TRP) family of ion channels [4,5]. It plays an important physiological role in Ca^{2+} reabsorbing intestinal and renal epithelia. However, TRPV6 is also aberrantly expressed in various cancers, such as prostate, breast, colon, and ovarian cancers [4,6]. In ovarian cancer, TRPV6 has increased expression in all stages when compared to normal tissue [7]. Furthermore, the inhibition of TRPV6 channels in an SKOV-3 xenograft model in mice led to reduced tumor formation. TRPV6 overexpression was also present in breast cancer, where it correlated with invasive areas of the tumor [8]. In the prostate cancer cell line LNCaP, TRPV6 inhibition can lead to lower levels of proliferation and increased apoptosis [9]. Translocation of TRPV6 to the plasma membrane and increased aggressiveness was also observed in LNCaP, indicating a clear role for TRPV6 in prostate cancer [10]. Overall, TRPV6 channels promote cancer cell proliferation, survival, migration, and invasion by modulating intracellular Ca^{2+} signaling and downstream pathways [11–14].

The expression and function of TRPV6 in PDAC are still unclear. A previous study indicated that the overexpression of TRPV6 in PDAC tissues and cell lines correlated with poor survival and chemoresistance [15]. Another study showed that TRPV6 has a reduced expression in micro-dissected PDAC samples [16]. These contradictory findings may reflect the heterogeneity and complexity of PDAC. Furthermore, it is known that TRPV6 impacts non-alcoholic early onset pancreatitis, a risk factor for the development of PDAC [17,18]. This was observed in several cohorts and appears to be correlated with the Ca^{2+} channel activity of TRPV6 [19]. In this study, we aimed to investigate how TRPV6 impacts PDAC aggressiveness in tumor tissue, in PDAC cell line Panc-1, and in vivo. To achieve that, TRPV6 expression was quantified in tumoral and peri-tumoral tissues from PDAC patients. Stable clones from Panc-1 cells were created, with a knockdown or an overexpression of TRPV6. These cells were evaluated for proliferation, viability or motility. These stable clones were also grafted into mice to assess the role of TRPV6 channels in PDAC tumor aggressiveness in vivo.

2. Materials and Methods

2.1. Human Tissue Data

Tumor and peri-tumoral tissues were obtained from patients with PDAC that was histopathologically confirmed by the medical staff of GHICL (Groupement des Hôpitaux de l'Institut Catholique de Lille, Lille, France) (TNM classification, 8th edition of the UICC 2016). The number of subjects is 46 and tissues were collected between January of 2014 and December of 2019 (RNIPH-2022-26).

For immunohistochemistry, four micrometer-thick conventional whole tissue sections were cut from formalin-fixed and paraffin-embedded (FFPE) tissue blocks. Immunohistochemical staining was performed using a BenchMark ULTRA system (Ventana Medical Systems Inc., Oro Valley, USA) and a revelation kit (ultraView DAB Detection Kit (Roche Diagnostics, Indianapolis, USA)). The sections were immunolabeled with anti-TRPV6 Clone Mab 82 antibody [20] or anti-Ki-67 by using heat-induced epitope retrieval (HIER) in a citrate-based buffer (CCS 2) at 91 °C for 8 min followed by primary antibody incubation for 32 min. TRPV6 expression was analyzed semi-quantitatively with a scoring system

ranging from 0 (no staining) to 3 (very intense staining). The staining intensity is based on the H-score, which is the result of the multiplication of the percentage of cells by the score given [21].

2.2. Cell Culture

Panc-1 and Capan-1 cells were incubated in a humidified atmosphere at 37 °C and 5% CO_2. The highly aggressive pancreatic adenocarcinoma cells were cultured in RPMI medium (Roswell Park Memorial Institute medium, Sigma-Aldrich, St. Louis, USA) supplemented with 10% fetal bovine serum (FBS Superior, Berlin, Germany) and 500 µM of geneticin (G418) (ThermoFischer Scientific, Waltham, USA).

2.3. Cell Transfection

For transfection, the cells were seeded in 6-well plates at a density of 1×10^5 cells per well and incubated overnight. The next day, the cells were transfected with one of the following plasmids: vEF1ap-5′UTR-TRPV6_CMVp-mCherry-Vektor, vEF1ap-5′UTR_CMVp-mCherry or pSingle-tTS-shRNA-Vektor (Clontech Laboratories, Mountain View, USA). The latter vector had Luciferase or TRPV6 as the shRNA sequence. The plasmids were diluted in Opti-MEM Reduced Serum Medium and mixed with Lipofectamine 3000 Transfection Reagent (Thermo Fisher Scientific) according to the manufacturer's instructions. The transfection complexes were added to the cells and incubated for 24 h. The medium was then replaced with fresh RPMI with 500 µM of geneticin (G418) in order to select transfected cells. After 2 weeks, a small group of cells (3–4 cells) was selected, and a new culture was prepared for each mixed clone. All the experiments were performed with the stable mixed clones.

2.4. RNA Sequencing

The cells were plated in 60 mm dishes at 75% confluence and the total RNA was extracted and purified from the cells using the NucleoSpin® RNA Plus kit (Machery-Nagel, Strasbourg, France) according to the manufacturer's recommendations. Each RNA sample was validated for RNA integrity using a 18S/28S ratio. In total, 1 µg of total RNA from each sample was used for library preparation. Library preparation was realized following the manufacturer's recommendations (Illumina Stranded mRNA Prep, Illumina, San Diego, USA). The final samples' pooled library prep was sequenced on ILLUMINA Novaseq 6000 with SP-200 cartridge (2×800 Millions of 100 bases reads), corresponding to 2×26 Millions of reads per sample after demultiplexing. This work benefited from equipment and services from the iGenSeq core facility, at ICM (Paris, France). The results were then evaluated as the fold change in the controls.

2.5. RT-PCR

cDNA amplification conditions included the initial denaturation step of 7 min at 95 °C and 36 cycles of 30 s at 95 °C, 30 s at 60 °C, 30 s at 72 °C, and finally 7 min at 72 °C. Quantitative real-time PCR of TRPV6 and hypoxanthine-phosphoribosytransferase (HPRT) mRNA transcripts were carried out using MESA GREEN qPCR MasterMix Plus for SYBR Assay (Eurogentec) on the Biorad CFX96 Real-Time PCR Detection System. The sequences of primers are as follows: *TRPV6*: Forward GCCTTCTATATCATCTTCC; Backward GGTGATGCTGTACATGAAGG; HPRT: Forward GGCGTCGTGATTAGTGATGAT; Backward CGAGCAAGACGTTCAGTCCT. The *HPRT* gene used has a housekeeping gene. To quantify the results, the comparative threshold cycle method ΔΔCt and CFX Manager Software v2.0 were used.

2.6. Western Blot

Western blot protocol was followed like in Haustrate et al. [20]. Briefly, the cells were treated with an ice-cold lysis buffer containing the following: 10 mM Tris-HCl, pH 7.4, 150 mM NaCl, 10 mM $MgCl_2$, 1 mM PMSF, 1% Nonidet P-40, and protease inhibitor cocktail

from Sigma-Aldrich. After centrifugation, the lysates were mixed with a sample buffer containing 125 mM Tris-HCl pH 6.8, 4% SDS, 5% β-mercaptoethanol, 20% glycerol, and 0.01% bromophenol blue, and boiled for 5 min at 95 °C. The total protein samples were subjected to 8% SDS-PAGE and transferred to a nitrocellulose membrane via semi-dry Western blotting (Bio-Rad Laboratories, Hercules, CA, USA). The membrane was blocked overnight in 5% milk containing TNT buffer (Tris-HCl, pH 7.5, 140 mM NaCl, and 0.05% Tween 20) and then probed using specific mouse monoclonal anti-TRPV6 antibodies (all at 1/500 dilution from the initial concentration of 0.5 µg/µL) and mouse monoclonal anti-β-actin (Lab Vision Co., Fremont, CA, USA, 1/1000) antibodies. Mouse monoclonal anti-mouse secondary antibodies (Chemicon International; Temecula, CA, USA, 1/200) were used. The bands on the membrane were visualized using an enhanced chemiluminescence method (Pierce Biotechnologies Inc., Escondido, CA, USA). Densitometric analysis was performed using a Bio-Rad image acquisition system (Bio-Rad Laboratories).

2.7. Mn^{2+} Quench Experiments

Panc-1 cells were stained with the Ca^{2+}-sensitive dye Fura2, coupled with the AM ester to be able to permeate the cell (3 µM, Invitrogen, Waltham, USA) in Ringer's solution (NaCl 140 mM, $CaCl_2$ 1.2 mM, $MgCl_2$ 0.8 mM, KCl 5.4 mM) with Hepes 20 mM for 30 min in a heating cabinet. The cells were then placed on the stage of a Axiovert 200 fluorescence microscope (Zeiss, Oberkochen, Germany) and continuously superfused with prewarmed (37 °C) HEPES-buffered Ringer's solution. During the experiment, a 3 min control period (Ringer's solution without Ca^{2+}) preceded the application of the test solution (Ringer's solution with 400 µM $MnCl_2$) for 3 min. Mn^{2+} has a higher binding affinity to Fura2 than Ca^{2+} and quenches its fluorescence. Images were taken every other 10 s. Fura2-loaded cells were excited at the isosbestic wavelength of 357 nm [22]. The mean cellular fluorescence intensity emitted at 510 nm was measured following background subtraction. Then, the slope of the fluorescence declines over 30 s for each time point during the Mn^{2+} influx was calculated, and the slope of the control period was subtracted. The steepest slope over 30 s was determined and taken as a surrogate of Ca^{2+} influx.

2.8. Cell Count

Cell proliferation was assessed through cell count. Briefly, the cells were plated in a T25 flask at a density of 30,000 cells per flask. Images of proliferating Panc-1 cells were acquired every other 30 min for 48 h, starting 2 h after plating. Cell proliferation was also assessed through mitosis count. This allowed us to exclude cells migrating from other areas. Images were obtained in a Zeiss Axio1040 microscope (Zeiss, Germany) with controlled temperature. The pictures were taken using MikroCamLab II 7.3.1.8 software (Bresser, Germany).

2.9. Cell Cycle Assay

Cell cycle analysis was performed by means of flow cytometry of cell populations cultured in triplicate in 30 cm^2 dishes, as described in the work of Lehen'kyi et al. 2011 [23]. Briefly, Panc-1 cells were washed with phosphate-buffered saline (PBS) and then trypsinized. After this procedure, they were fixed in cold methanol for 30 min at +4 °C. After this step, the cells were centrifuged and with PBS at 4 °C, resuspended in 100 µL PBS, treated with 100 µL RNAse A (1 mg/mL, Sigma-Aldrich), and stained with propidium iodide (PI, Sigma-Aldrich) at a final concentration of 50 µg/mL. The stained cells were stored at 4 °C in the dark and analyzed within 2 h. PI fluorescence was measured with a BD FACSCalibur (BD Biosciences, Franklin Lakes, NJ, USA). Data were acquired for 10,000 events, and red fluorescence was measured using a fluorescence detector 3 (FL3). The data were stored and analyzed using CellQuest software to assess the cell cycle distribution patterns between the different phases: subG1 (apoptotic), G0/G1, S, and G2/M phases.

were prepared for as soon as either a critical tumor size of 2500 mm^3 or a deviation of more than 10% of the body weight is reached.

2.15. Statistical Analysis

Experimental data are shown as mean ± SEM. The statistical analysis was performed in GraphPad Prism 8.0. ANOVA followed by the Holm–Sidak test, with multiple comparisons between the different clones in different time points or with different concentrations. *T*-test was used for differences between two groups with one variable. In the graphs, (*) denotes statistically significant differences with $p < 0.05$.

3. Results

3.1. TRPV6 Expression in PDAC Tumor Tissues Correlates with Tumor Stage, Differentiation and Proliferation

To investigate the role of TRPV6 in pancreatic ductal adenocarcinoma (PDAC), the expression of TRPV6 was analyzed in tissue samples from 46 patients with PDAC in different stages. The staining intensity of TRPV6 was compared in tumor tissues against peri-tumoral tissues (as the control) and graded according to the scoring system ranging from 0 (no staining) to 3 (very intense staining) (Figure 1A). For quantitative analysis, we used the H-score, meaning that the staining intensity is the result of the multiplication of the percentage of cells by a certain score given. Based on the TMN, the tumor tissues were separated into lower disease progression (T1/T2) or higher disease progression (T3/T4) (Figure 1B). Histopathological features were used to classify the tumor tissues as highly differentiated or poorly differentiated (Figure 1C). We also investigated the relationship between TRPV6 expression and cell proliferation in PDAC tumor tissues using the proliferation marker Ki-67. The tumor tissues were grouped into four categories based on the percentage of Ki-67 positive cells: 0–5% (lower proliferation), 5–25%, 25–50%, and >50% (higher proliferation). TRPV6 staining intensity was then analyzed as a function of Ki-67 expression (Figure 1C).

TRPV6 expression was found increased with the tumor stage, from the early stages (stages I and II) to the later ones (stages III and IV) (Figure 1D). TRPV6 staining intensity rises by 67.9 ± 23.1% for tumor tissues and 18.3 ± 10.5% for peri-tumoral tissues between the early and late stages. Furthermore, we found that poorly differentiated tumor tissues express more TRPV6 than highly differentiated ones (Figure 1E). Poorly differentiated tissues had a TRPV6 staining intensity of 126.9 ± 16.2. Well-differentiated tissues only had a staining intensity of 81.7 ± 10.1, indicating a 32% decrease in staining compared to poorly differentiated tissues.

A tendency can be observed for an increase in TRPV6 expression with increasing Ki-67 positivity (Figure 1F). It reaches significance for the group with >50% Ki-67 positive cells. The mean TRPV6 staining intensity for each group was as follows: 61.3 ± 9.7 for 0–5%, 72.2 ± 16.5 for 5–25%, 93.7 ± 16.2 for 25–50%, and 230 ± 30 for the group with >50% of Ki-67 positive cells. This indicates that TRPV6 expression is elevated in highly proliferative PDAC tumor cells.

Taken together, our results suggest that TRPV6 expression appears to correlate with PDAC aggressiveness. The following experiments are aimed at revealing how TRPV6 channels may contribute to PDAC aggressiveness.

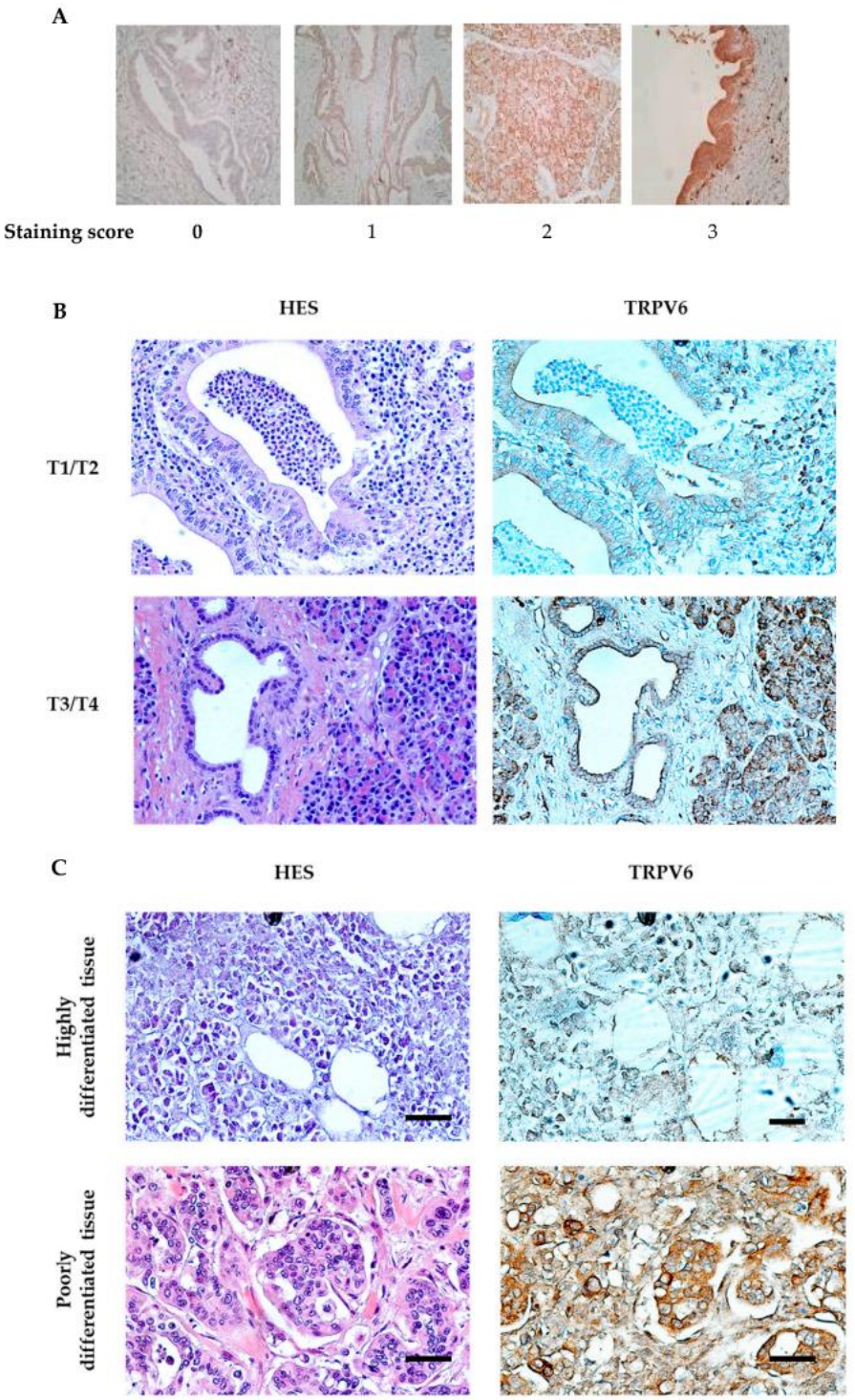

Figure 1. *Cont.*

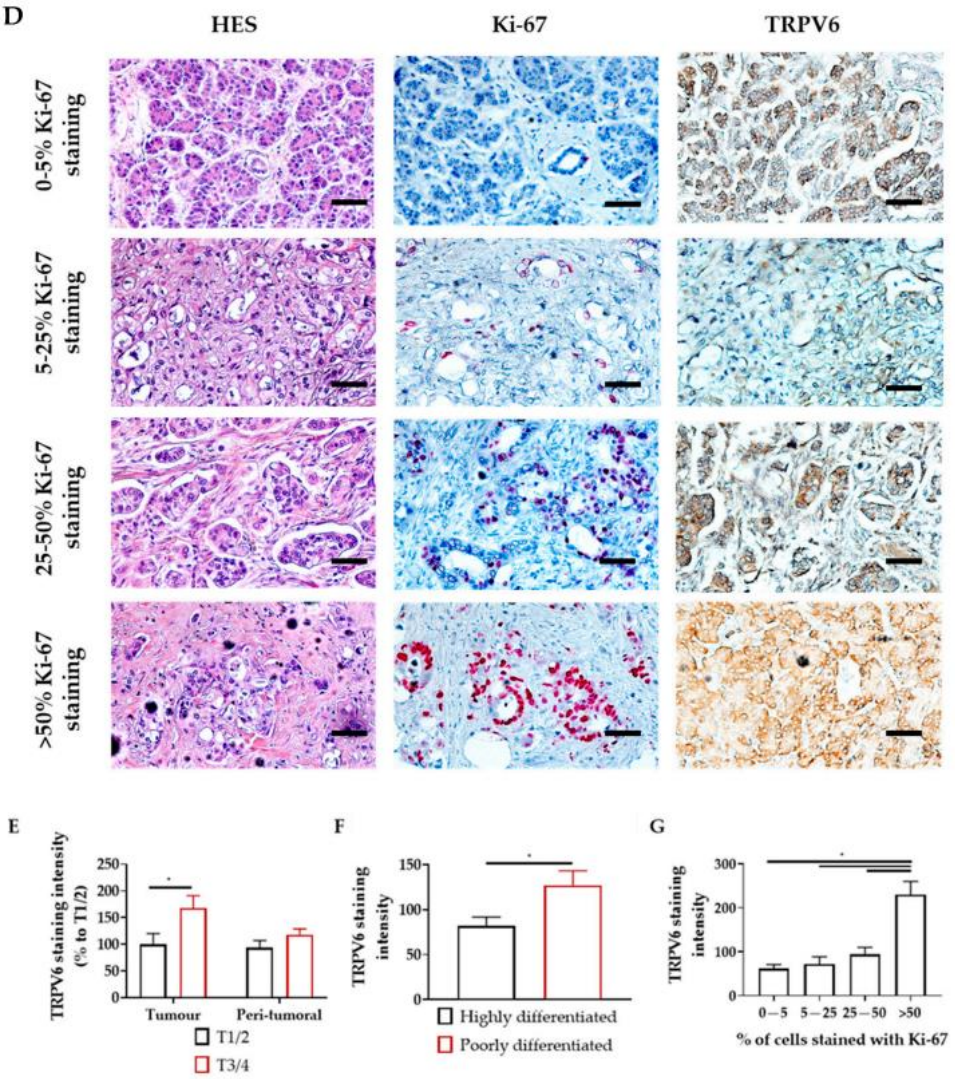

Figure 1. TRPV6 expression correlates with PDAC staging, tissue differentiation and cancer cell proliferation. (**A**) TRPV6 expression was analyzed semi-quantitatively with immunohistochemistry using the TRPV6 antibody Mab82. The expression was scored according to its intensity, ranging from 0 (no staining) to 3 (very intense staining). (**B**) TRPV6 in PDAC tissue from patients in the early stage (top right), late stage (bottom right), with HES staining in the left columns. Scale bars indicate 50 µm. (**C**) TRPV6 staining (brown color) in highly differentiated tissue (top right) or poorly differentiated tissue (bottom right), with HES staining in the left columns. Scale bars indicate 50 µm. (**D**) Ki-67 (blue) and TRPV6 (brown) staining in PDAC tissue. Ki-67 staining (middle column) allowed us to visualize tissue with diverse levels of proliferation. TRPV6 staining (brown color) of the same tissue sections indicates a correlation between TRPV6 expression and the proliferation marker Ki-67, with HES staining in the left columns. Scale bars indicate 50 µm. (**E**) Tumoral and peri-tumoral tissues of 46 PDAC patients were divided into two groups according to their pathological stage (early T1/2 or late T3/4). TRPV6 staining intensities were normalized to the mean values of those found in stage I and II specimen. Error bars represent standard error of the mean of at least three independent tissues. Statistical significance was determined using *t*-test. * $p < 0.05$. (**F**) Tissues were divided into two groups

according to their differentiation. Data represent the TRPV6 staining analysis of the two groups. Error bars represent standard error of the mean of at least three patient tissues. Statistical significance was determined using an unpaired *t*-test. * $p < 0.05$. (**G**) TRPV6 staining intensity as a function of the expression of the proliferation marker Ki-67. Error bars represent standard error of the mean of at least three independent tissues. Statistical significance was determined using one-way ANOVA with the Holm–Sidak method. * $p < 0.05$.

3.2. Characterization of Panc-1 Cells with Altered TRPV6 Expression

In order to investigate the role of TRPV6 channels in mechanistic studies, two groups of stable clones of both Panc-1 and Capan-1 cells were created: one with a knockdown of TRPV6 expression (Panc-1-shTRPV6 or Capan-1-shTRPV6) and one with an overexpression of TRPV6 (Panc-1-mCherry-TRPV6 or Capan-1-mCherry-TRPV6). Each group had a control clone with normal TRPV6 expression (Panc-1[Capan-1]-shLuciferase or Panc-1[Capan-1]-mCherry).

The altered expression of TRPV6 channels was assessed in multiple ways. RNA sequencing analysis revealed the expected difference in the respective mRNA levels in Panc-1 cells. Western blot demonstrated that the RNA levels of the stable clones do translate to changes in protein level in Panc-1 cells. TRPV6 levels in Capan-1 cells were assessed via RT-PCR. Moreover, we assessed the impact of altered TRPV6 expression on the Ca^{2+} influx into Panc-1 cells with the Mn^{2+} quench technique. It is based on the principle that Mn^{2+} enters the cells through similar pathways as Ca^{2+} and quenches the fluorescence of the Ca^{2+}-sensitive dye Fura2AM. The results are shown in Figure 2.

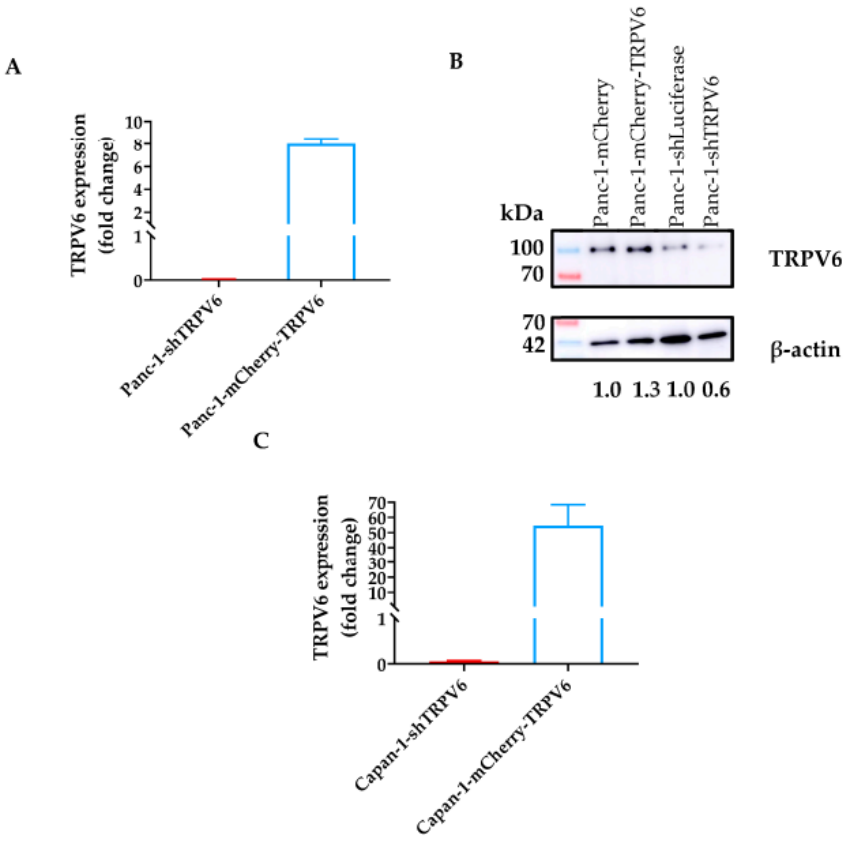

Figure 2. *Cont.*

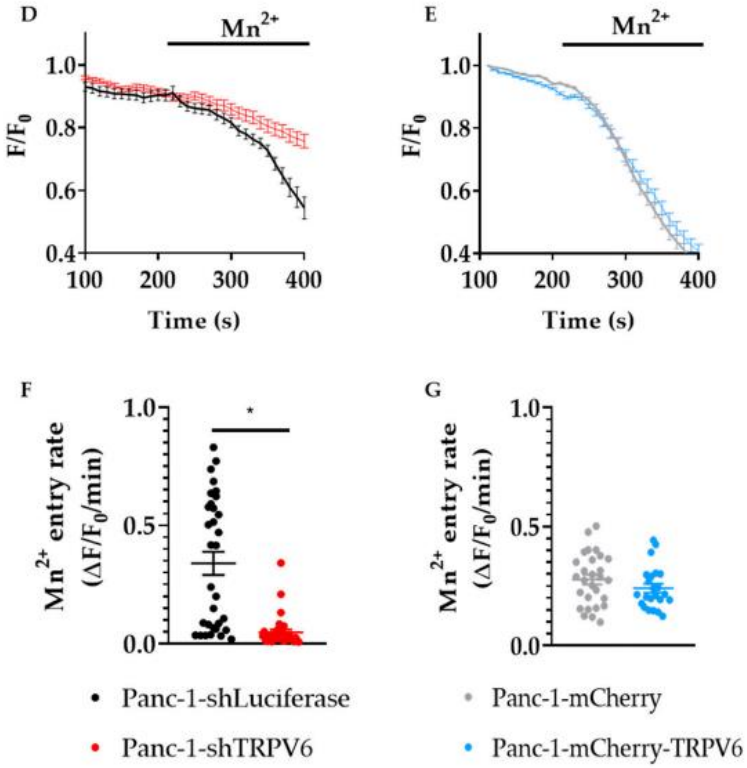

Figure 2. TRPV6 characterization in Panc-1 cells. (**A**) Change in TRPV6 mRNA expression in the knockdown and overexpression Panc-1 clones as determined via RNA sequencing. Changes were normalized to the respective control cell lines and results presented as fold-change. (**B**) Representative immunoblot of whole cell lysates obtained from the stable Panc-1 clones. Channel expression is revealed with a mouse monoclonal anti-TRPV6 antibody. (**C**) Change in TRPV6 mRNA expression in the knockdown and overexpression Capan-1 clones as determined via RT-PCR. (**D**,**E**) Graphical representation of Mn^{2+} quench experiments, evaluated as the fraction of the initial Fura2 fluorescence intensity. (**D**) Panc-1-shLuciferase (black) and Panc-1-shTRPV6 (red); (**E**) Panc-1-mCherry (grey) and Panc-1-mCherry-TRPV6 (blue). (**F**,**G**) Summary of the Mn^{2+} quench experiments. The Mn^{2+} entry rate is calculated as the ratio of the slope of Fura2 fluorescence decline under control conditions and in the presence of Mn^{2+}. Error bars represent standard error of the mean of three replicates. Statistical significance was determined using an unpaired *t*-test. * $p < 0.05$.

TRPV6 knockdown impairs the Ca^{2+} influx into Panc-1 cells, as the Mn^{2+}-induced decline of Fura2 fluorescence intensity occurs more slowly in Panc-1-shTRPV6 cells than in Panc-1-shLuciferase cells. We found no differences in the quench rate between the Panc-1-mCherry-TRPV6 group and the Panc-1-mCherry cells, suggesting that overexpressed TRPV6 channels are apparently not able to significantly impact the Ca^{2+} influx.

3.3. TRPV6 Knockdown Impairs Proliferation, Cell Survival and Cell Cycle Progression of Panc-1 Cells

The proliferation of Panc-1 cells was investigated as a function of TRPV6 expression by counting the cell numbers at t = 0 h, 24 h and 48 h after seeding. Panc-1-shTRPV6 cells proliferate more slowly than Panc-1-shLuciferase cells (186 ± 2.6% vs. 217 ± 6.5% at t = 48 h) (Figure 3A). On the other hand, Panc-1-mCherry-TRPV6 proliferates faster than the Panc-1-mCherry cells (215 ± 10.4% vs. 155 ± 20.7% at t = 48 h) (Figure 3B). To confirm that these results are not influenced by cell death or cells moving from the ocular field, we

counted the mitosis that occurred during the time of the experiment (Figure 3C,D). These results suggest that TRPV6 expression impacts the proliferation of Panc-1 cells positively.

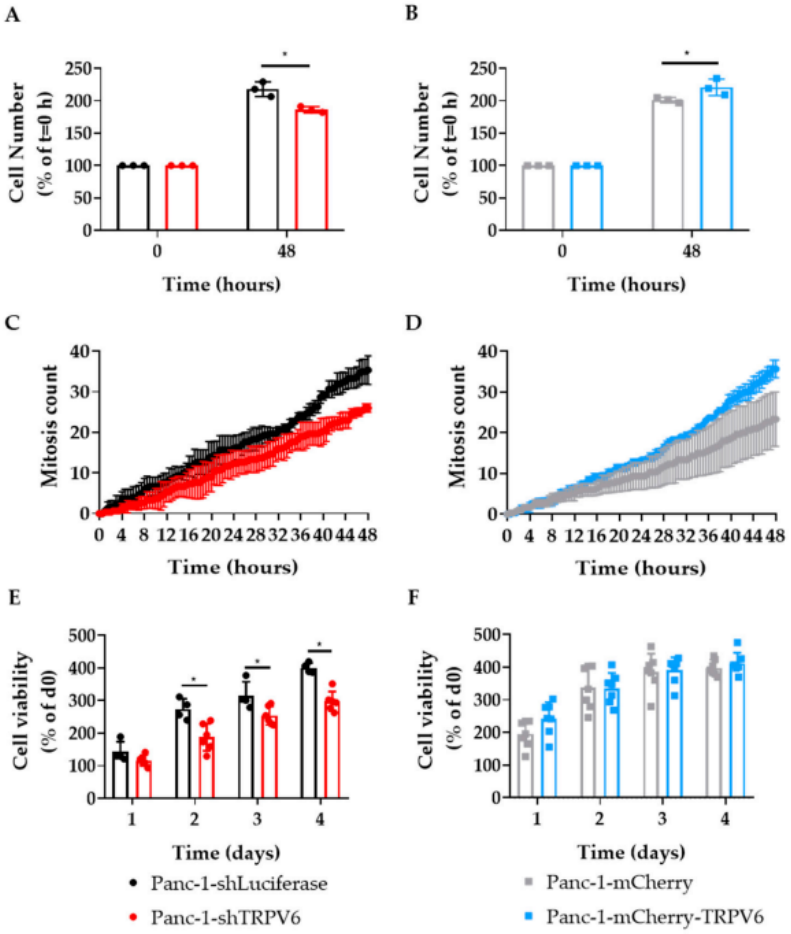

Figure 3. TRPV6 is involved in proliferation and viability of Panc-1 cells. (**A**,**B**) Proliferation of stable Panc-1 cell clones Panc-1-shLuciferase (black) and Panc-1-shTRPV6 (red), Panc-1-mCherry (grey) and Panc-1-mCherry-TRPV6 (blue), 48 h after seeding. Data are expressed as percentage of cell number compared to initial seeding density. Error bars represent standard error of the mean of three replicates. Statistical significance determined using an unpaired *t*-test * $p < 0.05$. (**C**,**D**) Mitosis count Proliferation of stable Panc-1 cell clones Panc-1-shLuciferase (black) and Panc-1-shTRPV6 (red), Panc-1-mCherry (grey) and Panc-1-mCherry-TRPV6 (blue), during 48 h of experiment. (**E**,**F**) Cell viability through ATP concentration of the four stable clones at 24, 48, 72, and 96 h after seeding measured via CellTiter-Glo assay. Data are expressed as percentage of daily luminescence from CellTiter, normalized to the initial luminescence values. Error bars represent standard error of the mean of 4–6 replicates. Statistical significance determined using two-way-ANOVA with Holm–Sidak method * $p < 0.05$.

In order to reveal whether the differences in TRPV6 expression impact cell viability, we measured their impact on the intracellular ATP concentration of our Panc-1 cell lines using CellTiter-Glo assay at 24, 48, 72, and 96 h after seeding. The Panc-1-shTRPV6 cells have lower ATP levels than the Panc-1-shLuciferase cells after 48 h (Figure 3E). This indicates that TRPV6 knockdown reduces the cell survival of Panc-1 cells. On the other hand, there

is no difference in the ATP levels between the Panc-1-mCherry-TRPV6 group and the Panc-1-mCherry group at any time point (Figure 3F).

These results were also similar in Capan-1 cells. The proliferation levels were dependent on TRPV6 expression. Similarly to Panc-1 cells, in Capan-1 cells, the knockdown of TRPV6 led to lower proliferation rates, as opposed to the overexpression of TRPV6 that generated higher proliferation rates (Figure 4A,B). Furthermore, cell viability was also impacted by TRPV6 expression (Figure 4C,D).

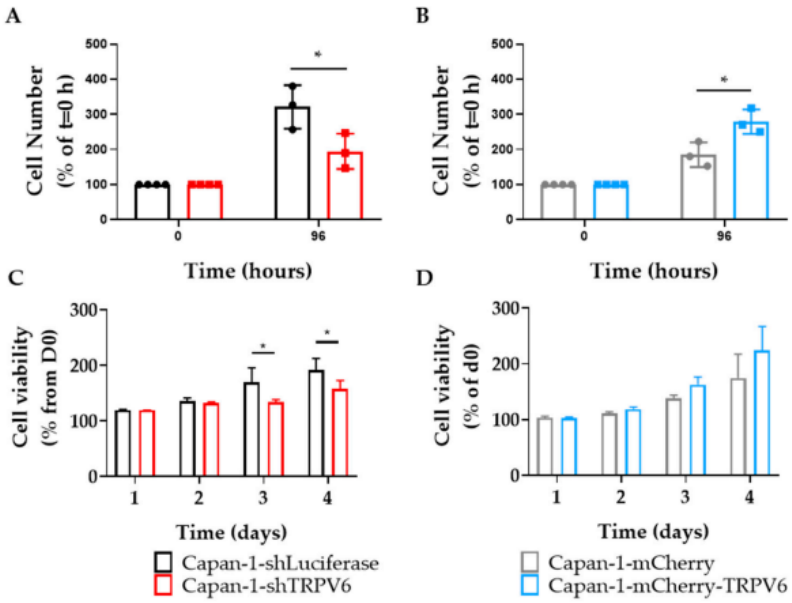

Figure 4. TRPV6 is involved in proliferation and viability of Capan-1 cells. (**A**,**B**) Proliferation of stable Capan-1 cell clones Capan-1-shLuciferase (black) and Capan-1-shTRPV6 (red), Capan-1-mCherry (grey) and Capan-1-mCherry-TRPV6 (blue), 48 h after seeding. Data are expressed as percentage of cell number compared to initial seeding density. Error bars represent standard error of the mean of three replicates. Statistical significance determined using an unpaired *t*-test * $p < 0.05$. (**C**,**D**) Cell viability through MTS of the four stable clones at 24, 48, 72, and 96 h after seeding. Data are expressed as percentage of daily absorbance from MTS reaction, normalized to the initial luminescence values. Error bars represent standard error of the mean of three replicates. Statistical significance determined using unpaired *t*-test * $p < 0.05$.

Cell cycle progression was assessed as a function of TRPV6 channel expression, through propidium iodide staining and flow cytometry, in Panc-1 cells. The focus of the experiment was on the sub-G1 phase of the cell cycle, which represents the fraction of cells with fragmented DNA indicating cell death (Figure 5A). There is a higher percentage of Panc-1-shTRPV6 than Panc-1-shLuciferase cells in the sub-G1 phase (10.8 ± 1.1% vs. 7.8 ± 0.3%) (Figure 5B). This indicates that TRPV6 knockdown induces apoptosis of Panc-1 cells. On the other hand, there is no difference in the sub-G1 phase between Panc-1-mCherry-TRPV6 and Panc-1-mCherry cells (6.5 ± 0.8% vs. 6.6 ± 0.4%) (Figure 5C), indicating that TRPV6 overexpression does not impact the cell cycle progression of Panc-1 cells.

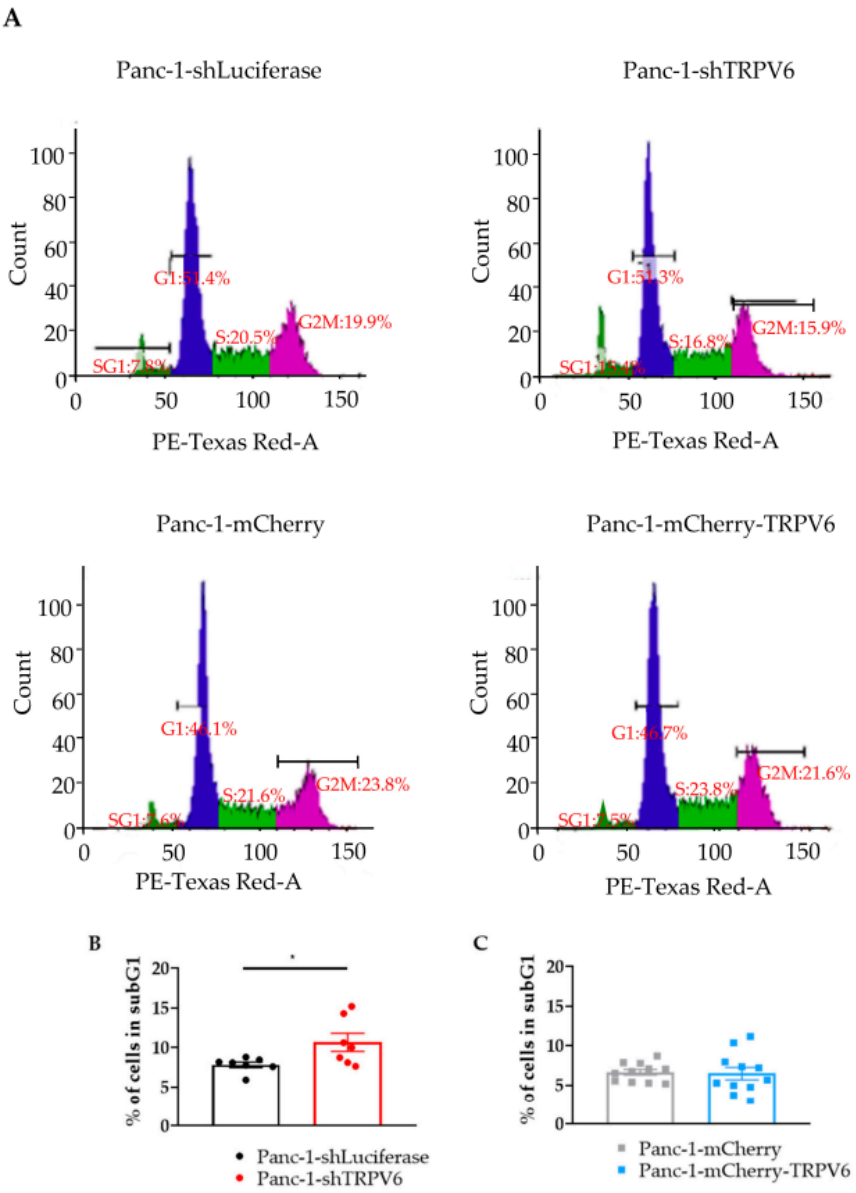

Figure 5. TRPV6 impacts cell cycle progression. (**A**) Representative histogram depicting the cell cycle phases of Panc-1-shLuciferase (top left) and Panc-1-shTRPV6 (top right), Panc-1-mCherry (bottom left) and Panc-1-mCherry-TRPV6 cells (bottom right) determined with propidium iodide staining and flow cytometry. Histograms are divided into four groups: SG1 (sub G1), G1, S and G2M (G2 and M phases). *Y* axis indicates the number of cells, whilst *X* axis indicates staining intensity (DNA quantity). (**B**,**C**) Quantification of cells in the sub-G1 phase, which represents apoptotic cells. Error bars represent standard error of the mean of 7–11 replicates. Statistical significance was determined with unpaired *t*-test * $p < 0.05$.

3.4. TRPV6 Increases Panc-1 Resistance to Chemotherapeutics

The aggressiveness of tumor cells also implies their resistance to chemotherapeutic drugs. We therefore evaluated the effect of TRPV6 expression on the resistance of Panc-1 cells to gemcitabine, cisplatin and 5-fluorouracil (5-FU). These drugs are commonly used in

the treatment of pancreatic cancer. The cells were treated with different concentrations of these agents for 96 h. First, we measured the intracellular ATP concentration of the clones as an indicator of cell viability. We found that TRPV6 knockdown sensitizes Panc-1 cells to 5-FU treatment, as the Panc-1-shTRPV6 cells have lower cell viability levels than the control cells (Panc-1-shLuciferase) after exposure to 1 and 10 µM of 5-FU for 96 h (Figure 6). This suggests that TRPV6 may confer resistance to 5-FU in pancreatic cancer cells. On the other hand, there was no difference in cell viability between the TRPV6 overexpressing cells (Panc-1-mCherry-TRPV6) and the control cells (Panc-1-mCherry) under any condition of 5-FU treatment. There was a tendency for the Panc-1-shTRPV6 cells to have lower cell viability than the Panc-1-shLuciferase group after 96 h of exposure to higher concentrations of gemcitabine or cisplatin. This implies that TRPV6 knockdown might also impact the resistance of Panc-1 cells to gemcitabine or cisplatin.

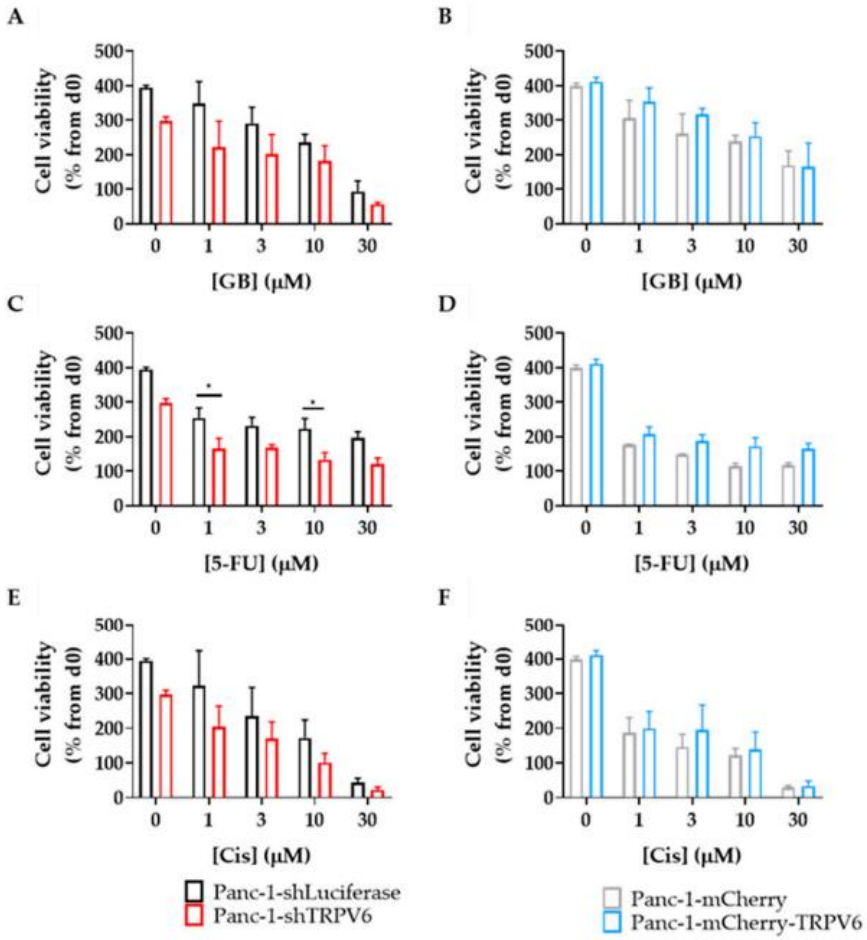

Figure 6. TRPV6 knockdown sensitizes Panc-1 to chemotherapeutics. Cell viability of Panc-1-shLuciferase (black) and Panc-1-shTRPV6 (red), Panc-1-mCherry (grey) and Panc-1-mCherry-TRPV6 cells (blue), after 96 h of treatment with chemotherapeutics, was measured via CellTiter-Glo assay. Stable clones were treated with different concentrations (1, 3, 10 and 30 µM) of (**A**,**B**) gemcitabine (GB), (**C**,**D**) 5-fluorouracil (5-FU) and (**E**,**F**) cisplatin (Cis). Error bars represent standard error of the mean of 4–6 replicates. Statistical significance determined using two-way ANOVA with Holm–Sidak method * $p < 0.05$.

The next goal was to understand whether the apoptosis of Panc-1 cells induced by chemotherapeutic agents is modulated by the expression level of TRPV6 channels.

Therefore, we evaluated annexin V binding to detect the early apoptosis of the cells that were treated with gemcitabine, cisplatin and 5-FU for 24 h. The results are shown in Figure 7. We found that TRPV6 knockdown increases the apoptosis of Panc-1 cells in response to 5-FU and gemcitabine treatment since Panc-1-shTRPV6 cells bind more annexin V than the Panc-1-shLuciferase cells. This confirms that TRPV6 may mediate resistance to 5-FU and, possibly, gemcitabine in pancreatic cancer cells.

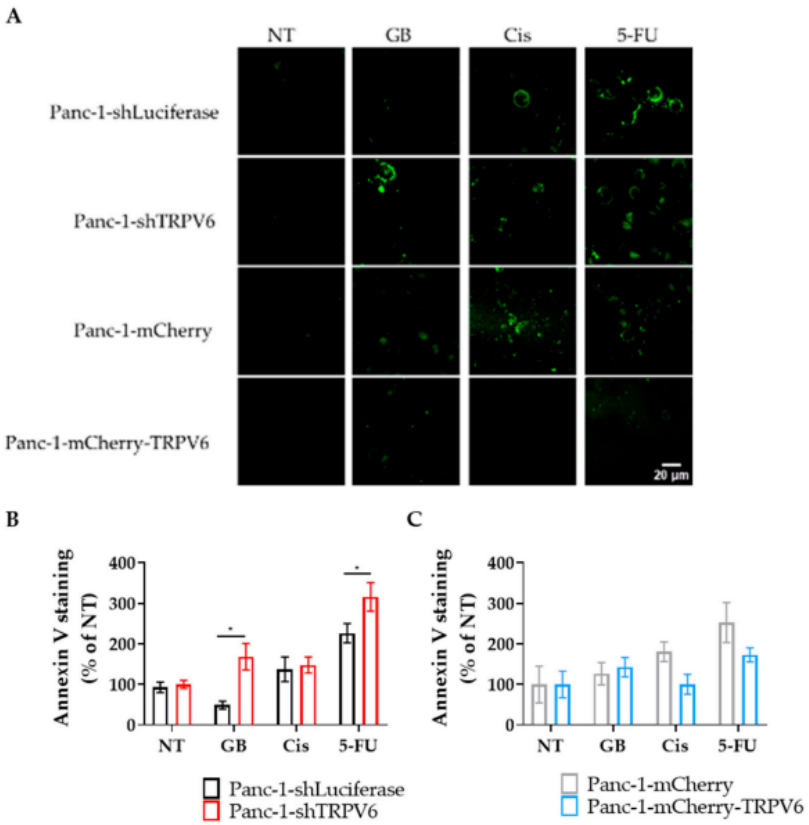

Figure 7. TRPV6 knockdown results in higher Panc-1 cells' apoptosis in response to chemotherapeutics. Panc-1-shLuciferase (black) and Panc-1-shTRPV6 (red), Panc-1-mCherry (grey) and Panc-1-mCherry-TRPV6 cells (blue) were treated with gemcitabine (GB), cisplatin (Cis) or 5-FU for 24 h. Non-treated cells (NT) served as controls. After that period, an annexin V assay was performed and fluorescence intensity of annexin V staining was measured to determine apoptotic cells. (**A**) Representative images of annexin V staining for the stable clones without treatment (NT) and treated with 3 µM of gemcitabine (GB), cisplatin (Cis) or 5-FU, after 24 h. Scale bar represents 20 µm. (**B**,**C**) Differences in annexin V staining between the TRPV6 knockdown or overexpressing Panc-1 cells and their respective controls. Data are expressed as the percentage of annexin staining intensity, compared to the non-treated group. Each replicate has the mean value of 10 cells per field in seven fields evaluated. Error bars represent standard error of the mean of three replicates. Statistical significance was determined using two-way ANOVA with Holm–Sidak method. * $p < 0.05$.

We observed no increase in annexin V binding in TRPV6 overexpressing cells under any of the treatments. Thus, TRPV6 overexpression prevents Panc-1 cells from undergoing apoptosis in response to chemotherapeutics. In contrast, the control cells (Panc-1-mCherry) do bind more annexin V after 5-FU treatment. Collectively, these results suggest that TRPV6 channels contribute to the resistance of pancreatic cancer cells to 5-FU and gemcitabine.

gathered indicate that cells overexpressing TRPV6 have nearly half of the wound area closed compared to the control group. This would normally translate to more proximity between the cells, hence dismissing the possibility that the overexpression of the channels is responsible for this effect.

3.6. TRPV6 Dysregulation Inhibits Tumor Formation In Vivo

So far, we have seen a correlation between TRPV6 staining and tumor aggressiveness in patient samples which we could, by and large, recapitulate in in vitro experiments. To lend further support to this view, we next examined the effect of TRPV6 expression on tumor growth in vivo in a mouse model. We grafted the four Panc-1 cell lines subcutaneously into nude mice and monitored the tumor size weekly for 10 weeks, either by using a caliper to establish a growth curve within a given time frame or by measuring mCherry intensity in the tumor area (for Panc-1-mCherry or Panc-1-mCherry-TRPV6 cells) (Figure 9A). Surprisingly, we found that both control clones form larger tumors than Panc-1-shTRPV6 and Panc-1-mCherry-TRPV6 cells (Figure 9B,C). The mean tumor volume at 10 weeks is 525 $\pm$ 132 mm^3 for Panc-1-mCherry cells, 410 $\pm$ 118 mm^3 for Panc-1-shLuciferase, 194 $\pm$ 30 mm^3 for Panc-1-shTRPV6 cells and 137 $\pm$ 55 mm^3 for Panc-1-mCherry-TRPV6 cells. These results suggest that TRPV6 expression modulates tumor growth in Panc-1 cells and that both low and high levels of TRPV6 channel expression are strongly inhibitory in our setting. The mice weights did not show any significant differences throughout the experiment (Figure S1). Only two mice were sacrificed due to human endpoints, on the 11th week of experimentation (Figure S2). Both of the mice were from the Panc-1-shLuciferase group.

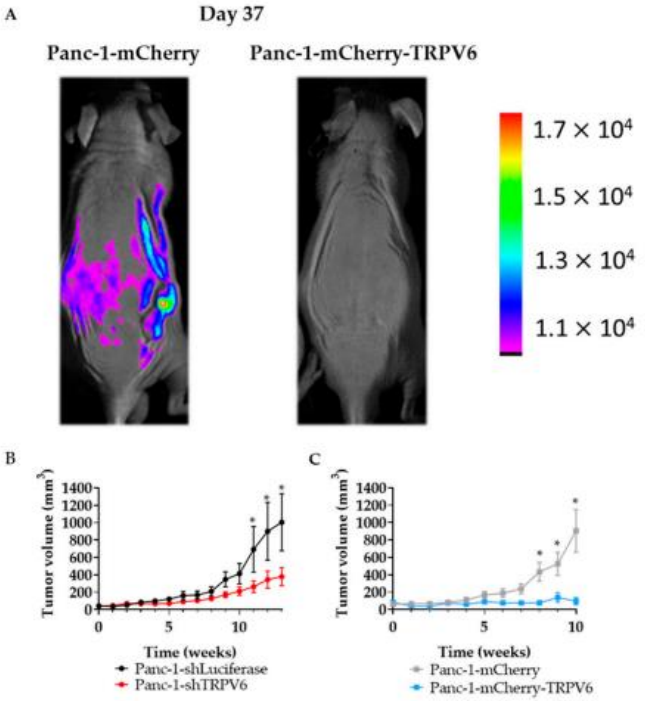

Figure 9. Stable clone with dysregulation of TRPV6 could not promote tumor growth. Nude mice were injected subcutaneously with the four different Panc-1 stable clones. (**A**) Tumor surveillance through mCherry. Representative image comparing the control group (Panc-1-mCherry) with the overexpression of TRPV6 group (Panc-1-mCherry-TRPV6). (**B**) Panc-1-shLuciferase (black) and Panc-1-shTRPV6 (red) (**C**) Panc-1-mCherry (grey) and Panc-1-mCherry-TRPV6 (blue). Tumor growth was evaluated for 10 weeks by measuring and calculating its volume (mm^3). Error bars represent standard error of the mean of 10 mice. Statistical significance was determined using unpaired *t*-test method between each modulated group and its control. * $p < 0.05$.

4. Discussion

In this study, we investigated the role of TRPV6 channels in pancreatic ductal adenocarcinoma (PDAC), a highly aggressive and lethal cancer type. We analyzed the expression of TRPV6 channels in tissue samples from 46 patients with PDAC of different stages and found that TRPV6 expression increased with the tumor stage and dedifferentiation status. Our results show that TRPV6 expression is upregulated in PDAC tumor tissues, but only in the later stages and especially in poorly differentiated ones. This suggests that TRPV6 may be involved in the progression and aggressiveness of PDAC. Previous studies have shown that TRPV6 is overexpressed in various cancers, such as prostate, breast, colon, and ovarian cancers [4–6]. Regarding PDAC, there are contradictory studies [15,16]. In our cohort, it appears that TRPV6 is prominent in the later, more aggressive stages. It should be stated that the tumor generally metastasizes to neighboring tissues in later stages. Furthermore, poorly differentiated tissues are connected to higher tumor progression [24,25]. Similarly to other tumors, TRPV6 appears to correlate with the aggressiveness of PDAC. Accordingly, the presence of the proliferation marker Ki-67 in patient samples correlates with increased TRPV6 expression. This effect was already demonstrated in prostate cancer tissues [10].

In order to investigate the function of TRPV6 channels in PDAC cell behavior, we generated four stable Panc-1 or Capan-1 cell lines with different levels of TRPV6 expression: a knockdown of TRPV6 expression (Panc-1-shTRPV6 or Capan-1-shTRPV6), an overexpression of TRPV6 (Panc-1-mCherry-TRPV6 or Capan-1-mCherry-TRPV6), and a control clone with normal TRPV6 expression (Panc-1[Capan-1]-shLuciferase or Panc-1[Capan-1]-mCherry). We used these cell lines for in vitro and in vivo experiments to assess the effect of TRPV6 expression on the viability, proliferation, resistance, migration, and tumor growth in nude mice.

These cell lines allowed us to confirm several of the findings in vitro that we made in patient tissue. We found that TRPV6 knockdown reduces the cell proliferation and cell viability in Panc-1 and Capan-1 cells, and the cell cycle progression of Panc-1 cells. Conversely, TRPV6 overexpression enhances proliferation. Capan-1 cells were only used to confirm the in vitro data of cell proliferation and viability, which is one of the major findings in our article. In addition to the proliferation and viability results, TRPV6 knockdown induces apoptosis in Panc-1 cells, as indicated by the increased percentage of cells in the sub-G1 phase. The lack of differences between the overexpression and the control in this experiment can be explained due to 3–5% of the cells being naturally in the sub-G1 phase. These results indicate that TRPV6 is involved in survival and growth of PDAC cells, and that its inhibition may trigger cell death. The mechanisms through which TRPV6 regulates these processes are not fully understood but may involve, at least in part, the modulation of Ca^{2+}-dependent signaling pathways. For example, calmodulin, a Ca^{2+}-dependent TRPV6 inhibitor, can control the KRas4B pathway that can impact proliferation [26,27]. The inhibition of calmodulin can lead to effects such as lower proliferation levels, inability to progress in the cell cycle or higher cell death [28,29]. Moreover, store-operated Ca2+ channels (SOCE) can act on Akt/mTor or NF-κB pathways modulating proliferation [30]. In prostate cancer, an interaction between SOCE and TRPV6 was already described and could in principle occur in PDAC as well [10]. TRPV6 was shown to increase proliferation, and lead cells to a more aggressive phenotype in prostate cancer cell lines.

Our results also show that TRPV6 expression influences therapy resistance and the migration of Panc-1 cells, two important features of cancer aggressiveness. We evaluated the effect of TRPV6 expression on the resistance of Panc-1 cells to three chemotherapeutic drugs: gemcitabine, cisplatin, and 5-FU. These drugs are commonly used in the treatment of pancreatic cancer, but often fail to achieve satisfactory outcomes due to the development of drug resistance [31–34]. We found that TRPV6 knockdown sensitizes Panc-1 cells to 5-FU treatment. On the other hand, we found that TRPV6 overexpression does not affect the sensitivity of Panc-1 cells to 5-FU. However, previous reports are inconclusive in this respect, which is likely due to the fact that chemotherapeutics elicit their cell toxicity by means of different mechanisms. 5-FU makes use of Ca^{2+} as a second messenger to induce

the apoptosis of HCT116 colon carcinoma cells [35]. Furthermore, calmodulin inhibition, e.g., through a reduction in the intracellular Ca^{2+} concentration, can impair this process. We therefore believe that our results on chemoresistance of the TRPV6-knockdown cells to 5-FU are unrelated to the Ca^{2+} channel activity of TRPV6 channels. In contrast, our experiments with gemcitabine are in line with the role of TRPV6 as a Ca^{2+} channel. Gemcitabine toxicity is activated by the blockage of calmodulin pathways [36]. The knockdown of TRPV6 can lead to lower levels of calmodulin activation and thereby increase the cytotoxicity of gemcitabine action in PDAC cells [27]. The lack of differences found in the overexpression group when compared to the control, in both chemoresistance and calcium influx, might be an indicator that TRPV6 overexpression does not necessarily translate into higher TRPV6 expression on the membrane. Recently, Kogel et al. indicated that in the HEK293 cell line, TRPV6 has a very short membrane period before a rapid endocytosis [37]. This internalization of TRPV6 might be impacting Ca^{2+} trafficking inside the cells. Thus, TRPV6 could be impacting intracellular homeostasis more than membrane homeostasis. This should be a subject for further studies.

We investigated the effect of TRPV6 expression on the migration of Panc-1 cells using a wound-healing assay. We found that TRPV6 expression negatively regulates the migration of Panc-1 cells. Hence, TRPV6 knockdown enhances the migration of Panc-1 cells, while TRPV6 overexpression impairs it. This effect was quite interesting, seeing that the overexpression of TRPV6 improves proliferation rates, whilst the knockdown gives preference to the migration of the cells. Even though the selection of these phenotypes in the tumor requires different specifications, it was shown that cells can interchange from a more proliferative phenotype to a more migratory one, as was previously suggested in different works [38,39]. Indeed, TRPV6 might rise as a promoter or a switch for these changes. TRPV6 knockdown cells have an increased number of cells in the sub-G1 phase, which clearly demonstrates a deviation from the proliferative phenotype; nonetheless, we could observe that the overexpression of TRPV6 decreases cell motility despite the higher proliferation levels. We also found that TRPV6 knockdown in particular promotes the clustering and a more cohesive movement of Panc-1 cells. In breast and prostate cancer tissues, TRPV6 knockdown appears to impact both cell migration and cell–cell adhesion negatively [12,14].

Our results also show that TRPV6 expression modulates tumor growth in vivo in a mouse model. Surprisingly, we found that both control cell lines form larger tumors than the Panc-1-shTRPV6 and Panc-1-mCherry-TRPV6 cell lines. These results suggest that TRPV6 expression has a biphasic effect on tumor growth in Panc-1 cells and that both low and high levels of TRPV6 can impact tumor development. Future studies will be made on this subject. These findings are unexpected as the in vitro results indicated a positive correlation between TRPV6 expression and cell proliferation. One possible explanation is that TRPV6 expression may affect other aspects of tumor biology, such as angiogenesis, inflammation, or immune response, which are not captured in the in vitro assays [40,41]. Finally, we cannot dismiss the possibility that properties of the tumor microenvironment yet to be identified increase the susceptibility of Panc-1 cells to alterations in their TRPV6 expression.

5. Conclusions

Taken together, our results suggest that the TRPV6 channels play a role in PDAC aggressiveness. The inhibition of TRPV6 may reduce the growth and aggressive phenotype of PDAC cells while rendering them more vulnerable to chemotherapy. This could come with the adverse effect of higher motility of the cancer cells. Further studies are needed to elucidate the molecular mechanisms through which TRPV6 regulates PDAC aggressiveness and to evaluate the therapeutic potential of TRPV6 inhibitors in other PDAC models, like pancreatic cancer organoids.

cells

MDPI

Review

Role of the TRP Channels in Pancreatic Ductal Adenocarcinoma Development and Progression

Gonçalo Mesquita [1,2,3], Natalia Prevarskaya [1,2], Albrecht Schwab [3] and V'yacheslav Lehen'kyi [1,2,*]

[1] Laboratory of Cell Physiology, INSERM U1003, Laboratory of Excellence Ion Channels Science and Therapeutics, Department of Biology, Faculty of Science and Technologies, University of Lille, 59650 Villeneuve d'Ascq, France; goncalo.mesquita@univ-lille.fr (G.M.); natacha.prevarskaya@univ-lille.fr (N.P.)
[2] PHYCELL—Laboratoire de Physiologie Cellulaire, INSERM U1003, University of Lille, 59655 Villeneuve d'Ascq, France
[3] Institute of Physiology II, University Münster, 48149 Münster, Germany; aschwab@uni-muenster.de
* Correspondence: vyacheslav.lehenkyi@univ-lille.fr; Tel.: +33-(0)-3-20-33-70-78; Fax: +33-(0)-3-20-43-40-66

Abstract: The transient receptor potential channels (TRPs) have been related to several different physiologies that range from a role in sensory physiology (including thermo- and osmosensation) to a role in some pathologies like cancer. The great diversity of functions performed by these channels is represented by nine sub-families that constitute the TRP channel superfamily. From the mid-2000s, several reports have shown the potential role of the TRP channels in cancers of multiple origin. The pancreatic cancer is one of the deadliest cancers worldwide. Its prevalence is predicted to rise further. Disappointingly, the treatments currently used are ineffective. There is an urgency to find new ways to counter this disease and one of the answers may lie in the ion channels belonging to the superfamily of TRP channels. In this review, we analyse the existing knowledge on the role of TRP channels in the development and progression of pancreatic ductal adenocarcinoma (PDAC). The functions of these channels in other cancers are also considered. This might be of interest for an extrapolation to the pancreatic cancer in an attempt to identify potential therapeutic interventions.

Keywords: ion channels; TRP channels; pancreatic ductal adenocarcinoma

Citation: Mesquita, G.; Prevarskaya, N.; Schwab, A.; Lehen'kyi, V. Role of the TRP Channels in Pancreatic Ductal Adenocarcinoma Development and Progression. *Cells* **2021**, *10*, 1021. https://doi.org/10.3390/cells10051021

Academic Editor: Saverio Marchi

Received: 18 March 2021
Accepted: 21 April 2021
Published: 26 April 2021

1. Introduction

Fifty years ago, the identification of a mutant fruit fly set the start to the discovery of a superfamily of channels [1]. The gene *trp* was only determined in 1989 and from then on, the TRP family started growing with several members being discovered in numerous independent studies [2]. In 2002 there was a standardization of the nomenclature that led to the formation of the superfamily TRP [3]. The TRP channel superfamily was divided into seven different groups based on sequence homology. For mammals, six subfamilies were reported: the TRPC or canonical family, the TRPV or vanilloid family, the TRPM or Melastatin family, the TRPP or polycystin family, the TRPML or mucolipin family, and the TRPA or ankyrin family (Figure 1). The channels belonging to these families have many diverse functions that include the sensation to pain, temperature, taste, pressure, and vision [4–8]. The role of these channels in diverse cancerous diseases has been established but there is a shortfall in the translation of this knowledge from bench-side to bed-side [9–11]. In pancreatic ductal adenocarcinoma (PDAC), there is a similar occurrence as there is still much work needed in order to better understand the possible roles of TRP channels and how can we take advantage of them clinically. The aim of this review is to summarise the data obtained so far on the expression and function of TRP channels in PDAC development and progression. It becomes evident that these channels have several functions in PDAC pathophysiology and could thereby be potential diagnostic and/or therapeutic targets for the disease.

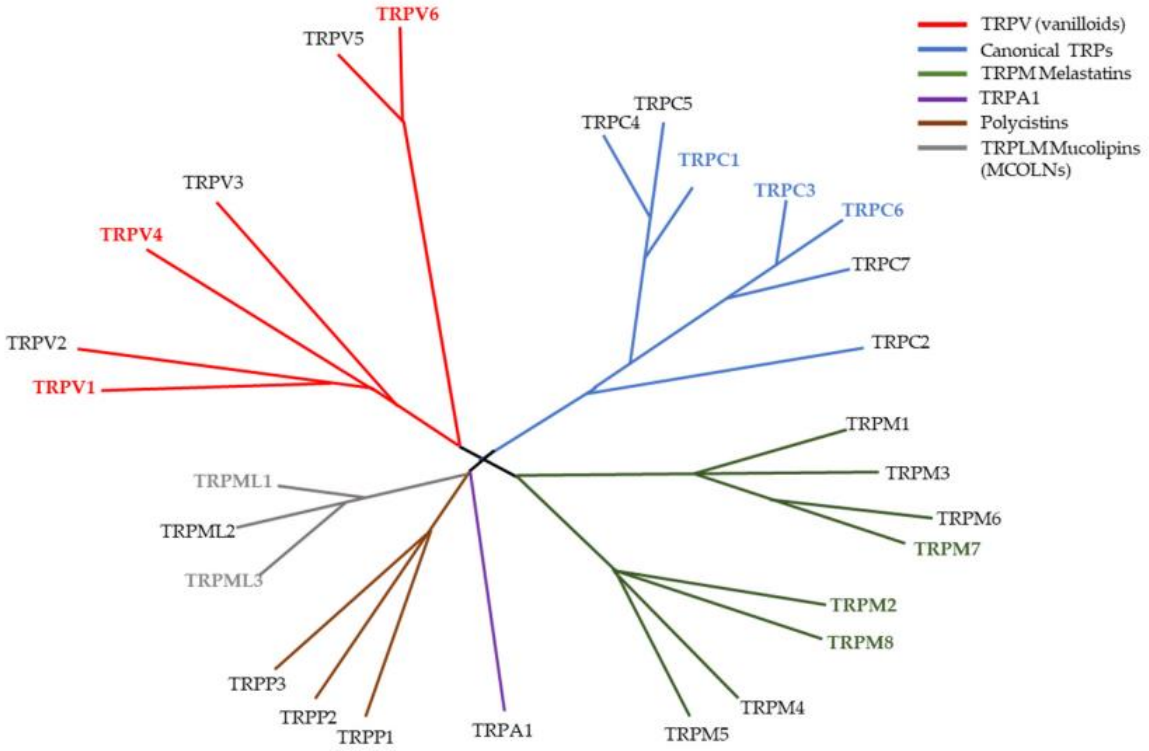

Figure 1. Phylogenetic tree of the TRP superfamily in vertebrates. Highlighted TRP channels (TRPV1, TRPV4, TRPV6, TRPC1, TRPC3. TRPC6, TRPM2, TRPM7, TRPM8, TRPML1 and TRPML3) identify channels that already been study in the context of PDAC and/or pancreatitis. Figure inspired by Clapham D. (2003) [12].

2. Pancreatic Ductal Adenocarcinoma

PDAC is one of the deadliest cancers with the one of the worst outcomes, as the 5-year survival is at 9% [13]. Sadly, there has hardly been any improvement during the last five years. In 2015 the five-year survival was 7.5%. The patients which undergo resection or radical surgery have the best prognosis, but only less than 20% of the patients are diagnosed in a phase when the tumor is resectable [14,15]. The advances in the understanding of this disease have not yet led to an improvement of the patients' outcome [16]. The PDAC microenvironment is very complex, consisting in an interrelationship between cancer cells, fibroblasts, epithelial, endothelial, and immune cells [17]. The formation of a dense stroma (that comprises nearly 90% of all tumor mass) is one of the hallmarks of this cancer [18]. This desmoplasia contributes to the development and progression of the cancer, either by secreting several factors that promote cell proliferation and matrix deposition [19], or by inducing immunosuppression in PDAC [20].

There is one aspect of PDAC pathophysiology that has not yet gained much attention. The development of this disease is also highly connected to Ca^{2+} signalling. Overall, Ca^{2+} has an important role in many cellular processes. The failure to regulate it can lead to known cancer hallmarks, like continued proliferation, tissue invasion and apoptosis resistance [21–23]. Ca^{2+} signalling can have a role in both cell proliferation and cell death. In proliferation, Ca^{2+} has a fundamental role for the initiation and progression of the cell cycle, as evidenced by the cell cycle arrest due to suppression of several Ca^{2+} channels [24].

The role of Ca^{2+} in apoptosis has also been assessed. Apoptosis can occur via the intrinsic or extrinsic pathway. Ca^{2+} plays an important role in the intrinsic pathway. In this pathway, there is an increase in the levels of Ca^{2+} inside the mitochondria which will lead to mitochondrial membrane permeabilization and the release of cytochrome c. This in

turn will start a signalling cascade that culminates in the death of the cell [25]. Cancer cells can find ways to avoid the Ca^{2+}-dependent apoptosis through modulation of Ca^{2+} levels inside the cell. For example, in breast cancer, overexpression of plasma membrane calcium-ATPase 2 helps controlling intracellular Ca^{2+} levels, conferring apoptosis resistance to the cells [26].

The migration processes are responsible for cancerous cell invasion into other tissues. Migrating cells exhibit Ca^{2+} gradients along their front–rear axis [27]. They are instrumental for directional migration. This Ca^{2+} gradient is either due to the activity of Ca^{2+} permeable channels in the plasma membrane or through the mobilization of Ca^{2+} from internal cell stores [28]. Furthermore, in order to migrate away from the primary tumor and invade surrounding tissues cells need to establish contacts with the extracellular-matrix (ECM). Ca^{2+} signalling leads to the disassembly of cell adhesions, with the cleavage of several focal adhesion proteins, through the Ca^{2+} sensitive protease calpain [29]. At the same time, Ca^{2+} signalling is also important for the formation of new adhesion points [30]. Ca^{2+} signalling can induce focal degradation of the ECM, through the upregulation of different matrix metalloproteinases [31,32]. The control and modulation of these Ca^{2+}-dependent processes revolves around the TRP channels. They are both the signaller and the target of Ca^{2+}-dependent processes and thus important players in Ca^{2+} modulated diseases, like cancer [33].

Furthermore, the specific PDAC tumor microenvironment might be impacted by TRP channels modulation. As previously stated, desmoplasia is a common feature in PDAC and consists of a dense layer of extracellular matrix (ECM) and fibroblasts, more known as cancer-associated fibroblasts (CAF) [34]. One of the cell types that can acquire this CAF phenotype are pancreatic stellate cells (PSC). These cells can contribute to the progression and metastasis of the tumor through secretion of cytokines and chemokines, raising of interstitial pressures and promotion of hypoxia [35–37]. TRP channels can be sensitive to all those stimuli or even participate in their signalling cascades (Figure 2).

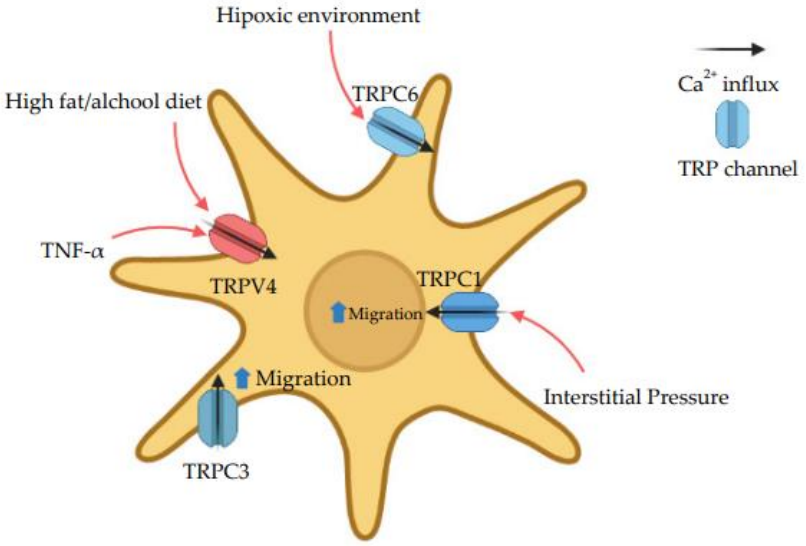

Figure 2. Ca^{2+} modulation by TRP channels in pancreatic stellate cells. These cells are important for the formation of the desmoplasia commonly found in PDAC [35–37]. Several reports have shown the impact that TRP channels might have on the activation and migration of stellate cells [29,38–40] This could bring to light potential therapies involving TRP channels and pancreatic stellate cells, to suppress the desmoplastic reaction.

3. TRP Channels

TRP channels are interesting due to the diversity of cation selectivity and specific activation mechanisms. All the channels possess a molecular structure similar to that of voltage-gated K^+ channels, with six-transmembrane (S1 to S6) polypeptide subunits (with a pore-forming re-entrant loop between S5 and S6) (Figure 3A). They assemble as tetramers to form cation-permeable pores. Their functions vary strongly according to the intracellular domains (Figure 3B) [41,42].

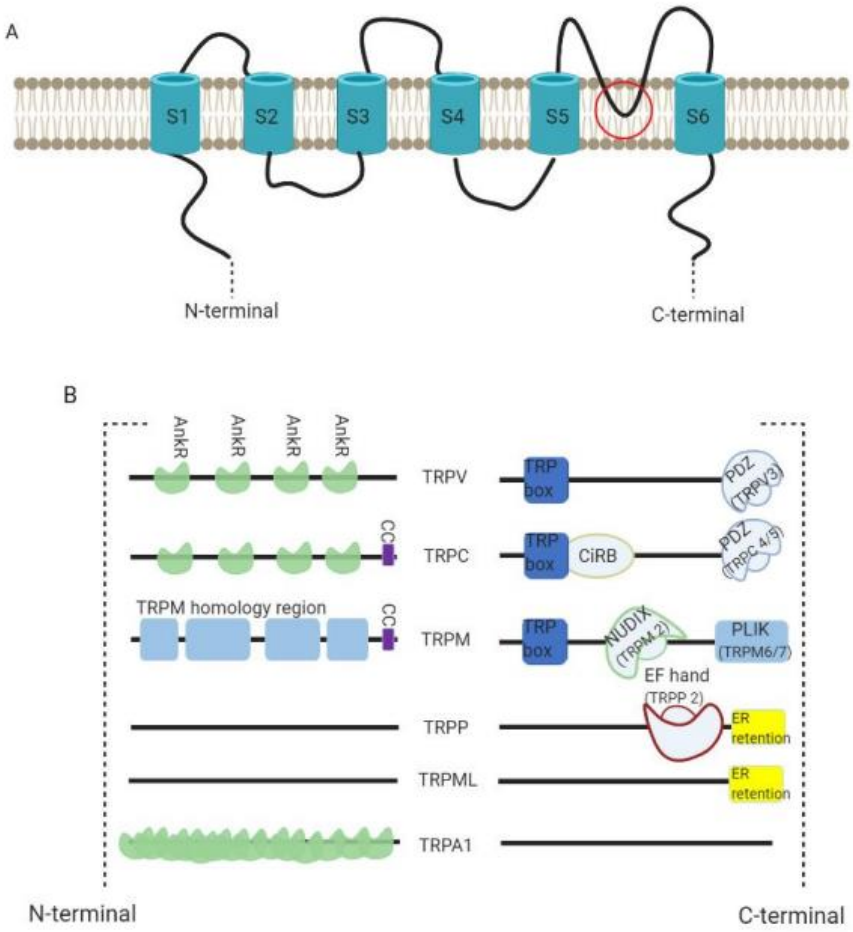

Figure 3. TRP channel structure. (**A**) All the channels possess a six-transmembrane (S1 to S6) polypeptide subunits (with a pore-forming re-entrant loop between S5 and S6 as marked in the figure) that assemble as tetramers to form cation-permeable pores. (**B**) The diversity of the channels is dependent on their C- and N- termini. All TRPV channels have a TRP box at their C-termini and TRPV3 has an additional PDZ binding motif. They have 3–4 Ankyrin repeats (AnkR) in their N-termini. TRPC channels have a TRP box containing the motif EWKFAR plus CIRB (a calmodulin- and inositol triphosphate receptor-binding site). Much like TRPV3, TRPC4/5 have a PDZ binding motif. This subfamily has 3–4 AnkR with an additional coiled-coil domain (CC) in the N-terminus. TRPM channels also have a TRP box in their C-termini. While TRPM2 has NUDIX (a NUDT9 hydrolase protein homologue binding ADP ribose), TRPLM6/7 have PLIK (a phospholipase-C-interacting kinase). In their N-termini, TRPM channels have a CC and a homology region whose functions are unknown. Both TRPP and TRPML have an endoplasmic reticulum retention signal (ER retention) in the C-terminal. TRPP2 also possess a EF-hand (a canonical Ca^{2+}-binding domain) in the N-terminus. TRPA1 channels have a much bigger number of AnkR than TRPV or TRPC. Figure inspired by Clapham D. (2003) [12].

4. TRPM

First described in 1998 by Duncan et al., the TRPM subfamily is the largest of the TRP superfamily [43]. The channels are quite diverse and can be grouped into four groups through phylogenetic analysis: TRPM1/3, TRPM2/8, TRPM4/5 and TRPM6/7 [44]. Several TRPM channels have roles in various cancers, but only TRPM2, 7 and 8 have been studied in PDAC. TRPM4 is connected to other cancers of epithelial origin, such as prostate cancer [45] and breast cancer [46]. Moreover, TRPM6 levels correlate positively with prolonged overall survival of colorectal cancer patients [47].

5. TRPM2

TRPM2 mutations have been associated with the survival time in patients with PDAC. Higher mRNA values of the channel correlate with lower survival times of the patients [48]. The in vitro results showed that TRPM2 is overexpressed in PANC-1 cells and that this overexpression results in enhanced cell proliferation and invasive ability. The authors also present a correlation between the expression levels of TRPM2 and the expression levels of ATP8B4, PARVG, TDRD9, TLR7, and SFMBT2. Of these, TLR7 seems to be the most important, as its expression is almost inexistent in healthy pancreas, but it is present in pancreatic tumor tissue and in pancreatic cancer cell lines [49,50]. TLR7 is implicated in the loss of expression of several players in cell cycle progression like PTEN, p21 or p27 [51]. Furthermore, SFMBT knockdown leads to higher levels of migration and invasion in prostate cancer cell lines [52]. This suggests that further research is required to investigate these associations. The mechanisms by which TRPM2 might impact PDAC progression is far from being understood. It was shown to have a role in promoting the expression of inflammatory cytokines by PDAC cells and enhancing their migratory capacity by importing Ca^{2+} in a pathway which sees SIRT6 modulating intracellular ADPr levels [53].

6. TRPM7

The study of this channel in pancreatic cancer started in zebrafish with a report stating that TRPM7 is functionally required for pancreatic epithelial proliferation [54]. In 2012, Rybarczyk and his colleagues showed that TRPM7 is present in the human pancreatic tissue and involved in magnesium-dependent processes of cell migration. They also showed that this channel is overexpressed in PDAC and inversely correlates with patient survival, which was further confirmed by Yee et al. [55,56]. Additional studies suggest a regulation of MMP expression by TRPM7. Indeed, a correlation between TRPM7 and Hsp90/uPA/MMP-2 pathway was demonstrated, as the silencing of the cation channel in different pancreatic cell lines leads to significantly decreased levels of the proteins of the pathway [57]. More recently, a study demonstrated that TRPM7 interacts with the ribosomal protein SA to promote MIA PaCa-2 cell migration stimulated by elastin-derived peptides [58].

7. TRPM8

The first TRPM channel being reported in pancreatic cancer was TRPM8. In 2010, much like TRPM7 and TRPM2, TRPM8 was reported to be overexpressed in pancreatic cancer cell lines (PANC-1 and BxPC-3) when compared to pancreatic ductal epithelia [59]. Furthermore, TRPM8 was required for maintaining cell proliferation. The silencing of this channel leads to morphological changes at cellular and nuclear levels, suggestive of replicative senescence. The silencing of TRPM8 also leads to an increased proportion of cells in G0/G1 phases and a decrease in S and G2/M phases. The aberrant expression of TRPM8 in humans was later confirmed [60]. The channel is required to prevent non-apoptotic cell death that involves replicative senescence of cancer cells. More studies have arisen to understand the possible role of TRPM8 in this type of cell death. For example, in breast cancer cells, TRPM8 can enhance basal autophagy by positively regulating AMPK [61].

In addition, TRPM8 expression could have a positive correlation with cancer development and metastasis formation. In BxPC-3 and MIAPaCa-2 cell lines, TRPM8 is crucial for the invasive ability of the cancer cells [62]. Furthermore, a comparison of 110 pairs of pan-

creatic cancer tissues and adjacent non-cancerous tissues revealed a correlation of higher expression levels of TRPM8 with worse overall survival and disease-free survival [63]. On the other hand, studies in PANC-1 cells showed that the silencing of TRPM8 stimulates cell migration and proliferation levels [64,65]. Through comparison between glycosylated and un-glycosylated TRPM8, using tunicamycin (an N-glycosylation inhibitor), Ulareanu et al. demonstrated that the un-glycosylated form may have a protective role in PDAC and that this is the form of the channel found in PANC-1 cells [65].

TRPM8 targeting can also be used to enhance the effects of gemcitabine, a common drug used in chemotherapy, in vitro [66]. Combining the silencing of TRPM8 and gemcitabine treatment elicits a more pronounced inhibition of cell proliferation and migration in BXPC-3 and PANC-1 cell lines. This might be explained by the down-regulation of multidrug resistance-related factors, P-gp, MRP-2, and LRP, that occur in response to TRPM8 silencing [66]. These proteins are responsible for cellular efflux of xenobiotics including gemcitabine. New cancer therapies seek the modulation of these proteins in order to achieve higher treatment efficacy [67].

8. TRPV

The Vanilloid subfamily of TRP got its name in 1997 because one of its members, TRPV1, was shown to be activated by the vanilloid compound capsaicin [68]. This subfamily is divided in two groups based on sequence homology; TRPV1 to 4 and TRPV5 and 6. The first four channels are all responsive to high temperatures (from 25 °C, in TRPV4, to 52 °C, in TRPV2) and have nonselective cation conducting pores. TRPV5 and 6 are the most Ca^{2+}-selective TRP channels. TRPV2 has an important role in the pancreatic endocrine system, more specifically in the process of insulin secretion [69]. Although there is no information on this channel regarding PDAC, TRPV2 has been connected to various types of carcinomas. TRPV2 levels are higher in prostate cancer and in human hepatoblastoma, while being lower in urothelial carcinoma [70–72]. Furthermore, it promotes the progression of prostate cancer to more aggressive stages [70]. The presence of TRPV2 in both ductal and acinar cells might be of interest in the study of PDAC [69,73].

9. TRPV1

In 2006 studies connected the role of TRPV1 channels to pancreatic cancer. Hartel et al. demonstrated the overexpression of the TRPV1 in patients with both PDAC and chronic pancreatitis. This overexpression was higher in PDAC than in the chronic pancreatitis. Moreover, there was a positive correlation between pain levels and expression of TRPV1 in PDAC patients [74]. More recently, TRPV1 was found to be an important regulator of EGFR expression [75]. EGFR has been known for a long time as an interesting target in the pathology of cancer in general and PDAC, in particular [76]. It has a relevant role in the development and progression of the disease, like its interaction with the KRAS oncogene or the signalling induction for pancreatic cancer cell migration [77]. Overexpression of TRPV1 (or a TRPV1 agonist) downregulates EGFR expression and its signalling. The opposite occurs upon silencing of TRPV1 [75].

Another important program in PDAC progression is epithelial-to-mesenchymal transition (EMT). One of the EMT activators is Zeb1. Krebs et al. demonstrated that the depletion of Zeb1 leads to reduced invasion, distant metastasis and colonization capabilities in KPC mice [78]. These mice possess a mutation in the *Kras* and *Trp53* genes, which allows the study of PDAC in immunocompetent animals, while experiencing several features observed in human PDAC. TRPV1 might be controlling Zeb1 in pancreatic cancer as it has been shown in hepatocellular carcinoma. The knockout of TRPV1 channels in mice leads to an upregulation of Zeb1 and subsequent promotion of hepatocarcinogenesis [79]. So far, it is not known whether such a link between TRPV1 and Zeb1 also exists in PDAC.

10. TRPV4

Chronic pancreatitis is a major risk factor for the development of PDAC and other pancreatic cancers. The risk of PDAC in a chronic pancreatitis patient is elevated 16-fold [80]. Chronic pancreatitis can develop among others from alcohol, smoking, genetic predisposition, and autoimmunity. Some lesions that occur in pancreatitis (like acinar-ductal metaplasia, activation of PSCs leading to fibrosis) are present in Pancreatic Intraepithelial Neoplasia, which can further evolve into PDAC [81,82].

A correlation between high fat/alcohol and TRPV4 was found in pancreatic stellate cells from Lewis rats [38]. The high fat/alcohol diet leads to increased cytosolic Ca^{2+} mobilization in PSCs which is TRPV4-dependent. Furthermore, this process is enhanced by TNF-α. TRPV4 might be an important player in the development of PDAC from pancreatitis as it modulates Ca^{2+} mobilization in stellate cells and is up-regulated in pancreatic cancer tissues [83]. More recently, a report demonstrated that pressure-induced pancreatitis is promoted by Piezo-1 [84]. The continuous activation of this channel induces Ca^{2+} overload which leads to mitochondrial depolarization and trypsinogen activation in pancreatic acinar cells [85]. TRPV4 is activated by Piezo-1 so that the use of TRPV4 receptor antagonists inhibits the sustained Ca^{2+} elevation. In a mouse model of pancreatitis due to pressure (by pancreatic duct obstruction), TRPV4-KO mice are significantly more protected [85]. This relationship between TRPV4 and Piezo-1 might not be strictly linked to stellate cells. Stress-induced deformation of immune cells occurs in both pancreatitis and PDAC. This occurs as a result of the high interstitial pressure found on these affected tissues and might be activated by cell responses Piezo-1 dependently [36,86].

11. TRPV6

TRPV6 is one of the newest TRP channels studied in the context of PDAC. However, it has several connections to the pancreas. This channel has been described to regulate proliferation of INS-1E cells, which are a model of pancreatic β-cells, and BON-1 cells, which are a model of endocrine tumor cells [87,88]. Furthermore, increasing evidence suggests that the overexpression of TRPV6 is a common event in cancers of epithelial origin, such as ovary, prostate, thyroid and colon [89–92]. This subject can be controversial in PDAC as reports have presented contradictory information. While Zaccagnino et al. found a reduced expression of TRPV6 channels in micro-dissected PDAC samples [93], Song et al. reported an overexpression in PDAC tissues [94]. However, both of these studies did not take into account whether the tissue samples were from invasive or non-invasive parts of the tumor. This is a relevant distinction, as a preponderance of TRPV6 expression was shown for the invasive parts of breast cancer [89]. The silencing of TRPV6 in Capan-2 and SW1900 cells leads to decreased proliferation, increased apoptosis, lower levels of migration and invasion and cell cycle arrest. A phase I clinical trial for SOR-C13, a TRPV6 inhibitor, has been made with some positive results [61]. This trial had included 23 patients with different types of advanced solid tumors, two of whom had PDAC. Stable disease was observed in both patients. One of the patients had a 27% reduction from baseline in the sum of tumor diameters (by RECIST criteria), with a decrease of 55% in tumor marker CA19-9 [95]. TRPV6 levels also correlate with lower survival rates on patients with PDAC [94]. Adding to the fact that TRPV6 is also linked to early onset chronic pancreatitis, a risk factor for the development of PDAC, makes it indispensable to undertake a more detailed analysis of TRPV6 channels in pancreatic cancer [96].

12. TRPML

The TRPML subfamily is represented in mammals by TRPML1, 2 and 3 (also known as MCOLN-1 to 3). Mutations on TRPML1 or TRPML3 can lead to several disorders such as Mucolipidosis type IV (TPLM1) or deafness and pigmentation defects (TPLM3). On the other hand, no disease phenotype has been associated with TRPML2 [97]. Furthermore, this channel has a reduced presence in the pancreas [98].

13. TRPML1

TRPML1 is the founding member of the mucolipins subfamily of TRP. In pancreatic cancer this channel might predict poor survival of the patients with PDAC. In a study with 80 PDAC patients, high levels of TRPML1 are associated with a short overall survival and relapse-free survival compared to the patients with lower levels of the channel. Furthermore, downregulating the expression of TRPLM1 in BxPC-3 and PANC-1 pancreatic cancer cell lines leads to lower proliferation levels. When transfecting PANC-1 cells into the mice, the tumors have significantly less volume when the TRPML1 channel was silenced [99].

14. TRPML3

TRPML3 belongs to a set of nine genes whose signature was identified in an in-silico analysis to predict overall survival of PDAC patients [100]. Based on the role of TRPML3 in autophagy in HEK293T cells [101], the authors proposed that TRPML3 might exert its tumor suppressive effects in PDAC by this mechanism, too. So far, functional data are missing.

15. TRPC

This subfamily consists in seven members (TRPC1-7), all expressed in humans, except for TRPC2, which is a pseudogene. Although these channels contribute to the progression of several different cancers, their function in pancreatic cancer cells has not yet been studied in greater detail. However, a role of this subfamily has been described for pancreatic stellate cells.

16. TRPC1

The role of TRPC1 in migration of PDAC cell lines (BxPC-3) was investigated [102,103]. Firstly, in BxPC-3 cells, TGF-β could induce PKC-α through its translocation to the plasma membrane. This activation could be the result of the mobilization of intracellular Ca^{2+} by TGF-β. Furthermore, they confirmed that TGF-β can induce PTEN suppression and increase cell motility PKC-α dependently [102]. The only TRPC channels present in BxPC-3 are TRPC1, 4, and 6. Of these three, co-silencing of TRPC1 and NCX1 was able to inhibit TGF-β induced cell motility [103]. On another note, Fels et al. suggested that TRPC1 channels contribute to the pressure-induced activation of pancreatic stellate cells [39,104]. Using primary stellate cells from mice, it was observed that the knock-out of TRPC1 leads to significantly lower levels of cell migration after pressure incubation. Cell migration was used as a functional read-out of pancreatic stellate cell activation. Furthermore, the loss of TRPC1 channels causes a reduced Ca^{2+} influx after pressure incubation. These differences were not noticed under control conditions [39].

17. TRPC3

Not much is known about the role of TRPC3 in PDAC, but a recent study in RLT-PSC (pancreatic stellate cell line) opened the discussion on this channel. TRPC3 plays a role in the migration of stellate cells. It does so through an interplay with the Ca^{2+} sensitive K^+ channel of intermediate conductance, $K_{Ca}3.1$. Moreover, the suggested hypothesis is that the $K_{Ca}3.1$ takes advantage of Ca^{2+} entering the cells through TRPC3 channels to activate calpain and promote deadhesion of the stellate cells [29].

18. TRPC6

As observed with TRPC1 and TRPC3, TRPC6 also modulates pancreatic stellate cell behaviour [40]. In primary murine pancreatic stellate cells, the knock-out of TRPC6 leads to impaired cell migration when the cells were exposed to a hypoxic environment. Pre-treating the cells in a hypoxic environment or inducing chemical hypoxia with dimethyloxalylglycine (DMOG), leads to increased migratory activity of wild-type cells but not of TRPC6 knock-out cells. Similarly, hypoxia increases Ca^{2+} influx and cytokine secretion in a TRPC6-

dependent manner in pancreatic stellate cells. These TRPC6-dependent processes can lead to a continuous autocrine activation of pancreatic stellate cells and PDAC progression [40].

TRPC6 channels are also crucial for CXCR2-mediated responses of neutrophils. This has a great importance due to the role of neutrophils in the development of PDAC [105]. Neutrophils are part of the desmoplastic tumor microenvironment and a high density of intratumoral neutrophil granulocytes is associated with poor patient survival. Their recruitment needs CXCR2 signaling, which is TRPC6-dependent [106].

19. Targeting TRP Channels in PDAC

The current treatment of PDAC varies depending on the phase the cancer is diagnosed. Surgery is the still the only way to cure PDAC, but that it is a choice for patients diagnosed with resectable tumors only. Such an early diagnosis only occurs in ~20% of the cases [107,108]. This calls for better diagnostic tools and for a bigger array of biomarkers for PDAC. The TRPM channels appear to be overexpressed in PDAC. TRPM2 and 7 are overexpressed in humans while TRPM8 is reported overexpressed in pancreatic cancer cell lines. Further studies should focus on understanding on which PDAC stage these channels start being overexpressed, in order to understand the potential for these channels as diagnostic markers. For later stages of PDAC, the commonly used treatments are FOLFIRINOX and nab-paclitaxel–gemcitabine [107]. One example of a possible targeted therapy in the silencing of TRPM8, which enhances the effects of gemcitabine in vitro, in pancreatic cancer cell lines [66]. Nonetheless, the patients' average time of survival in these later stages is below 12 months. The future strategies might involve more co-adjuvants that lead to better efficacy of the current drugs. The desmoplastic stroma is a hindrance to the development of more effective treatments for PDAC. Much of the chemo-resistance and high interstitial pressure derives from the desmoplasia processes. Furthermore, stomal cells like PSCs are crucial in the development of PDAC. Pothula et al. presented a novel therapeutic approach to PDAC by targeting a factor secreted by PSCs [109]. This treatment, in mice, managed to surpass the efficacy of gemcitabine in reducing tumor angiogenesis and metastasis. TRP channels could be a target to control the activation of PSCs and prevent the continuous stroma-tumor interactions. Both TRPV4 and TRPC1 are possible targets due to their role in PSCs pressure-induced activation [39,85]. A therapy with focus on TRP channels could be the key to augment the efficacy of current treatments by focusing the specific tumor microenvironment present in PDAC.

Nonetheless, to this day, no pharmacological agents targeting TRP channels have succeed in becoming a normalized treatment. A phase I clinical trial has been undertaken for an antagonist for TRPV6 in solid tumors. As mentioned above, this trial demonstrated that the use of SOR-C13 leads to reduced tumor size and CA19-9 marking. This treatment was made on patients with advanced tumors. One of the biggest obstacles to the development of TRP-related therapies might be to find specific inhibitors for each TRP channel. Not all TRP channels possess a specific antagonist like TRPM3 [110] or TRPV4 [111]. Some antagonists have achieved phase I clinical trials, like AMG 517 (TRPV1 antagonist), but ended up failing, as the treatment in humans elicited long-lasting hyperthermia [112].

For palliative care, a targeted therapy against TRPV1 might be of interest. As stated before, the intensity of pain reported by PDAC patients is correlated with the expression of TRPV1 [74]. Using an in vivo bone cancer model, Ghilardi et al. demonstrated the potential in targeting TRPV1 with an antagonist (JNJ-17203212) [113]. Mice with TRPV1 knockout and TRPV1 antagonist experienced a significant attenuation in pain-related behaviors in comparison to wild-type animals [113].

20. Conclusions

Despite of multiple efforts to understand and treat PDAC, the overall survival of the patients has not been vastly improved. Nonetheless, a lot of data has been surging in the past years. Taking advantage of that, in the last decade, the TRP channels have been appearing in a diversity of scientific works concerning their expression in the tumor

tissue and the possible effects that they exert on the development and progression of PDAC. Almost every TRP subfamily present in humans seems to play a role in this disease. These ion channels might be a crucial tool, not only in the diagnosis of PDAC, but also as a therapeutic target that can be combined with traditional treatments. Numerous possibilities might arise from further studies on the TRP family, as there are still many unanswered questions. How can we translate this knowledge from bench to bed-side? There is a gap in our understanding of redundancy among these channels. Several studies demonstrated that the knockdown of a TRP channel leads to the upregulation of other TRP channels in order to balance it [39,114,115]. How can we circumvent these mechanisms to achieve better efficacy in treatment? Furthermore, a better understanding on the relationship between these ion channels and the immune system is pivotal as demonstrated by the role of TRPC6 in neutrophil chemotaxis [106]. Lastly, the increasing attention given to the stroma cells should be correlated with the TRP superfamily. Several of these channels have an impact on stellate cell migration and activation. Further study is needed to better understand the possible roles of TRP channels in the development of the specific tumor microenvironment found in PDAC.

The critical need for better diagnosis tools and new therapeutics might have a solution in this big family of ion channels that can affect both pancreatic cancer cells and pancreatic stellate cells and have roles in cell proliferation, migration, invasion, and death, as summarized in Figure 4.

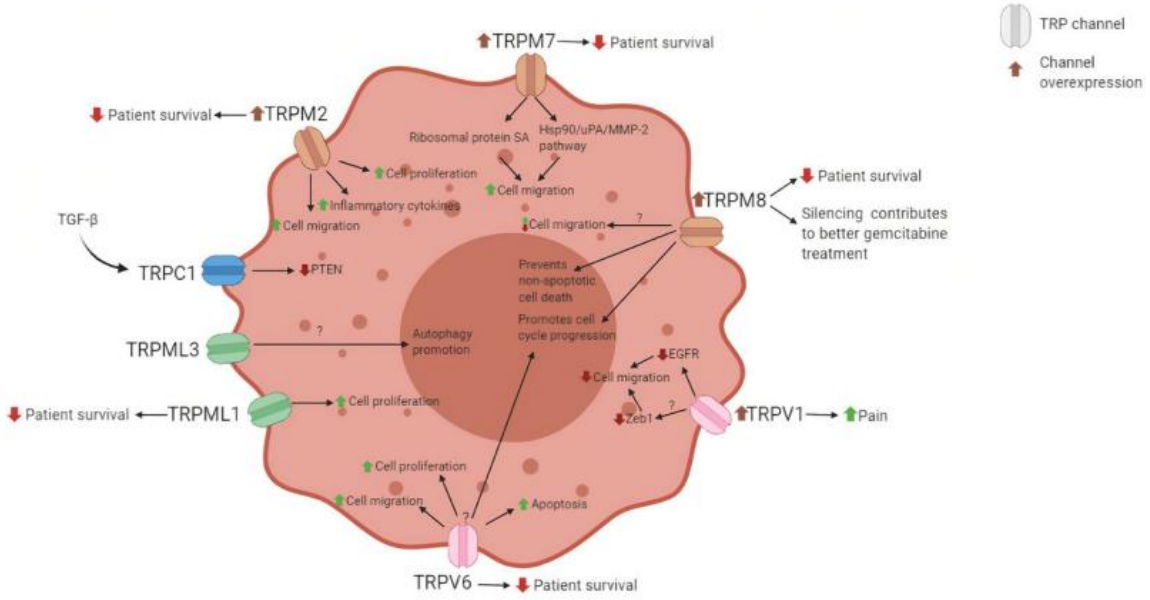

Figure 4. Summary of the roles and possible effects of the TRP channels in the pancreatic cancer cell. The TRP channels exert several changes to the PDAC cells. The expression of these channels correlates negatively with patient survival and may act on the level of cell proliferation, migration and apoptosis.

9. References

Andersen, A. P., J. M. Moreira and S. F. Pedersen (2014). "Interactions of ion transporters and channels with cancer cell metabolism and the tumour microenvironment." Philos Trans R Soc Lond B Biol Sci **369**(1638): 20130098.

Bai, S., Y. Wei, R. Liu, Y. Chen, W. Ma, M. Wang, L. Chen, Y. Luo and J. Du (2023). "The role of transient receptor potential channels in metastasis." Biomed Pharmacother **158**: 114074.

Berchtold, M. W. and A. Villalobo (2014). "The many faces of calmodulin in cell proliferation, programmed cell death, autophagy, and cancer." Biochim Biophys Acta **1843**(2): 398-435.

Bernardini, M., A. Brossa, G. Chinigo, G. P. Grolez, G. Trimaglio, L. Allart, A. Hulot, G. Marot, T. Genova, A. Joshi, V. Mattot, G. Fromont, L. Munaron, B. Bussolati, N. Prevarskaya, A. Fiorio Pla and D. Gkika (2019). "Transient Receptor Potential Channel Expression Signatures in Tumor-Derived Endothelial Cells: Functional Roles in Prostate Cancer Angiogenesis." Cancers (Basel) **11**(7).

Bettaieb, L., M. Brule, A. Chomy, M. Diedro, M. Fruit, E. Happernegg, L. Heni, A. Horochowska, M. Housseini, K. Klouyovo, A. Laratte, A. Leroy, P. Lewandowski, J. Louvieaux, A. Moitie, R. Tellier, S. Titah, D. Vanauberg, F. Woesteland, N. Prevarskaya and V. Lehen'kyi (2021). "Ca(2+) Signaling and Its Potential Targeting in Pancreatic Ductal Carcinoma." Cancers (Basel) **13**(12).

Bhardwaj, R., S. Lindinger, A. Neuberger, K. D. Nadezhdin, A. K. Singh, M. R. Cunha, I. Derler, G. Gyimesi, J. L. Reymond, M. A. Hediger, C. Romanin and A. I. Sobolevsky (2020). "Inactivation-mimicking block of the epithelial calcium channel TRPV6." Sci Adv **6**(48).

Bianco, S. D., J. B. Peng, H. Takanaga, Y. Suzuki, A. Crescenzi, C. H. Kos, L. Zhuang, M. R. Freeman, C. H. Gouveia, J. Wu, H. Luo, T. Mauro, E. M. Brown and M. A. Hediger (2007). "Marked disturbance of calcium homeostasis in mice with targeted disruption of the Trpv6 calcium channel gene." J Bone Miner Res **22**(2): 274-285.

Bodding, M. (2005). "Voltage-dependent changes of TRPV6-mediated Ca2+ currents." J Biol Chem **280**(8): 7022-7029.

Bodding, M., U. Wissenbach and V. Flockerzi (2002). "The recombinant human TRPV6 channel functions as Ca2+ sensor in human embryonic kidney and rat basophilic leukemia cells." J Biol Chem **277**(39): 36656-36664.

Bodkin, J. V. and S. D. Brain (2011). "Transient receptor potential ankyrin 1: emerging pharmacology and indications for cardiovascular biology." Acta Physiol (Oxf) **203**(1): 87-98.

Bolanz, K. A., M. A. Hediger and C. P. Landowski (2008). "The role of TRPV6 in breast carcinogenesis." Mol Cancer Ther **7**(2): 271-279.

Borowiec, A. S., G. Bidaux, N. Pigat, V. Goffin, S. Bernichtein and T. Capiod (2014). "Calcium channels, external calcium concentration and cell proliferation." Eur J Pharmacol **739**: 19-25.

Bortner, C. D. and J. A. Cidlowski (2014). "Ion channels and apoptosis in cancer." Philos Trans R Soc Lond B Biol Sci **369**(1638): 20130104.

Bose, T., A. Cieslar-Pobuda and E. Wiechec (2015). "Role of ion channels in regulating Ca(2)(+) homeostasis during the interplay between immune and cancer cells." Cell Death Dis **6**(2): e1648.

Bovelstad, H. M. and O. Borgan (2011). "Assessment of evaluation criteria for survival prediction from genomic data." Biom J **53**(2): 202-216.

Brassart-Pasco, S., S. Brezillon, B. Brassart, L. Ramont, J. B. Oudart and J. C. Monboisse (2020). "Tumor Microenvironment: Extracellular Matrix Alterations Influence Tumor Progression." Front Oncol **10**: 397.

Bryant, K. L., J. D. Mancias, A. C. Kimmelman and C. J. Der (2014). "KRAS: feeding pancreatic cancer proliferation." Trends Biochem Sci **39**(2): 91-100.

Buch, T. R. H., E. A. M. Buch, I. Boekhoff, D. Steinritz and A. Aigner (2018). "Role of Chemosensory TRP Channels in Lung Cancer." Pharmaceuticals (Basel) **11**(4).

Bulk, E., L. M. Todesca and A. Schwab (2021). "Ion Channels in Lung Cancer." Rev Physiol Biochem Pharmacol **181**: 57-79.

Can, G., B. Akpinar, Y. Baran, B. Zhivotovsky and M. Olsson (2013). "5-Fluorouracil signaling through a calcium-calmodulin-dependent pathway is required for p53 activation and apoptosis in colon carcinoma cells." Oncogene **32**(38): 4529-4538.

Cannon, A., C. Thompson, B. R. Hall, M. Jain, S. Kumar and S. K. Batra (2018). "Desmoplasia in pancreatic ductal adenocarcinoma: insight into pathological function and therapeutic potential." Genes Cancer **9**(3-4): 78-86.

Carrato, A., A. Falcone, M. Ducreux, J. W. Valle, A. Parnaby, K. Djazouli, K. Alnwick-Allu, A. Hutchings, C. Palaska and I. Parthenaki (2015). "A Systematic Review of the Burden of Pancreatic Cancer in Europe: Real-World Impact on Survival, Quality of Life and Costs." J Gastrointest Cancer **46**(3): 201-211.

Chemaly, E. R., L. Troncone and D. Lebeche (2018). "SERCA control of cell death and survival." Cell Calcium **69**: 46-61.

Chen, Y. F., Y. T. Chen, W. T. Chiu and M. R. Shen (2013). "Remodeling of calcium signaling in tumor progression." J Biomed Sci **20**: 23.

Chigurupati, S., R. Venkataraman, D. Barrera, A. Naganathan, M. Madan, L. Paul, J. V. Pattisapu, G. A. Kyriazis, K. Sugaya, S. Bushnev, J. D. Lathia, J. N. Rich and S. L. Chan (2010). "Receptor channel TRPC6 is a key mediator of Notch-driven glioblastoma growth and invasiveness." Cancer Res **70**(1): 418-427.

Chinigo, G., H. Castel, O. Chever and D. Gkika (2021). "TRP Channels in Brain Tumors." Front Cell Dev Biol **9**: 617801.

Chow, J., M. Norng, J. Zhang and J. Chai (2007). "TRPV6 mediates capsaicin-induced apoptosis in gastric cancer cells--Mechanisms behind a possible new "hot" cancer treatment." Biochim Biophys Acta **1773**(4): 565-576.

Clapham, D. E. (2003). "TRP channels as cellular sensors." Nature **426**(6966): 517-524.

Cook, N., R. Brais, W. Qian, C. C. Hak and P. G. Corrie (2015). "Endothelin-1 and endothelin B receptor expression in pancreatic adenocarcinoma." J Clin Pathol **68**(4): 309-313.

Cosens, D. J. and A. Manning (1969). "Abnormal electroretinogram from a Drosophila mutant." Nature **224**(5216): 285-287.

D'Souza, R. S., J. Y. Lim, A. Turgut, K. Servage, J. Zhang, K. Orth, N. G. Sosale, M. J. Lazzara, J. Allegood and J. E. Casanova (2020). "Calcium-stimulated disassembly of focal adhesions mediated by an ORP3/IQSec1 complex." Elife **9**.

Dardare, J., A. Witz, J. L. Merlin, P. Gilson and A. Harle (2020). "SMAD4 and the TGFbeta Pathway in Patients with Pancreatic Ductal Adenocarcinoma." Int J Mol Sci **21**(10).

De Donatis, A., F. Ranaldi and P. Cirri (2010). "Reciprocal control of cell proliferation and migration." Cell Commun Signal **8**: 20.

Dhaka, A., V. Uzzell, A. E. Dubin, J. Mathur, M. Petrus, M. Bandell and A. Patapoutian (2009). "TRPV1 is activated by both acidic and basic pH." J Neurosci **29**(1): 153-158.

Dhennin-Duthille, I., M. Gautier, M. Faouzi, A. Guilbert, M. Brevet, D. Vaudry, A. Ahidouch, H. Sevestre and H. Ouadid-Ahidouch (2011). "High expression of transient receptor potential channels in human breast cancer epithelial cells and tissues: correlation with pathological parameters." Cell Physiol Biochem **28**(5): 813-822.

Fang, Y., G. Liu, C. Xie, K. Qian, X. Lei, Q. Liu, G. Liu, Z. Cao, J. Fu, H. Du, S. Liu, S. Huang, J. Hu and X. Xu (2018). "Pharmacological inhibition of TRPV4 channel suppresses malignant biological behavior of hepatocellular carcinoma via modulation of ERK signaling pathway." Biomed Pharmacother **101**: 910-919.

Fedchenko, N. and J. Reifenrath (2014). "Different approaches for interpretation and reporting of immunohistochemistry analysis results in the bone tissue - a review." Diagn Pathol **9**: 221.

Fels, B., E. Bulk, Z. Petho and A. Schwab (2018). "The Role of TRP Channels in the Metastatic Cascade." Pharmaceuticals (Basel) **11**(2).

Fiorio Pla, A. and D. Gkika (2013). "Emerging role of TRP channels in cell migration: from tumor vascularization to metastasis." Front Physiol **4**: 311.

Fiorio Pla, A. and L. Munaron (2014). "Functional properties of ion channels and transporters in tumour vascularization." Philos Trans R Soc Lond B Biol Sci **369**(1638): 20130103.

Foulon, A., P. Rybarczyk, N. Jonckheere, E. Brabencova, H. Sevestre, H. Ouadid-Ahidouch and L. Rodat-Despoix (2022). "Inositol (1,4,5)-Trisphosphate Receptors in Invasive Breast Cancer: A New Prognostic Tool?" Int J Mol Sci **23**(6).

Fu, S., H. Hirte, S. Welch, T. T. Ilenchuk, T. Lutes, C. Rice, N. Fields, A. Nemet, D. Dugourd, S. Piha-Paul, V. Subbiah, L. Liu, J. Gong, D. Hong and J. M. Stewart (2017). "First-in-human phase I study of SOR-C13, a TRPV6 calcium channel inhibitor, in patients with advanced solid tumors." Invest New Drugs **35**(3): 324-333.

Fusi, C., S. Materazzi, D. Minocci, V. Maio, T. Oranges, D. Massi and R. Nassini (2014). "Transient receptor potential vanilloid 4 (TRPV4) is downregulated in keratinocytes in human non-melanoma skin cancer." J Invest Dermatol **134**(9): 2408-2417.

Gallaher, J. A., J. S. Brown and A. R. A. Anderson (2019). "The impact of proliferation-migration tradeoffs on phenotypic evolution in cancer." Sci Rep **9**(1): 2425.

Garcia-Sanz, N., A. Fernandez-Carvajal, C. Morenilla-Palao, R. Planells-Cases, E. Fajardo-Sanchez, G. Fernandez-Ballester and A. Ferrer-Montiel (2004). "Identification of a tetramerization domain in the C terminus of the vanilloid receptor." J Neurosci **24**(23): 5307-5314.

Giuliano, K., A. Ejaz and J. He (2017). "Technical aspects of pancreaticoduodenectomy and their outcomes." Chin Clin Oncol **6**(6): 64.

Gkika, D. and N. Prevarskaya (2011). "TRP channels in prostate cancer: the good, the bad and the ugly?" Asian J Androl **13**(5): 673-676.

Glazer, E. S., E. Welsh, J. M. Pimiento, J. K. Teer and M. P. Malafa (2017). "TGFbeta1 overexpression is associated with improved survival and low tumor cell proliferation in patients with early-stage pancreatic ductal adenocarcinoma." Oncotarget **8**(1): 999-1006.

Han, Y., C. Liu, D. Zhang, H. Men, L. Huo, Q. Geng, S. Wang, Y. Gao, W. Zhang, Y. Zhang and Z. Jia (2019). "Mechanosensitive ion channel Piezo1 promotes prostate cancer development through the activation of the Akt/mTOR pathway and acceleration of cell cycle." Int J Oncol **55**(3): 629-644.

Hasan, R. and X. Zhang (2018). "Ca(2+) Regulation of TRP Ion Channels." Int J Mol Sci **19**(4).

Haustrate, A., A. Mihalache, C. Cordier, P. Gosset, N. Prevarskaya and V. Lehen'kyi (2022). "A Novel Anti-TRPV6 Antibody and Its Application in Cancer Diagnosis In Vitro." Int J Mol Sci **24**(1).

Heinrich, M. A., A. Mostafa, J. P. Morton, L. Hawinkels and J. Prakash (2021). "Translating complexity and heterogeneity of pancreatic tumor: 3D in vitro to in vivo models." Adv Drug Deliv Rev **174**: 265-293.

Hellenthal, K. E. M., L. Brabenec, E. R. Gross and N. M. Wagner (2021). "TRP Channels as Sensors of Aldehyde and Oxidative Stress." Biomolecules **11**(10).

Hellmich, U. A. and R. Gaudet (2014). "Structural biology of TRP channels." Handb Exp Pharmacol **223**: 963-990.

Hirnet, D., J. Olausson, C. Fecher-Trost, M. Bodding, W. Nastainczyk, U. Wissenbach, V. Flockerzi and M. Freichel (2003). "The TRPV6 gene, cDNA and protein." Cell Calcium **33**(5-6): 509-518.

Ho, W. J., E. M. Jaffee and L. Zheng (2020). "The tumour microenvironment in pancreatic cancer - clinical challenges and opportunities." Nat Rev Clin Oncol **17**(9): 527-540.

Hoenderop, J. G., R. Vennekens, D. Muller, J. Prenen, G. Droogmans, R. J. Bindels and B. Nilius (2001). "Function and expression of the epithelial Ca(2+) channel family: comparison of mammalian ECaC1 and 2." J Physiol **537**(Pt 3): 747-761.

Hsu, W. H., K. A. LaBella, Y. Lin, P. Xu, R. Lee, C. E. Hsieh, L. Yang, A. Zhou, J. M. Blecher, C. J. Wu, K. Lin, X. Shang, S. Jiang, D. J. Spring, Y. Xia, P. Chen, J. P. Shen, S. Kopetz and R. A. DePinho (2023). "Oncogenic KRAS drives lipo-fibrogenesis to promote angiogenesis and colon cancer progression." Cancer Discov.

Hu, J. X., C. F. Zhao, W. B. Chen, Q. C. Liu, Q. W. Li, Y. Y. Lin and F. Gao (2021). "Pancreatic cancer: A review of epidemiology, trend, and risk factors." World J Gastroenterol **27**(27): 4298-4321.

Huang, J., C. H. Liu, S. A. Hughes, M. Postma, C. J. Schwiening and R. C. Hardie (2010). "Activation of TRP channels by protons and phosphoinositide depletion in Drosophila photoreceptors." Curr Biol **20**(3): 189-197.

Huber, S. M. (2013). "Oncochannels." Cell Calcium **53**(4): 241-255.

Iamshanova, O., A. Fiorio Pla and N. Prevarskaya (2017). "Molecular mechanisms of tumour invasion: regulation by calcium signals." J Physiol **595**(10): 3063-3075.

Inoue, R., L. J. Jensen, Z. Jian, J. Shi, L. Hai, A. I. Lurie, F. H. Henriksen, M. Salomonsson, H. Morita, Y. Kawarabayashi, M. Mori, Y. Mori and Y. Ito (2009). "Synergistic activation of vascular TRPC6 channel by receptor and mechanical stimulation via phospholipase C/diacylglycerol and phospholipase A2/omega-hydroxylase/20-HETE pathways." Circ Res **104**(12): 1399-1409.

Ishiguro, H., A. Yamamoto, M. Nakakuki, L. Yi, M. Ishiguro, M. Yamaguchi, S. Kondo and Y. Mochimaru (2012). "Physiology and pathophysiology of bicarbonate secretion by pancreatic duct epithelium." Nagoya J Med Sci **74**(1-2): 1-18.

James, A. D., A. Chan, O. Erice, A. K. Siriwardena and J. I. Bruce (2013). "Glycolytic ATP fuels the plasma membrane calcium pump critical for pancreatic cancer cell survival." J Biol Chem **288**(50): 36007-36019.

Jiang, Y., H. Gou, J. Zhu, S. Tian and L. Yu (2016). "Lidocaine inhibits the invasion and migration of TRPV6-expressing cancer cells by TRPV6 downregulation." Oncol Lett **12**(2): 1164-1170.

Jiang, Y., H. Gou, J. Zhu, S. Tian and L. Yu (2023). "Erratum: [Corrigendum] Lidocaine inhibits the invasion and migration of TRPV6-expressing cancer cells by TRPV6 downregulation." Oncol Lett **26**(3): 371.

Jogi, A., M. Vaapil, M. Johansson and S. Pahlman (2012). "Cancer cell differentiation heterogeneity and aggressive behavior in solid tumors." Ups J Med Sci **117**(2): 217-224.

Julius, D. (2013). "TRP channels and pain." Annu Rev Cell Dev Biol **29**: 355-384.

Karki, T., E. K. Rajakyla, A. Acheva and S. Tojkander (2020). "TRPV6 calcium channel directs homeostasis of the mammary epithelial sheets and controls epithelial mesenchymal transition." Sci Rep **10**(1): 14683.

Kehlet, S. N., R. Sanz-Pamplona, S. Brix, D. J. Leeming, M. A. Karsdal and V. Moreno (2016). "Excessive collagen turnover products are released during colorectal cancer progression and elevated in serum from metastatic colorectal cancer patients." Sci Rep **6**: 30599.

Khalil, M., K. Alliger, C. Weidinger, C. Yerinde, S. Wirtz, C. Becker and M. A. Engel (2018). "Functional Role of Transient Receptor Potential Channels in Immune Cells and Epithelia." Front Immunol **9**: 174.

Kim, H. J., H. N. Lee, M. S. Jeong and S. B. Jang (2021). "Oncogenic KRAS: Signaling and Drug Resistance." Cancers (Basel) **13**(22).

Kim, J. M., M. Lee, N. Kim and W. D. Heo (2016). "Optogenetic toolkit reveals the role of Ca2+ sparklets in coordinated cell migration." Proc Natl Acad Sci U S A **113**(21): 5952-5957.

Klatte, D. C. F., B. Boekestijn, M. Wasser, S. Feshtali Shahbazi, I. S. Ibrahim, J. S. D. Mieog, S. A. C. Luelmo, H. Morreau, T. P. Potjer, A. Inderson, J. J. Boonstra, F. W. Dekker, H. F. A. Vasen, J. E. van Hooft, B. A. Bonsing and M. E. van Leerdam (2022). "Pancreatic Cancer Surveillance in Carriers of a Germline CDKN2A Pathogenic Variant: Yield and Outcomes of a 20-Year Prospective Follow-Up." J Clin Oncol **40**(28): 3267-3277.

Kleeff, J., M. Korc, M. Apte, C. La Vecchia, C. D. Johnson, A. V. Biankin, R. E. Neale, M. Tempero, D. A. Tuveson, R. H. Hruban and J. P. Neoptolemos (2016). "Pancreatic cancer." Nat Rev Dis Primers **2**: 16022.

Koda, S., J. Hu, X. Ju, G. Sun, S. Shao, R. X. Tang, K. Y. Zheng and J. Yan (2023). "The role of glutamate receptors in the regulation of the tumor microenvironment." Front Immunol **14**: 1123841.

Kogel, A., C. Fecher-Trost, U. Wissenbach, V. Flockerzi and M. Schaefer (2022). "Ca(2+) transport via TRPV6 is regulated by rapid internalization of the channel." Cell Calcium **106**: 102634.

Koltai, T., S. J. Reshkin, T. M. A. Carvalho, D. Di Molfetta, M. R. Greco, K. O. Alfarouk and R. A. Cardone (2022). "Resistance to Gemcitabine in Pancreatic Ductal Adenocarcinoma: A Physiopathologic and Pharmacologic Review." Cancers (Basel) **14**(10).

Kotarba, G., E. Krzywinska, A. I. Grabowska, A. Taracha and T. Wilanowski (2018). "TFCP2/TFCP2L1/UBP1 transcription factors in cancer." Cancer Lett **420**: 72-79.

Kulkarni, N. M., E. V. Soloff, P. P. Tolat, G. P. Sangster, J. B. Fleming, O. R. Brook, Z. J. Wang, E. M. Hecht, M. Zins, P. R. Bhosale, H. Arif-Tiwari, L. Mannelli, A. R. Kambadakone and E. P. Tamm (2020). "White paper on pancreatic ductal adenocarcinoma from society of abdominal radiology's disease-focused panel for pancreatic ductal adenocarcinoma: Part I, AJCC staging system, NCCN guidelines, and borderline resectable disease." Abdom Radiol (NY) **45**(3): 716-728.

Lafitte, M., I. Moranvillier, S. Garcia, E. Peuchant, J. Iovanna, B. Rousseau, P. Dubus, V. Guyonnet-Duperat, G. Belleannee, J. Ramos, A. Bedel, H. de Verneuil, F. Moreau-Gaudry and S. Dabernat (2013). "FGFR3 has tumor suppressor properties in cells with epithelial phenotype." Mol Cancer **12**: 83.

Lee, B. M., G. S. Lee, E. M. Jung, K. C. Choi and E. B. Jeung (2009). "Uterine and placental expression of TRPV6 gene is regulated via progesterone receptor- or estrogen receptor-mediated pathways during pregnancy in rodents." Reprod Biol Endocrinol **7**: 49.

Lehen'kyi, V., M. Flourakis, R. Skryma and N. Prevarskaya (2007). "TRPV6 channel controls prostate cancer cell proliferation via Ca(2+)/NFAT-dependent pathways." Oncogene **26**(52): 7380-7385.

Lehen'kyi, V., M. Raphael, A. Oulidi, M. Flourakis, S. Khalimonchyk, A. Kondratskyi, D. V. Gordienko, B. Mauroy, J. L. Bonnal, R. Skryma and N. Prevarskaya (2011). "TRPV6 determines the effect of vitamin D3 on prostate cancer cell growth." PLoS One **6**(2): e16856.

Lehen'kyi, V., M. Raphael and N. Prevarskaya (2012). "The role of the TRPV6 channel in cancer." J Physiol **590**(6): 1369-1376.

Leung, E. L. H., L. X. Luo, Z. Q. Liu, V. K. W. Wong, L. L. Lu, Y. Xie, N. Zhang, Y. Q. Qu, X. X. Fan, Y. Li, M. Huang, D. K. Xiao, J. Huang, Y. L. Zhou, J. X. He, J. Ding, X. J. Yao, D. C. Ward and L. Liu (2018). "Inhibition of KRAS-dependent lung cancer cell growth by deltarasin: blockage of autophagy increases its cytotoxicity." Cell Death Dis **9**(2): 216.

Li, F., N. Abuarab and A. Sivaprasadarao (2016). "Reciprocal regulation of actin cytoskeleton remodelling and cell migration by Ca2+ and Zn2+: role of TRPM2 channels." J Cell Sci **129**(10): 2016-2029.

Lieben, L. and G. Carmeliet (2012). "The Involvement of TRP Channels in Bone Homeostasis." Front Endocrinol (Lausanne) **3**: 99.

Litan, A. and S. A. Langhans (2015). "Cancer as a channelopathy: ion channels and pumps in tumor development and progression." Front Cell Neurosci **9**: 86.

Liu, J., C. Qu, C. Han, M. M. Chen, L. J. An and W. Zou (2019). "Potassium channels and their role in glioma: A mini review." Mol Membr Biol **35**(1): 76-85.

Lodola, F., U. Laforenza, E. Bonetti, D. Lim, S. Dragoni, C. Bottino, H. L. Ong, G. Guerra, C. Ganini, M. Massa, M. Manzoni, I. S. Ambudkar, A. A. Genazzani, V. Rosti, P. Pedrazzoli, F. Tanzi, F. Moccia and C. Porta (2012). "Store-operated Ca2+ entry is remodelled and controls in vitro angiogenesis in endothelial progenitor cells isolated from tumoral patients." PLoS One **7**(9): e42541.

Loeck, T. and A. Schwab (2023). "The role of the Na(+)/Ca(2+)-exchanger (NCX) in cancer-associated fibroblasts." Biol Chem **404**(4): 325-337.

Lu, C., Z. Ma, X. Cheng, H. Wu, B. Tuo, X. Liu and T. Li (2020). "Pathological role of ion channels and transporters in the development and progression of triple-negative breast cancer." Cancer Cell Int **20**: 377.

Ma, X., Y. Cai, D. He, C. Zou, P. Zhang, C. Y. Lo, Z. Xu, F. L. Chan, S. Yu, Y. Chen, R. Zhu, J. Lei, J. Jin and X. Yao (2012). "Transient receptor potential channel TRPC5 is essential for P-glycoprotein induction in drug-resistant cancer cells." Proc Natl Acad Sci U S A **109**(40): 16282-16287.

Maddalena, M., G. Mallel, N. B. Nataraj, M. Shreberk-Shaked, O. Hassin, S. Mukherjee, S. Arandkar, R. Rotkopf, A. Kapsack, G. Lambiase, B. Pellegrino, E. Ben-Isaac, O. Golani, Y. Addadi, E. Hajaj, R. Eilam, R. Straussman, Y. Yarden, M. Lotem and M. Oren (2021). "TP53 missense mutations in PDAC are associated with enhanced fibrosis and an immunosuppressive microenvironment." Proc Natl Acad Sci U S A **118**(23).

Madge, O., A. Brodey, J. Bowen, G. Nicholson, S. Sivakumar and M. J. Bottomley (2022). "The COVID-19 Pandemic Is Associated with Reduced Survival after Pancreatic Ductal Adenocarcinoma Diagnosis: A Single-Centre Retrospective Analysis." J Clin Med **11**(9).

Masamune, A., H. Kotani, F. L. Sorgel, J. M. Chen, S. Hamada, R. Sakaguchi, E. Masson, E. Nakano, Y. Kakuta, T. Niihori, R. Funayama, M. Shirota, T. Hirano, T. Kawamoto, A. Hosokoshi, K. Kume, L. Unger, M. Ewers, H. Laumen, P. Bugert, M. X. Mori, V. Tsvilovskyy, P. Weissgerber, U. Kriebs, C. Fecher-Trost, M. Freichel, K. N. Diakopoulos, A. Berninger, M. Lesina, K. Ishii, T. Itoi, T. Ikeura, K. Okazaki, T. Kaune, J. Rosendahl, M. Nagasaki, Y. Uezono, H. Algul, K. Nakayama, Y. Matsubara, Y. Aoki, C. Ferec, Y. Mori, H. Witt and T. Shimosegawa (2020). "Variants That Affect Function of Calcium Channel TRPV6 Are Associated With Early-Onset Chronic Pancreatitis." Gastroenterology **158**(6): 1626-1641 e1628.

McGoldrick, L. L., A. K. Singh, K. Saotome, M. V. Yelshanskaya, E. C. Twomey, R. A. Grassucci and A. I. Sobolevsky (2018). "Opening of the human epithelial calcium channel TRPV6." Nature **553**(7687): 233-237.

Mesquita, G., N. Prevarskaya, A. Schwab and V. Lehen'kyi (2021). "Role of the TRP Channels in Pancreatic Ductal Adenocarcinoma Development and Progression." Cells **10**(5).

Mezencev, R., L. V. Matyunina, G. T. Wagner and J. F. McDonald (2016). "Acquired resistance of pancreatic cancer cells to cisplatin is multifactorial with cell context-dependent involvement of resistance genes." Cancer Gene Ther **23**(12): 446-453.

Minke, B. (2010). "The history of the Drosophila TRP channel: the birth of a new channel superfamily." J Neurogenet **24**(4): 216-233.

Molenaar, R. J. (2011). "Ion channels in glioblastoma." ISRN Neurol **2011**: 590249.

Monteith, G. R., N. Prevarskaya and S. J. Roberts-Thomson (2017). "The calcium-cancer signalling nexus." Nat Rev Cancer **17**(6): 367-380.

Montell, C., L. Birnbaumer, V. Flockerzi, R. J. Bindels, E. A. Bruford, M. J. Caterina, D. E. Clapham, C. Harteneck, S. Heller, D. Julius, I. Kojima, Y. Mori, R. Penner, D. Prawitt, A. M. Scharenberg, G. Schultz, N. Shimizu and M. X. Zhu (2002). "A unified nomenclature for the superfamily of TRP cation channels." Mol Cell **9**(2): 229-231.

Muller, C., P. Morales and P. H. Reggio (2018). "Cannabinoid Ligands Targeting TRP Channels." Front Mol Neurosci **11**: 487.

Neuberger, A., K. D. Nadezhdin and A. I. Sobolevsky (2021). "Structural mechanisms of TRPV6 inhibition by ruthenium red and econazole." Nat Commun **12**(1): 6284.

Neuberger, A., Y. A. Trofimov, M. V. Yelshanskaya, J. Khau, K. D. Nadezhdin, L. S. Khosrof, N. A. Krylov, R. G. Efremov and A. I. Sobolevsky (2023). "Molecular pathway and structural mechanism of human oncochannel TRPV6 inhibition by the phytocannabinoid tetrahydrocannabivarin." Nat Commun **14**(1): 4630.

Nielsen, N., O. Lindemann and A. Schwab (2014). "TRP channels and STIM/ORAI proteins: sensors and effectors of cancer and stroma cell migration." Br J Pharmacol **171**(24): 5524-5540.

Niemeyer, B. A., C. Bergs, U. Wissenbach, V. Flockerzi and C. Trost (2001). "Competitive regulation of CaT-like-mediated Ca2+ entry by protein kinase C and calmodulin." Proc Natl Acad Sci U S A **98**(6): 3600-3605.

Nilius, B. and G. Owsianik (2011). "The transient receptor potential family of ion channels." Genome Biol **12**(3): 218.

Nishimoto, A. (2022). "Effective combinations of anti-cancer and targeted drugs for pancreatic cancer treatment." World J Gastroenterol **28**(28): 3637-3643.

Norton, J., D. Foster, M. Chinta, A. Titan and M. Longaker (2020). "Pancreatic Cancer Associated Fibroblasts (CAF): Under-Explored Target for Pancreatic Cancer Treatment." Cancers (Basel) **12**(5).

O'Day, D. H., S. Mathavarajah, M. A. Myre and R. J. Huber (2020). "Calmodulin-mediated events during the life cycle of the amoebozoan Dictyostelium discoideum." Biol Rev Camb Philos Soc **95**(2): 472-490.

Oancea, E., J. T. Wolfe and D. E. Clapham (2006). "Functional TRPM7 channels accumulate at the plasma membrane in response to fluid flow." Circ Res **98**(2): 245-253.

Ogawa, F., M. S. Walters, A. Shafquat, S. L. O'Beirne, R. J. Kaner, J. G. Mezey, H. Zhang, P. L. Leopold and R. G. Crystal (2019). "Role of KRAS in regulating normal human airway basal cell differentiation." Respir Res **20**(1): 181.

Okada, Y., P. S. Reinach, K. Shirai, A. Kitano-Izutani, M. Miyajima, O. Yamanaka, T. Sumioka and S. Saika (2015). "Transient Receptor Potential Channels and Corneal Stromal Inflammation." Cornea **34 Suppl 11**: S136-141.

Okeke, E., T. Parker, H. Dingsdale, M. Concannon, M. Awais, S. Voronina, J. Molgo, M. Begg, D. Metcalf, A. E. Knight, R. Sutton, L. Haynes and A. V. Tepikin (2016). "Epithelial-mesenchymal transition, IP3 receptors and ER-PM junctions: translocation of Ca2+ signalling complexes and regulation of migration." Biochem J **473**(6): 757-767.

Orrenius, S., B. Zhivotovsky and P. Nicotera (2003). "Regulation of cell death: the calcium-apoptosis link." Nat Rev Mol Cell Biol **4**(7): 552-565.

Palamaris, K., E. Felekouras and S. Sakellariou (2021). "Epithelial to Mesenchymal Transition: Key Regulator of Pancreatic Ductal Adenocarcinoma Progression and Chemoresistance." Cancers (Basel) **13**(21).

Peleg, S., J. H. Sellin, Y. Wang, M. R. Freeman and S. Umar (2010). "Suppression of aberrant transient receptor potential cation channel, subfamily V, member 6 expression in hyperproliferative colonic crypts by dietary calcium." Am J Physiol Gastrointest Liver Physiol **299**(3): G593-601.

Peng, J. B., E. M. Brown and M. A. Hediger (2003). "Epithelial Ca2+ entry channels: transcellular Ca2+ transport and beyond." J Physiol **551**(Pt 3): 729-740.

Peng, J. B., X. Z. Chen, U. V. Berger, P. M. Vassilev, H. Tsukaguchi, E. M. Brown and M. A. Hediger (1999). "Molecular cloning and characterization of a channel-like transporter mediating intestinal calcium absorption." J Biol Chem **274**(32): 22739-22746.

Peng, J. B., X. Z. Chen, U. V. Berger, S. Weremowicz, C. C. Morton, P. M. Vassilev, E. M. Brown and M. A. Hediger (2000). "Human calcium transport protein CaT1." Biochem Biophys Res Commun **278**(2): 326-332.

Peng, J. B., L. Zhuang, U. V. Berger, R. M. Adam, B. J. Williams, E. M. Brown, M. A. Hediger and M. R. Freeman (2001). "CaT1 expression correlates with tumor grade in prostate cancer." Biochem Biophys Res Commun **282**(3): 729-734.

Peppicelli, S., J. Ruzzolini, M. Lulli, A. Biagioni, F. Bianchini, A. Caldarella, C. Nediani, E. Andreucci and L. Calorini (2022). "Extracellular Acidosis Differentially Regulates Estrogen Receptor beta-Dependent EMT Reprogramming in Female and Male Melanoma Cells." Int J Mol Sci **23**(23).

Peters, A. A., P. T. Simpson, J. J. Bassett, J. M. Lee, L. Da Silva, L. E. Reid, S. Song, M. O. Parat, S. R. Lakhani, P. A. Kenny, S. J. Roberts-Thomson and G. R. Monteith (2012). "Calcium channel TRPV6 as a potential therapeutic target in estrogen receptor-negative breast cancer." Mol Cancer Ther **11**(10): 2158-2168.

Phillips, A. M., A. Bull and L. E. Kelly (1992). "Identification of a Drosophila gene encoding a calmodulin-binding protein with homology to the trp phototransduction gene." Neuron **8**(4): 631-642.

Pinto, M. C., A. H. Kihara, V. A. Goulart, F. M. Tonelli, K. N. Gomes, H. Ulrich and R. R. Resende (2015). "Calcium signaling and cell proliferation." Cell Signal **27**(11): 2139-2149.

Prevarskaya, N., R. Skryma and Y. Shuba (2011). "Calcium in tumour metastasis: new roles for known actors." Nat Rev Cancer **11**(8): 609-618.

Prevarskaya, N., R. Skryma and Y. Shuba (2018). "Ion Channels in Cancer: Are Cancer Hallmarks Oncochannelopathies?" Physiol Rev **98**(2): 559-621.

Prevarskaya, N., L. Zhang and G. Barritt (2007). "TRP channels in cancer." Biochim Biophys Acta **1772**(8): 937-946.

Principe, D. R., A. F. Aissa, S. Kumar, T. N. D. Pham, P. W. Underwood, R. Nair, R. Ke, B. Rana, J. G. Trevino, H. G. Munshi, E. V. Benevolenskaya and A. Rana (2022). "Calcium channel blockers potentiate gemcitabine chemotherapy in pancreatic cancer." Proc Natl Acad Sci U S A **119**(18): e2200143119.

Prior, I. A., P. D. Lewis and C. Mattos (2012). "A comprehensive survey of Ras mutations in cancer." Cancer Res **72**(10): 2457-2467.

Prole, D. L. and C. W. Taylor (2019). "Structure and Function of IP(3) Receptors." Cold Spring Harb Perspect Biol **11**(4).

Provenzano, P. P. and S. R. Hingorani (2013). "Hyaluronan, fluid pressure, and stromal resistance in pancreas cancer." Br J Cancer **108**(1): 1-8.

Pulido, I., S. Ollosi, S. Aparisi, J. H. Becker, A. Aliena-Valero, M. Benet, M. L. Rodriguez, A. Lopez, E. Tamayo-Torres, L. Chulia-Peris, J. C. Garcia-Canaveras, M. Soucheray, A. V. Dalheim, J. B. Salom, W. Qiu, S. Kaja, J. A. Fernandez-Coronado, S. Alandes, J. Alcacer, F. Al-Shahrour, J. A. Borgia, O. Juan, M. I. Nishimura, A. Lahoz, J. Carretero and T. Shimamura (2020). "Endothelin-1-Mediated Drug Resistance in EGFR-Mutant Non-Small Cell Lung Carcinoma." Cancer Res **80**(19): 4224-4232.

Raphael, M., V. Lehen'kyi, M. Vandenberghe, B. Beck, S. Khalimonchyk, F. Vanden Abeele, L. Farsetti, E. Germain, A. Bokhobza, A. Mihalache, P. Gosset, C. Romanin, P. Clezardin, R. Skryma and N. Prevarskaya (2014). "TRPV6 calcium channel translocates to the plasma membrane via Orai1-mediated mechanism and controls cancer cell survival." Proc Natl Acad Sci U S A **111**(37): E3870-3879.

Rawla, P., T. Sunkara and V. Gaduputi (2019). "Epidemiology of Pancreatic Cancer: Global Trends, Etiology and Risk Factors." World J Oncol **10**(1): 10-27.

Rhana, P., R. R. J. Trivelato, P. S. L. Beirao, J. S. Cruz and A. L. P. Rodrigues (2017). "Is there a role for voltage-gated Na+ channels in the aggressiveness of breast cancer?" Braz J Med Biol Res **50**(7): e6011.

Rhim, A. D., P. E. Oberstein, D. H. Thomas, E. T. Mirek, C. F. Palermo, S. A. Sastra, E. N. Dekleva, T. Saunders, C. P. Becerra, I. W. Tattersall, C. B. Westphalen, J. Kitajewski, M. G. Fernandez-Barrena, M. E. Fernandez-Zapico, C. Iacobuzio-Donahue, K. P. Olive and B. Z. Stanger (2014). "Stromal elements act to restrain, rather than support, pancreatic ductal adenocarcinoma." Cancer Cell **25**(6): 735-747.

Richardson, D. A., P. Sritangos, A. D. James, A. Sultan and J. I. E. Bruce (2020). "Metabolic regulation of calcium pumps in pancreatic cancer: role of phosphofructokinase-fructose-bisphosphatase-3 (PFKFB3)." Cancer Metab **8**: 2.

Rohacs, T., C. M. Lopes, I. Michailidis and D. E. Logothetis (2005). "PI(4,5)P2 regulates the activation and desensitization of TRPM8 channels through the TRP domain." Nat Neurosci **8**(5): 626-634.

Sakipov, S., A. I. Sobolevsky and M. G. Kurnikova (2018). "Ion Permeation Mechanism in Epithelial Calcium Channel TRVP6." Sci Rep **8**(1): 5715.

Saldias, M. P., D. Maureira, O. Orellana-Serradell, I. Silva, B. Lavanderos, P. Cruz, C. Torres, M. Caceres and O. Cerda (2021). "TRP Channels Interactome as a Novel Therapeutic Target in Breast Cancer." Front Oncol **11**: 621614.

Santoni, G., F. Maggi, M. B. Morelli, M. Santoni and O. Marinelli (2019). "Transient Receptor Potential Cation Channels in Cancer Therapy." Med Sci (Basel) **7**(12).

Saotome, K., A. K. Singh, M. V. Yelshanskaya and A. I. Sobolevsky (2016). "Crystal structure of the epithelial calcium channel TRPV6." Nature **534**(7608): 506-511.

Schindl, R., I. Frischauf, H. Kahr, R. Fritsch, M. Krenn, A. Derndl, E. Vales, M. Muik, I. Derler, K. Groschner and C. Romanin (2008). "The first ankyrin-like repeat is the minimum indispensable key structure for functional assembly of homo- and heteromeric TRPC4/TRPC5 channels." Cell Calcium **43**(3): 260-269.

Schwarz, E. C., U. Wissenbach, B. A. Niemeyer, B. Strauss, S. E. Philipp, V. Flockerzi and M. Hoth (2006). "TRPV6 potentiates calcium-dependent cell proliferation." Cell Calcium **39**(2): 163-173.

Shi, Y., X. Ding, Z. H. He, K. C. Zhou, Q. Wang and Y. Z. Wang (2009). "Critical role of TRPC6 channels in G2 phase transition and the development of human oesophageal cancer." Gut **58**(11): 1443-1450.

Shinkawa, T., K. Ohuchida, Y. Mochida, K. Sakihama, C. Iwamoto, T. Abe, N. Ideno, Y. Mizuuchi, K. Shindo, N. Ikenaga, T. Moriyama, K. Nakata, Y. Oda and M. Nakamura (2022). "Subtypes in pancreatic ductal adenocarcinoma based on niche factor dependency show distinct drug treatment responses." J Exp Clin Cancer Res **41**(1): 89.

Singh, A. K., L. L. McGoldrick, E. C. Twomey and A. I. Sobolevsky (2018). "Mechanism of calmodulin inactivation of the calcium-selective TRP channel TRPV6." Sci Adv **4**(8): eaau6088.

Skrzypski, M., N. Khajavi, S. Mergler, D. Szczepankiewicz, P. A. Kolodziejski, D. Metzke, T. Wojciechowicz, M. Billert, K. W. Nowak and M. Z. Strowski (2015). "TRPV6 channel modulates proliferation of insulin secreting INS-1E beta cell line." Biochim Biophys Acta **1853**(12): 3202-3210.

Skrzypski, M., P. A. Kolodziejski, S. Mergler, N. Khajavi, K. W. Nowak and M. Z. Strowski (2016). "TRPV6 modulates proliferation of human pancreatic neuroendocrine BON-1 tumour cells." Biosci Rep **36**(4).

Sohn, B. S., Y. J. Yuh, H. S. Song, B. S. Kim, K. H. Lee, J. S. Jang and S. R. Kim (2015). "Triplet cytotoxic chemotherapy with gemcitabine, 5-fluorouracil and cisplatin for advanced pancreatic cancer." Oncol Lett **10**(2): 1204-1210.

Song, H., M. Dong, J. Zhou, W. Sheng, X. Li and W. Gao (2018). "Expression and prognostic significance of TRPV6 in the development and progression of pancreatic cancer." Oncol Rep **39**(3): 1432-1440.

Song, M. Y. and J. X. Yuan (2010). "Introduction to TRP channels: structure, function, and regulation." Adv Exp Med Biol **661**: 99-108.

Spivak-Kroizman, T. R., G. Hostetter, R. Posner, M. Aziz, C. Hu, M. J. Demeure, D. Von Hoff, S. R. Hingorani, T. B. Palculict, J. Izzo, G. M. Kiriakova, M. Abdelmelek, G. Bartholomeusz, B. P. James and G. Powis (2013). "Hypoxia triggers hedgehog-mediated tumor-stromal interactions in pancreatic cancer." Cancer Res **73**(11): 3235-3247.

Stewart, J. M. (2020). "TRPV6 as A Target for Cancer Therapy." J Cancer **11**(2): 374-387.

Stoklosa, P., A. Borgstrom, S. Kappel and C. Peinelt (2020). "TRP Channels in Digestive Tract Cancers." Int J Mol Sci **21**(5).

Stopa, K. B., F. Lozinski, A. A. Kusiak, J. Litewka, D. Krzysztofik, S. Mosiolek, J. Morys, P. E. Ferdek and M. A. Jakubowska (2023). "Driver Mutations of Pancreatic Cancer Affect Ca(2+) Signaling and ATP Production." Function (Oxf) **4**(5): zqad035.

Storck, H., B. Hild, S. Schimmelpfennig, S. Sargin, N. Nielsen, A. Zaccagnino, T. Budde, I. Novak, H. Kalthoff and A. Schwab (2017). "Ion channels in control of pancreatic stellate cell migration." Oncotarget **8**(1): 769-784.

Strotmann, R., C. Harteneck, K. Nunnenmacher, G. Schultz and T. D. Plant (2000). "OTRPC4, a nonselective cation channel that confers sensitivity to extracellular osmolarity." Nat Cell Biol **2**(10): 695-702.

Suzuki, M., K. Ishibashi, G. Ooki, S. Tsuruoka and M. Imai (2000). "Electrophysiologic characteristics of the Ca-permeable channels, ECaC and CaT, in the kidney." Biochem Biophys Res Commun **274**(2): 344-349.

Suzuki, Y., A. Pasch, O. Bonny, M. G. Mohaupt, M. A. Hediger and F. J. Frey (2008). "Gain-of-function haplotype in the epithelial calcium channel TRPV6 is a risk factor for renal calcium stone formation." Hum Mol Genet **17**(11): 1613-1618.

Taylor, C. W. and S. C. Tovey (2010). "IP(3) receptors: toward understanding their activation." Cold Spring Harb Perspect Biol **2**(12): a004010.

Tiwari, A. and L. Kumar (2018). "Pancreatic ductal adenocarcinoma: Role of chemotherapy & future perspectives." Indian J Med Res **148**(3): 254-257.

Valero, M. L., F. Mello de Queiroz, W. Stuhmer, F. Viana and L. A. Pardo (2012). "TRPM8 ion channels differentially modulate proliferation and cell cycle distribution of normal and cancer prostate cells." PLoS One **7**(12): e51825.

VanHouten, J., C. Sullivan, C. Bazinet, T. Ryoo, R. Camp, D. L. Rimm, G. Chung and J. Wysolmerski (2010). "PMCA2 regulates apoptosis during mammary gland involution and predicts outcome in breast cancer." Proc Natl Acad Sci U S A **107**(25): 11405-11410.

Varghese, E., S. M. Samuel, Z. Sadiq, P. Kubatka, A. Liskova, J. Benacka, P. Pazinka, P. Kruzliak and D. Busselberg (2019). "Anti-Cancer Agents in Proliferation and Cell Death: The Calcium Connection." Int J Mol Sci **20**(12).

Vriens, J., B. Nilius and T. Voets (2014). "Peripheral thermosensation in mammals." Nat Rev Neurosci **15**(9): 573-589.

Wang, T., Z. Chen, Y. Zhu, Q. Pan, Y. Liu, X. Qi, L. Jin, J. Jin, X. Ma and D. Hua (2015). "Inhibition of transient receptor potential channel 5 reverses 5-Fluorouracil resistance in human colorectal cancer cells." J Biol Chem **290**(1): 448-456.

Wang, W. B., Y. Yang, Y. P. Zhao, T. P. Zhang, Q. Liao and H. Shu (2014). "Recent studies of 5-fluorouracil resistance in pancreatic cancer." World J Gastroenterol **20**(42): 15682-15690.

Weber, K., R. G. Erben, A. Rump and J. Adamski (2001). "Gene structure and regulation of the murine epithelial calcium channels ECaC1 and 2." Biochem Biophys Res Commun **289**(5): 1287-1294.

Wei, C., X. Wang, M. Zheng and H. Cheng (2012). "Calcium gradients underlying cell migration." Curr Opin Cell Biol **24**(2): 254-261.

Weissgerber, P., U. Kriebs, V. Tsvilovskyy, J. Olausson, O. Kretz, C. Stoerger, R. Vennekens, U. Wissenbach, R. Middendorff, V. Flockerzi and M. Freichel (2011). "Male fertility depends on Ca(2)+ absorption by TRPV6 in epididymal epithelia." Sci Signal **4**(171): ra27.

Wissenbach, U., B. A. Niemeyer, T. Fixemer, A. Schneidewind, C. Trost, A. Cavalie, K. Reus, E. Meese, H. Bonkhoff and V. Flockerzi (2001). "Expression of CaT-like, a novel calcium-selective channel, correlates with the malignancy of prostate cancer." J Biol Chem **276**(22): 19461-19468.

Wood, L. D., M. I. Canto, E. M. Jaffee and D. M. Simeone (2022). "Pancreatic Cancer: Pathogenesis, Screening, Diagnosis, and Treatment." Gastroenterology **163**(2): 386-402 e381.

Xu, X., N. Li, Y. Wang, J. Yu and J. Mi (2021). "Calcium channel TRPV6 promotes breast cancer metastasis by NFATC2IP." Cancer Lett **519**: 150-160.

Xue, H., Y. Wang, T. J. MacCormack, T. Lutes, C. Rice, M. Davey, D. Dugourd, T. T. Ilenchuk and J. M. Stewart (2018). "Inhibition of Transient Receptor Potential Vanilloid 6 channel, elevated in human ovarian cancers, reduces tumour growth in a xenograft model." J Cancer **9**(17): 3196-3207.

Yang, D. and J. Kim (2020). "Emerging role of transient receptor potential (TRP) channels in cancer progression." BMB Rep **53**(3): 125-132.

Yasuda, K., T. Torigoe, T. Mariya, T. Asano, T. Kuroda, J. Matsuzaki, K. Ikeda, M. Yamauchi, M. Emori, H. Asanuma, T. Hasegawa, T. Saito, Y. Hirohashi and N. Sato (2014). "Fibroblasts induce expression of FGF4 in

ovarian cancer stem-like cells/cancer-initiating cells and upregulate their tumor initiation capacity." Lab Invest **94**(12): 1355-1369.

You, M., Z. Xie, N. Zhang, Y. Zhang, D. Xiao, S. Liu, W. Zhuang, L. Li and Y. Tao (2023). "Signaling pathways in cancer metabolism: mechanisms and therapeutic targets." Signal Transduct Target Ther **8**(1): 196.

Zaccagnino, A., C. Pilarsky, D. Tawfik, S. Sebens, A. Trauzold, I. Novak, A. Schwab and H. Kalthoff (2016). "In silico analysis of the transportome in human pancreatic ductal adenocarcinoma." Eur Biophys J **45**(7): 749-763.

Zhang, P., X. Liu, H. Li, Z. Chen, X. Yao, J. Jin and X. Ma (2017). "TRPC5-induced autophagy promotes drug resistance in breast carcinoma via CaMKKbeta/AMPKalpha/mTOR pathway." Sci Rep **7**(1): 3158.

Zhang, Y., N. Cruickshanks, F. Yuan, B. Wang, M. Pahuski, J. Wulfkuhle, I. Gallagher, A. F. Koeppel, S. Hatef, C. Papanicolas, J. Lee, E. E. Bar, D. Schiff, S. D. Turner, E. F. Petricoin, L. S. Gray and R. Abounader (2017). "Targetable T-type Calcium Channels Drive Glioblastoma." Cancer Res **77**(13): 3479-3490.

Zhang, Z., H. Zhang, X. Liao and H. I. Tsai (2023). "KRAS mutation: The booster of pancreatic ductal adenocarcinoma transformation and progression." Front Cell Dev Biol **11**: 1147676.

Zhao, H., L. Wu, G. Yan, Y. Chen, M. Zhou, Y. Wu and Y. Li (2021). "Inflammation and tumor progression: signaling pathways and targeted intervention." Signal Transduct Target Ther **6**(1): 263.

Zhao, X. L., Y. Lin, J. Jiang, Z. Tang, S. Yang, L. Lu, Y. Liang, X. Liu, J. Tan, X. G. Hu, Q. Niu, W. J. Fu, Z. X. Yan, D. Y. Guo, Y. F. Ping, J. M. Wang, X. Zhang, H. F. Kung, X. W. Bian and X. H. Yao (2017). "High-mobility group box 1 released by autophagic cancer-associated fibroblasts maintains the stemness of luminal breast cancer cells." J Pathol **243**(3): 376-389.

Zhuang, L., J. B. Peng, L. Tou, H. Takanaga, R. M. Adam, M. A. Hediger and M. R. Freeman (2002). "Calcium-selective ion channel, CaT1, is apically localized in gastrointestinal tract epithelia and is aberrantly expressed in human malignancies." Lab Invest **82**(12): 1755-1764.